AN EXPERIMENTAL INVESTIGATION OF NATURAL CONVECTION FROM HOT VEE CORRUGATED PLATES TO A COLD FLAT PLATE
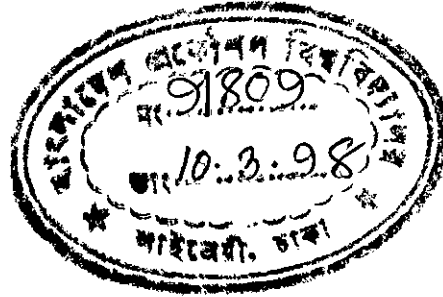
By

LATIFA BEGUM

A THESIS SUBMITTED TO THE DEPARTMENT OF MECHANICAL ENGINEERING
IN PARTIAL FULFILMENT OF THE DEGREE OF
MASTER OF SCIENCE IN MECHANICAL ENGINEERING

BANGLADESH UNIVERSITY OF ENGINEERING AND TECHNOLOGY , DHAKA.
JANUARY, 1998

CERTIFICATE OF APPROVAL

The thesis titled " An Experimental Investigation of Natural Convection From Hot Vee Corrugated Plates to a Cold Flat Plate" submitted by Latifa Begum, Roll Number : 891403F, Registration Number : 83342 of M.Sc. Engineering (Mechanical) has been accepted as satisfactory in partial fulfillment of the degree of Master of Science in Engineering (Mechanical) on the 24 th January, 1998.
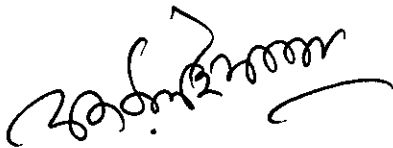

Dr. Md. Abdur Razzaq Akhanda (Supervisor)   Chairman
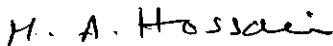Professor
Mechanical Engineering Department
BUET , Dhaka.

Dr. Md. Abu Taher Ali   Member
Professor
Mechanical Engineering Department
BUET , Dhaka.

Dr. A. K. M. Sadrul Islam   Member (Ex - officio)
Professor and Head of
Mechanical Engineering Department
BUET , Dhaka.
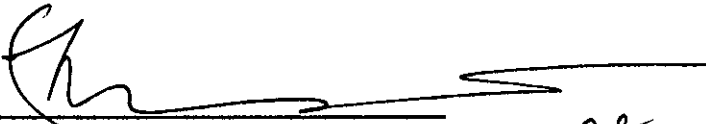
Professor Dr. M. Anwar Hossain   Member
Department of Mechanical & Chemical Engineering   (External)
Islamic Institution of Technology
Dhaka.
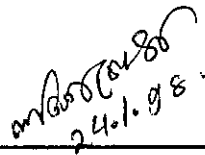
CERTIFICATE OF RESEARCH

This is to certify that the work presented in this thesis is an outcome of the investigation carried out by the author under the supervision of Dr. Md. Abdur Razzaq Akhanda, Professor of Department of Mechanical Engineering, Bangladesh University of Engineering & Technology, Dhaka.

Dr. Md. Abdur Razzaq Akhanda 24, 1. 98
Supervisor

Latifa Begum
Author

ACKNOWLEDGEMENT

ABSTRACT

This experimental investigation deals with the steady state natural convection heat transfer through air at atmospheric pressure from hot vee corrugated plates to a cold flat plate placed above and parallel to it, where the surroundings were maintained at constant temperature. Different amplitudes of corrugation i.e., H = 10mm, 15mm, 25mm were used. The effects of angle of inclination, aspect ratio, temperature difference and Rayleigh number on average convective heat transfer co-efficients were studied which covers the ranges of :

$$0^0 \leq \theta \leq 75^0, \quad 1.4 \leq A \leq 9.5, 10^0 C \leq \Delta T \leq 35^0 C, \quad 3.294 \times 10^4 \leq Ra_L \leq 1.881 \times 10^6$$

From these sets of corrugation it is investigated that for the same Rayleigh number an increase in amplitude of corrugation increases the convective heat transfer coefficient and the values are

Nu_L for H = 25mm > Nu_L for H = 10 mm by 15%

Nu_L for H = 25mm > Nu_L for H = 15 mm by 08%

The results are compared with those available in literature and it is found that for lower Rayleigh number i.e., Ra_L = 0.4 x 10^6 the Nusselt number is maximum for vee-corrugation and minimum for square corrugation, and the values are,

Nu_L for Vee corrugation > Nu_L for Square corrugation of H =25mm by 40%

Nu_L for Vee corrugation > Nu_L for Rectangular corrugation of H =25mm by 28%

Nu_L for Vee corrugation > Nu_L for Trapezoidal corrugation of H =25mm by 22%

Nu_L for Vee corrugation > Nu_L for Sinusoidal corrugation of H =25mm by 12%

These differences are also lower for higher Rayleigh numbers i.e., 1.0 X 10^6.

Finally correlation for vee corrugation was developed which correlates almost all the data within ± 12 %

$$Nu_L = 0.276 [Ra_L \cos \theta]^{0.294} . [A]^{-0.331}$$

Besides this, the experimental results are compared with the results of Chinnappa (1970), who carried out an experimental investigation from a horizontal lower vee corrugated plate to an upper cold flat plate at Rayleigh number, Ra_L = 0.4 x 10^6 and H = 25mm, it was found that the Nusselt number of this experiment was higher by 0.6% than the value of Chinnappa.

By uncertainty analysis it was found that for calculation the value of Nusselt number in vee corrugated enclosure the estimated uncertainty was 1.2477 %.

CONTENTS

NOMENCLATURE

SYMBOL	MEANING	UNITS
A	Aspect ratio, L/H	dimensionless
A_{COR}	Project area of the test section	m^2
A_{COLD}	Area of the cold plate	m^2
A_P	Area of any plane rectangular surface	m^2
A_i	Area of surface i	m^2
A_j	Area of surface j	m^2
A_s	Area of wooden surface	m^2
C	Constant	dimensionless
C_P	Specific heat of air at constant pressure	KJ/Kg K
E_b	Emissive power for a black surface, σT^4	Watt/ m^2
F	Shape factor	
Gr	Grashof number, $g.\beta . \Delta T d^3 / v^2$	dimensionless
g	Acceleration due to gravity	m / sec^2
h	Average natural convective heat transfer co-efficient	Watt/m^2 K
H	Amplitude of the corrugation	mm
I_{safe}	Safe current capacity of the heater coil	ampere
J	Radiosity [Emissive power for a black surface, E_b]	Watt/ m^2
K	Thermal conductivity of air	Watt/ m K
L_c	Characteristic length ($= A_p$)	m
L	Mean plate spacing	mm
m	Exponent	dimensionless
n	Exponent	dimensionless
Nu_L	Average Nusselt number, hL / k	dimensionless
Pr	Prandtl number , $\mu. C_p /k$	dinensionless
q	Heat transfer rate	Watt/ m^2
q"	Heat flux rate into the test hot plate	Watt/ m^2
r	Unit electrical resistance	ohms/m
Ra_L	Rayleigh number based on mean plate spacings (L), $g.\beta.\Delta T.L^3/v\alpha$	dimensionless
s	Maximum width of corrugation	mm
t	Time	sec
T	Temperature	K
T_a , T_∞	Ambient air temperature	K
T_f	Fluid film temperature , $[T_{COR} + T_{COLD}] / 2$	K
T_{COR}	Temperature of the hot corrugated plate	K
T_{COLD}	Temperature of the cold flat plate	K
ΔT	Temperature difference between the hot corrugated plate and flat cold plate	K
ΔT_c	Conduction correction	K
T_s	Temperature of the wooden surfaces	K

u,v,w	Velocity components in the direction of x,y,z respectively	m/sec
V_{safe}	Safe voltage across the heater coil	volts
W	Width of the enclosure	m
x,y,z	Spatial coordinates	
X_{COR}	Longitudinal side of the test section of the corrugated plate	mm
X_{COLD}	Longitudinal side of the cold flat plate	mm
ΔX	Thickness along x direction	m
Y_{COR}	Lateral side of the test section of the corrugated plate	mm
Y_{COLD}	Lateral side of the cold flat plate	mm

GREEK ALPHABET:

α	Thermal diffusivity , $k / \rho\, Cp$	m^2/sec
β	Volumetric thermal expansion coefficient , $1/T_f$	1/K
Δ	Difference	
ε	Long wave emmissivities	dimensionless
ε_H	Hemispherical emittance	dimensionless
ε_S	Long wave emmissivities of the wooden surface	dimensionless
θ	Tilt angle of inclination of the enclosed air layers with the horizontal	degree
ν	Kinematic viscosity of the convecting fluid (air)	m^2/sec
ρ	Density	kg/m^3
σ	Stefan Boltzman's constant [$= 5.67 \times 10^{-8}$]	Watt/ $m^2 K^4$
ϕ	Phase angle of the current	degree
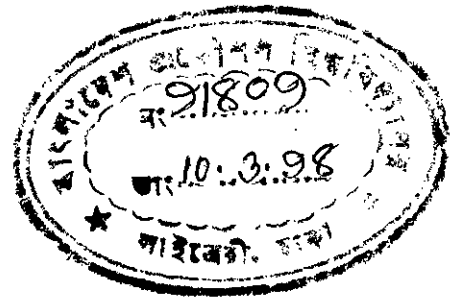
1.1 General

The fluid flow in "free" or "natural" convection arises as a result of density variations caused by thermal expansion of the fluid in a non uniform temperature distribution. The movement of fluid in natural convection results from the buoyancy forces imposed on the fluid when its density in the proximity of the heat transfer surface is decreased as a result of a heating process. Buoyancy is due to the combined presence of a fluid density gradient and a body force. The body force is usually gravitational, although gravity is not the only type of force field which can produce the natural convection currents, a fluid enclosed in a rotating machine is acted upon by a centrifugal force field, and thus could experience natural convection currents if one or more surfaces in contact with the fluid were heated. There are several ways in which a mass density gradient may arise in a fluid but in the most common situation it is due to the presence of a temperature gradient. The density of gases and liquids depends on temperature, generally decreasing due to liquid expansion with increasing temperature.

Natural convection currents transfer internal energy stored in fluid elements in the same manner as forced convection currents. However the intensity of mixing is generally less in natural convection and consequently the heat transfer co-efficients in natural convection are lower than those in forced convection. The analysis of heat transfer by convection is complicated by the fact that the motion of the fluid plays an important role in heat transfer. The temperature distribution in natural convection depends on the intensity of the fluid currents which is really depended on the temperature potential itself. So the qualitative and quantitative analysis of natural convection heat transfer are quite difficult. For this reason the theoretical analysis of natural convection heat transfer for most of the practical situations is absent in the literature. So , at this present stage the necessity of the experimental investigation is seriously felt.

1.2 Natural convection in an enclosure :

A large number of engineering applications frequently involve heat transfer between surfaces that are at different temperatures and are separated by an enclosed fluid. These applications span such diverse fields as solar energy collections, nuclear reactor operation and safety, the energy efficient design of buildings, rooms and machinery, waste disposal and fire prevention and safety, also cooling of microelectric components. The surfaces may be plan horizontal or vertical or inclined.

Recently the heat transfer characteristics for non plan (sinusoidal, rectangular & trapezoidal, square corrugated) horizontal as well as inclined fluid layers have been reported. The main feature of these types of natural convection heat transfer problems is that the boundary layer thickness, if there be any , is comparable with the dimensions of the enclosed fluid layers.

1.2.a Horizontal fluid layers

In fluids whose density decreases with the increasing of temperature, no natural convection currents occur in such a fluid which is enclosed between two parallel horizontal plates as long as

the temperature of the upper plate is higher than the temperature of the lower one. In that case heat will be transferred only by the conduction. The situation is different when a fluid is enclosed between two horizontal surfaces of which the upper surface is at lower temperature than the lower one. For fluids whose density decreases with increasing temperature leads to an unstable situation. Benard (1900) mentioned this instability as a "top heavy" situation. In that case fluid is completely stationary and heat is transferred across the layer by the conduction mechanism only. Rayleigh (1916) recognized that the unstable situation must break down at a certain value of Rayleigh number above which a convective motion must be generated. Jeffrey's (1928) and Low (1929) calculated this limiting value of Ra_L to be 1708, when the air layer is bounded on both sides by solid walls. With the optical investigation in a trough filled with water carried out by Schmidt and Saunders (1938) this limiting value [Ra_L = 1708] also has been confirmed. Above the critical value of Ra_L a peculiar natural convection flow pattern arises. The flow field becomes a cellular structure with more or less regular hexagonal cells. In the interior of these cells the flow moves in an upward direction and along the rim of the cells it returns down. According to Ostrach (1957) when the top and the bottom surfaces are rigid, the turbulence first appears at Ra_L = 4380 and the flow becomes fully turbulent at Ra_L = 4500 for plane horizontal air layers but at lower values of Ra_L for water with same boundaries.

1.2.b   Inclined fluid layers :

The convective motion of an inclined fluid layer heated from below is more or less similar to horizontal fluid layer . Purely convective motion is gained after decaying of tow distinct flow regimes : (i.) Conductive regime and (ii) Postconductive regime . At very small Rayleigh number the motion is relatively simple . It consists of one large cell which fills the whole slot , the fluid rising from the hot wall , falling down the cold wall and turning at the opposite ends of the slot . This flow pattern is known as base flow according to Ayyaswamy (1973). The heat transfer in this flow regime is purely conductive [i.e. , Nu= 1] except at the extreme ends where there is some convective heat transfer associated with the fluid turning . For air this conductive regime exits if the Rayleigh number is less than a critical value Ra_C. This limit has been defined by Buchberg et al. (1976) as follows:

Nu   =   1   for $Ra_L < 1708/ Cos\theta$

i.e, $Ra_C = 1708/ Cos\theta$

At Ra_C , the base flow becomes marginally unstable and the resulting flow begins to take the form of steady longitudinal rolls i.e. , rolls with their axis along the up slope.

At $Ra_L >> Ra_C$, the flow becomes convective. The resulting flow begins to take the boundary layer structure with the resistance to heat transfer lying exclusively in two boundary layers, one on each of the boundary surfaces.

1.3 Motivation behind the selection of present work :

Most works have addressed natural convection in rectangular geometries in horizontal or vertically imposed heat flux of temperature difference. Little work has been carried out in which

the conditions are neither horizontal nor vertical. Natural convective heat transfer across inclined fluid (air) layer heated from below is of importance in many engineering applications. It is of particular importance in flat-plate collectors where it can constitute the main mode of heat loss. Solar engineers are concerned about natural convection heat loss from the absorber plate of the flat plate solar collector to the adjacent flat glass covers. The efficiency of the collector among other things increase with the decreasing of heat loss through the cover plates. Generally the absorber plate is made flat. Several studies have proved the advantageous effect of vee corrugated absorber plate. Investigation carried out by Arnold et al. (1978), Buchberg et al. (1976), Hert et al. (1971), Hollands et al. (1976, 1975, 1973, 1965, 1963), Koschmieder et al. (1974), O'Toole et al.(1961) and Schluter et al.(1965) have already discussed the natural convection heat transfer across air layer bounded by two parallel flat plates at different angles of inclination, including $\theta = 0^0$, Chinnappa (1970) the natural convection heat transfer from a hot vee corrugated plate to a cold flat plate in horizontal position.

Feroz (1992) reported results on natural convection heat transfer from hot trapezoidal and rectangular corrugated plates to a cold flat plate for different aspect ratios and different angles of inclination including horizontal.

Kabir (1988) reported results on natural convection heat transfer from a hot sinusoidal corrugated plate to a cold flat plate for different aspect ratios and different angles of inclination including horizontal.

Saiful (1995) reported results on natural convection heat transfer from a hot square corrugated plate to a cold flat plate for different aspect ratios and different angles of inclination including horizontal.

Works are reported on natural convection heat transfer across air layer in an enclosure bounded by two flat plates, from a hot sinusoidal plate to a cold flat plate, from hot trapezoidal and rectangular corrugated plates to a cold flat plate , from hot square corrugated plates to a cold flat plate. But no work is reported on natural convection heat transfer from hot vee corrugated plates to a cold flat plate in different angle of inclination . In previous works no report has focused attention on the variation of natural convection with the variation of amplitude of corrugation (amplitude H =10mm,15mm,25mm). Hence through the present investigation an effort has been made to fill up the existing gap in the information on natural convection heat transfer.

1.4 The present study :

Previously no work has reported the variation of natural convection with the variation of amplitude of corrugation. So , the present study is an experimental investigation on the natural convection heat transfer rate from hot vee corrugated plates to a cold plate with air as the working fluid. The geometry and dimensions of the corrugated plates tested are reported in figure 3.1 from the sketch of the inclined air layer bounded by vee corrugated plate and flat plate.

Main Objective (s) of the present work were :

a. To design an experimental set-up for studying the natural convection heat transfer from vee-corrugation.

3

b. To determine the average natural convective heat transfer co-efficient [h].

c. To determine the dependence of average natural convective heat transfer co-efficient [h] on aspect ratio [A].

d. To study the variation of average natural convective heat transfer co-efficient [h] with the angle of inclination [θ] of the v-corrugated plate with the horizontal.

e. To observe the variation of average natural convective heat transfer co-efficient [h] with different thermal potential [Δ T].

f. To observe the variation of average natural convective heat transfer co-efficient [h] with the variation of amplitude H of v-corrugation.

g. To compare the results of this study with earlier relevant investigations.

h. To develop possible correlation's which will correlate all the experimental data within reasonable limit.

Here to meet the above objectives, experimental set-up of Saiful (1995) was redesigned and modified for the present investigation. Supply of power to the experimental rig by electrical heater was varied by using a Variac with the variation of aspect ratio to keep a particular constant thermal potential (Δ T). The cooled flat plate was cooled by continuous water circulation. In the fabrication of hot plate assembly, vee corrugated plates of different depths (amplitudes H= 10mm, 15mm, 25mm) were fabricated from G.I. sheets.

The aspect ratio was varied between 1.40 and 9.50 by changing the mean plate spacing (L). The angle of inclination (θ) covered was between 0^0 and 75^0 and the range of temperature difference in the experiment was in between 10^0 C and 35^0 C .

The Rayleigh number covered in this study was :

$3.294 \times 10^4 \leq Ra_L \leq 1.881 \times 10^6$

Correlation in the form of $Nu_L = C [Ra_L Cos \theta]^n [A]^m$ was developed. The results obtained in the present study are compared with other studies related to the problem under investigation, in the form of plots and percentage variation.

4

CHAPTER 2

LITERATURE REVIEW

2.1 General :

Natural convection heat transfer through a layer of air bounded by two parallel plates heated from below is important in numerous engineering problems. Specially the natural convection heat loss across an inclined air layer is of interest to the designers of solar collectors, because any reduction of heat loss from the absorber plate through the cover plates improves the efficiency of the collector. A large number of engineering applications frequently involve heat transfer between surfaces that are at different temperatures and are separated by an enclosed fluid. These applications span such diverse fields as solar energy collectors, nuclear reactor operation and safety, the energy efficient design of buildings, rooms and machinery, waste disposal and fire prevention and safety, also on cooling of microelectric components. The surfaces may be plane horizontal or vertical or inclined.

Natural convection currents occur in a fluid enclosed between two parallel horizontal plates if the temperature of the lower plate is higher than that of the upper one. For fluids whose density decrease with the increasing temperature, an unstable state, named as "top heavy", is observed at a very small Rayleigh number. In this state, the fluid is completely stationary and heat is transferred across the fluid layer by a conduction mechanism. This unstable state breaks down at a certain critical value of Rayleigh number (which depends on the boundary conditoins).

At Ra_C, the unstable state becomes marginally unstable as any disturbance in the fluid will result in fluid motion with no dampening. This flow state is known as postconductive state. It is laminar and has nearly hexagonal cell structure. The flow moves upward in the interior of these cells and returns downward along its rim.

At $Ra_L \gg Ra_C$, the flow becomes convective with the breaking down of laminar flow into turbulent flow. The resulting flow begins to take the boundary layer structure in which the resistance to heat transfer lie exclusively in two boundary layers on the two boundary surfaces.

2.2 Natural convective heat transfer in plane horizontal fluid layers :

In most researches heat transfer in confined spaces have been carried out with the parallel plates in a horizontal position. A considerable number of experiments have been conducted on air, on water and on oil and the results have been reported by investigators.

An experimental investigation performed by Thomson (1882) on natural convection heat transfer through a layer of soapy water between horizontal plates heated from below. He noted the presence of cellular patterns in soapy water whose mean temperature was greater than the ambient. Benard (1900) also performed similar experimental investigation but his working fluid was paraffin oil and published photographs taken with a beam of parallel light which had passed through the layer of this paraffin oil. Those photographs clearly indicated the presence of hexagonal cellular convection patterns. Sterling and Scriven (1964) concluded that the cellular

convection patterns observed by Thomson and Benard were caused by surface tension rather than by thermal gradient.

Most elaborated experiment performed by Mull and Reiher (1930) on free convection heat transfer in horizontal air layer, who presented their experimental results by plotting K_e / K_C versus Gr_L and obtained a smooth curve in the range of $2.1 \times 10^3 < Gr_L < 8.89 \times 10^8$. They assumed K_e as an equivalent thermal conductivity considering the effect of conduction, convection and radiation i.e., $K_e = K_C + K_r$, where K_C is equivalent thermal conductivity taking into effects both conduction and convection, and K_r an equivalent thermal conductivity for radiation. Jakob (1946) plotted the data of Mull and Reiher in log-log coordinates and showed that there is at least one point of inflection in the curve and finally developed the following corelations :

$$Nu = 0.195 \,(Gr_L)^{1/4} \; ; \qquad \text{for } 10^4 < Gr_L < 4 \times 10^5$$

$$= 0.068 \,(Gr_L)^{1/3} \; ; \qquad \text{for } Gr_L < 4 \times 10^5$$

Hollands, et. al. (1974) carried out an experimental investigation on natural convection through an air layer between two parallel copper plates, heated from below. They performed their experiment by varying pressure from 10 Pa to 700 Kpa by inserting the plates in a pressure vassel. Actually the variation in Rr_L over a wide range without altering the plate spacing or the temperature difference between the plates was attained through the variation of pressure. Tests were carried out at mean plate spacings of 10mm, 25mm and 35mm covering the range of Rr_L from subcritical to 4×10^6. They reported that when their data along with the data of Chu and Goldstein (1969) for air were analyzed, the value of the index for Ra were the same as one-third (1/3) while Chu and Goldstein for their data found that :

$$Nu \; \alpha \; (Ra_L)^{0.294} \qquad \text{------------------ --------- (air)}$$

$$Nu \; \alpha \; (Ra_L)^{0.278} \qquad \text{------------------ --------- (water)}$$

Rossby (1969) also reported different power law for different prandlt number fluids as follows :

$$Nu \; \alpha \; (Ra_L)^{0.281} \; ; \quad \text{for sillicon oil (Pr } = 11600)$$
$$Nu \; \alpha \; (Ra_L)^{0.257} \; ; \quad \text{for mercury (Pr } = 0.025)$$

O' Toole and Silveston (1961) developed the correlation equations for natural convection heat transfer across horizontal fluid layers by taking all the data available in the literature at that time. On the basis of Ra_L they differentiated the flow into the following three regions :

Initial region : $1700 < Ra_L < 3500$
Laminar region : $3500 < Ra_L < 10^5$
Turbulent region : $10^5 < Ra_L < 10^9$

They also developed the following correlations :

$$Nu = 0.229 \,(Ra_L \cos\theta)^{0.22} \; ; \quad 5900 < Ra_L \cos\theta < 10^5$$

$Nu \quad \alpha \quad (Ra_L)^{0.305} \quad ; \quad$ for turbulent region

A number of investigators have also reported the 1/3 power law of dependency of Nusselt number on Rayleigh number. Mulkus (1963) and Globe et. al. (1959) also found the asymptotic behaviour of Nusselt number and obtained $Nu \; \alpha \; (Ra_L)^{1/3}$ .Through numerical solution of the governing differential equations Herring (1965, 1964) also predicted $Nu \; \alpha \; (Ra_L)^{1/3}$ by neglecting the non linear interaction terms.

2.3 Natural convection heat transfer in plane inclined fluid layer :

Natural convection in inclined layers of fluid heated from below and cooled from above has received extensive attention owing to its importance in engineering applications, including solar heating, nuclear reactor operation and safety, energy efficient design of buildings, machinery and cooling of microelectronic components.

Investigation was carried out by Graaf et. al. (1953). They performed measurements on heat transfer rate for the angles of inclination ranging from 0^0 to 90^0 in 10^0 steps and covered the range, $10^3 < Ra_L Cos\theta < 10^5$.

Dropkin et. al.(1965) performed an experimental investigation of natural convection heat transfer in liquids (water, silicon oils and mercury) confined in two parallel plates, inclined at various angles with respect to the horizontal. They carried out their experiments in rectangular and circular containers having copper plates and insulated walls and covered the range, $5 \times 10^4 < Ra_L < 7.17 \times 10^8$ and $0.02 < Pr < 11560$. They got the following correlations :
$$Nu = C (Ra_L)^{1/3} (Pr)^{0.074}$$

where the constant C is a function of the angle of inclination. It varies from C = 0.069 for the horizontal plates to C = 0.049 for vertical plates.

Ayyaswamy et. Al. (1974) carried out a theoretical investigation on natural convection heat transfer in an inclined rectangular region and their results were limited to $0^0 < \theta < 120^0$, $0.2 < A < 20$ and Ra upto 10^6 . But Ayyaswamy et. al. (1973) investigated the boundary layer domain and observed that :

$$Nu_{(\theta)} = Nu_{(\theta = 90^0)} (Sin \, \theta)^{1/4} ; \quad 0^0 < \theta < 110^0$$

Hollands et. al. (1975) performed an experimental investigation on free convection heat transfer rates through inclined air layers of high aspect ratio (A), heated from below. The covered range of Rayleigh number was from subcritical to 10^5 and angle of inclination was $0^0 \le \theta \le 70^0$. They gave the following correlations :

$$Nu = 1 + 1.44 (1 - 1708/ Ra_L Cos\theta)^* + [1 - (Sin 1.8\theta)^{1.6} \times 1708/ Ra_L Cos\theta] + [(Ra_L Cos\theta)^{1/3} / (5830)^{1/3} - 1]^*$$

[* denotes that when the arguments inside the bracketed terms become negative, the value of bracketed terms must be taken as zero].

7

Computation of natural convection heat transfer characteristics of flat plate enclosures, using interferometric techniques, was carried out by Randall et. al. (1977) . The effects of Grashof number, tilt angle and aspect ratio on both the local and average heat transfer coefficient were determined. The Grashof number range tested was 4×10^3 to 3.1×10^5 and the aspect ratio, defined as the ratio of enclosure length to plate spacing, varied between 9 and 36. The angles of inclination of the enclosure were 45^0, 60^0, 75^0 and 90^0. they reported that the average heat transfer rate at an angle of inclination of 90^0 decreased by 18% from that at 45^0 and developed the following correlation :

$$Nu_L = 0.118 \, [\, Gr_L \, Pr \cos^2 (\theta\text{-}45 \,) \,]^{0.29}$$

2.4 Natural convection heat transfer in Vee corrugated enclosures :

Experimental investigations on natural convection heat transfer from a horizontal lower vee corrugated plate to an upper cold flat plate for Rayleigh number from 7×10^3 to 7×10^5 were first carried out by Chinnappa (1970). The vee angle was 60^0 and aspect ratios were 0.64, 0.931, 0.968, 1.1875 and 1.218. Experimental fluid was air in all the test runs. The following correlations were obtained :

$$Nu_L = 0.54 \, [\, Gr_L \,]^{0.36} \; ; \qquad 7 \times 10^3 < Ra_L < 5.6 \times 10^4$$

$$Nu_L = 0.139 \, [\, Gr_L \,]^{0.278} \; ; \qquad 5.6 \times 10^4 < Ra_L < 7 \times 10^5$$

2.5 Natural convection heat transfer in sinusoidal corrugated enclosures :

The experimental investigation on the natural convection heat transfer from a lower horizontal sinusoidal corrugated plate to an upper cold flat plate for a range of Rayleigh number 5.50×10^3 to 2.34×10^6 and angle of inclination (θ), from 0^0 to 75^0 was carried out by Kabir (1988). The sinusoidal leading angle was 72^0 and aspect ratios covered were 2.0 to 5.75. experimental fluid was air in all the test runs. Finally the following correlation was obtained.

$$Nu_L = 0.0132 \, (Ra_L \cos\theta)^{0.51} \, (\, A \,)^{-0.35}$$

The above equation correlates all the experimental data within ± 10% and is valid for

$$5.56 \times 10^3 \leq Ra_L \leq 2.3 \times 10^6, \quad 2.0 \leq A \leq 5.75 \quad \text{and} \quad 0^0 \leq \theta \leq 75^0$$

2.6 Natural convection heat transfer in rectangular and trapezoidal corrugated enclosures :

The experimental investigation on the natural convection heat transfer from a lower horizontal rectangular and trapezoidal corrugated plates to an upper cold flat plate for a range of Rayleigh number $9.84 \times 10^4 \leq Ra_L \leq 2.29 \times 10^6$ and angle of inclination (θ) from 0^0 to 75^0 was carried by Feroz (1992). The aspect ratios covered was $2.6 \leq A \leq 5.22$. Experimental fluid was air in all test runs. Finally the following correlations were developed.

$$Nu_L = 0.0112 \, (Ra_L \cos\theta)^{0.521} \, (\, A \,)^{-0.4546} \; \text{----------------------------- (Trapezoidal Corrugation)}$$

$$Nu_L = 0.0102 \, (Ra_L \cos\theta)^{0.530} \, (A)^{-0.4923} \quad \text{------------------------- (Rectangular Corrugation)}$$

Both of these correlations correlate data to $\pm 15\%$.

2.7 Natural convection heat transfer in square corrugated enclosures :

This experimental investigation deals with the steady state natural convection heat transfer through air at atmospheric pressure from hot square corrugated plates to a cold flat plate placed above and parallel to it, where the surroundings were maintained at constant temperature was carried by Saiful (1995). Different amplitudes of corrugation i.e., H = 10mm, 15mm, 25mm were used. The effects of angle of inclination, aspect ratio, temperature difference and Rayleigh number on average convective heat transfer co-efficients were studied which covers the ranges of :

$$0^0 \leq \theta \leq 75^0, \; 1.4 \leq A \leq 9.5, \; 10^0 C \leq \Delta T \leq 35^0 C, \; 3.294 \times 10^4 \leq Ra_L \leq 1.881 \times 10^6$$

The following correlation for square corrugation was developed which correlates almost all the data within $\pm 20\%$.

$$Nu_L = 0.295 \, [Ra_L \cos\theta]^{0.265} \cdot [A]^{-0.442}$$

2.8 Table-A : Review Works on Different Types of Corrugated Enclosures.

Type of Corrugated Enclosures	Correlation's	Author
Vee corrugated enclosures	$Nu_L = 0.54 \, [Gr_L]^{0.36}$ $Nu_L = 0.139 \, [Gr_L]^{0.278}$	Chinnappa (1970)
Sinusoidal corrugated enclosures	$Nu_L = 0.0132 \, (Ra_L \cos\theta)^{0.51} \, (A)^{-0.35}$	Kabir (1988)
Trapezoidal corrugated enclosures	$Nu_L = 0.0112 \, (Ra_L \cos\theta)^{0.521} \, (A)^{-0.4546}$	Feroz (1992)
Rectangular corrugated enclosures	$Nu_L = 0.0102 \, (Ra_L \cos\theta)^{0.530} \, (A)^{-0.4923}$	Feroz (1992)
Square corrugated enclosures	$Nu_L = 0.295 [Ra_L \cos\theta]^{0.265} \cdot [A]^{-0.442}$	Saiful (1995)

9

CHAPTER 3

THEORY

3.1 General description :

The movement of the fluid in free convection , whether it is a gas or liquid , results from the buoyancy forces imposed on the fluid when its density in the proximity of the heat-transfer surface is decreased as a result of the heating process. The buoyancy forces would not be present if the fluid were not acted upon by some external force field such as gravity , although gravity is not the only type of force field which can produce the free-convection currents; a fluid enclosed in a rotating machine is acted upon by a centrifugal force field, and thus could experience free-convection currents if one or more of the surfaces in contact with the fluid were heated. The buoyancy forces which give rise to the free-convection currents are called body forces.

In order to get clear concept of above analogy and to measure we should discuss some dimensionless groups. These groups are named according to the name of scientist who gradually improved the Ranould's analogy.

a. **Prandtl Number (Pr)** : It represents one of the most significant heat transfer parameter being a measure of relative magnitude of momentum and thermal diffusion in the fluid.
$Pr = [C_p \mu / k]$ Where, C_p = Specific heat at constant pressure, usually kJ /kg K,
μ = Dynamic viscosity, k = Thermal conductivity, usually W/m K

b. **Reynold's Number(Re)** : This is the ratio of inertia force to viscous force.
$Re = [\rho u x]/ \mu$; Where , ρ = density, usually kg/ m^3 , u = free stream velocity ,
x = distance from leading edge , μ = Dynamic viscosity

c. **Nusselt Number (Nu)** : It is the most important number to get heat transfer co-efficient is the ratio of the temperature gradient in the fluid immediately in contact with the surface to the reference temperature.
It is given by $Nu = [hx]/ k$; Where , h = Heat transfer co-efficient, usually W/ m^2 K,
x = distance from leading edge, k = Thermal conductivity, usually W/m K

d. **Grashof Number (Gr):** It is the results from the inclusion of buoyancy forces in the equation of motion and would be absent in case where buoyancy is absent. This group is written as :
$$Gr = [g\beta (T_w - T_\infty)x^3] / v^2$$
Where, g = Acceleration of gravity , β = Volume co-efficient of expansion = 1/T, 1/K ,
T_w, T_∞ = Temperature at wall & infinity, x = distance from leading edge , v = Kinematic viscosity

It has a role similar to that played by the Reynolds number in Forced convection systems and is the primary variable used as a criterion for transition from laminar to turbulent boundary layer flow.

e. **Eckert Number (Ec):** It arises from the term representing the rate of dissipation of energy in the energy equation. $Ec = u_\infty^2 / [C_p (T_\infty - T_w)]$

f. **Rayleigh number (Ra)** : It is the product of Grashof and Prandtl numbers.

$$Ra = Gr \ Pr$$

If the average heat transfer coefficient is evaluated by integration over the body surface , the spatial variable are neglected the average Nusselt number is related in the following way :

$$N_{Nu} = f (n \, N_{Re} , N_{Gr} , N_{Ec} , N_{Pr})$$

In forced convection on neglects the effect of buoyancy forces So that ,

$$N_{Nu} = f (n \, N_{Re} , N_{Ec} , N_{Pr})$$

If the viscous dissipation is neglected. So that, $\mathbf{N_{Nu} = f (n \, N_{Re} , N_{Pr})}$

In natural convection system the average Nusselt number is related in the following way :

$$N_{Nu} = f (n \, N_{Re} , N_{Gr} , N_{Ec} , N_{Pr})$$

If the viscous dissipation is neglected. So that, $\mathbf{N_{Nu} = f (n \, N_{Re} , N_{Gr} , N_{Pr})}$

The new dimensionless variable , the Grashof number, which is important in all free-convection problems. But as in some forced-convection problems, experimental measurements must be relied upon to obtain relations for heat transfer in other circumstances. These circumstances are usually those in which it is difficult to predict temperature and velocity profiles analytically. Turbulent free convection is an important example , just as is turbulent forced convection, of a problem area in which experimental data are necessary; however the problem is more acute with free-convection flow systems than with forced-convection systems because the velocities are usually so small that they are very difficult to measure. Because of small velocities in free-convection system, the significance of Renoulds number (Re) is neglected.

So in natural convection system the average Nusselt number is :

$$N_{Nu} = f (n \, N_{Gr} , N_{Pr})$$

In the present experiment the investigation was carried out with only one confined convective fluid (air). So Prandlt number (Pr) was assumed as constant property in above equation. When the value of Prandlt number is 1, then the velocity and thermal distribution is equal. Therefore the Nusselt number (Nu), in natural-convection system, which measures the thermal convective property of the fluid mainly depends on Grashof number (Gr) i.e. Rayleigh number (Ra_L) . So the final form of Nusselt number becomes :

$$N_{Nu} = f (n \, N_{Gr}) = f (n \, N_{RaL})$$

Rayleigh number has been considered in this investigation in the range of,
$3.294 \times 10^4 \leq Ra_L \leq 1.881 \times 10^6$

The corrections for the radiant and back losses becomes relatively large at low Rayleigh number, and there is usually a large uncertainty in both these corrections. In the present measurements, every effort was made to minimize the radiant and back losses.

3.2 Description of the problem :

Natural convection heat transfer in an inclined rectangular enclosure is a function of temperature difference between the hot and cold plates, boundary conditions, angle of inclination of the enclosure with the horizontal and the properties of geometry of confined convective fluid . Also the natural convection heat transfer is a function of geometry of the hot plate , which is the basis for sketching the present problem of variation of natural convection from hot vee corrugated plate to a cold flat plate.

The present investigation in rectangular region was carried out with three sets of bottom hot vee corrugated plates having amplitude of 10mm,15mm and 25mm. In all cases the upper cold plate was flat. The convective fluid was air The side walls of the enclosure were made adiabatic and flat .

In the present experimental setup the spacing between the hot and cold plate was varied to get different aspect ratio 'A' defined as the ratio of mean plate spacing to amplitude of corrugation. The vertical side walls of the enclosure and the bottom hot corrugated plates were maintained at the same temperature. Also the upper wall of the lower guard heater assembly was maintained at the same temperature same as that of lower hot corrugated plate. At steady state the heat flux [q″] to the cold flat plate was by conduction, convection and radiation. But for Rayleigh number well above the critical value, conduction heat transfer was considered insignificant. So total heat flux, q″ had two components. Convection heat flux, $q_{CONV}″$ and radiation heat flux $q_r″$. In case of a fixed temperature potential (ΔT) the radiative heat flux becomes constant and the convective heat transfer varies on aspect ratio 'A' and angle of inclination of the enclosure.

The radiative heat flux, $q_r″$ was calculated by using the formula drived in Appendix-A by considering hot corrugated plate and cold flat plate behaved as black bodies. The convective heat flux $q_{CONV}″$ was calculated by subtracting the value of $q_r″$ from the total heat flux, q″ . Heat flux from the hot corrugated plate was calculated by measuring the current and the voltage supply of the main heater. In this chapter article 3.3 describes the mathematical equations required for calculating $q_r″$, $q_{CONV}″$ and natural convective heat transfer co-efficient (h).

3.3 Mathematical Equations :

The mathematical equations that were used to calculate h, Nu_L and Ra_L are given below :

$q_r″ = σ. ε_{COR} . [(T_{COR})^4 - (T_{COLD})^4]$ --[3.1]

$q″ = VI \cos φ / A_{COR}$ --[3.2]

$h = [q″ - q_r″] / [T_{COR} - T_{COLD}]$ --[3.3]

$Nu_L = h. L /K$ --[3.4]

$Ra_L = g. β [T_{COR} - T_{COLD}] . L^3 / v.α$ --[3.5]

All properties of the air were evaluated at film temperature , T_f

where, $T_f = [T_{COR} + T_{COLD}] /2$

CHAPTER 4

EXPERIMENTAL SET-UP
AND
TEST PROCEDURE

4.1. General Description of the Set-up :

The existing experimental set-up made by Saiful [1992] was redesigned to meet the requirements of the present experiment. The details of the experimental set up and test section is shown in Figures 4.1 and 4.2. There is a provision for the experimental set up to incline by an alignment plate in the range. 0^0 to 90^0 at a step of 15^0. The air gap depth was varied by changing the position of the cold plate in relation to the hot plate from 35mm to 95mm. Experimental hot plate assembly was heated by the main electric heater sandwiched in between the hot corrugated plates by supplying a constant voltage from the voltage stabilizer. The guard heater assemblies were also heated by electric heaters sandwiched in between the inner and outer wooden strips. The cold flat plate was placed above the corrugated assembly by four vertical clamps, fixed on the upper guard heater. This cold plate assembly was cooled by passing a steady flow of cooling water from the overhead tank, where the head of over head tank was kept constant. A digital milli-voltmeter was used to measure the temperature of the test section of the hot plate and cold plate through thermocouples no. 1 to 9 and 37 to 41 respectively. It was also used to monitor the surface temperatures of the guard heater assemblies through 27 chromel-Alumel thermocouples. To obtain the total heat input to the experimental test section of the hot plate, the input current to the corresponding heater [main heater] was measured by a digital ammeter and the voltage across the main heater was by a precision digital voltmeter.

4.2 The Test Section :

The test section consisted of

    a. The hot plate assembly.
    b. The outer guard heater assembly.
    c. The cold plate assembly.
    d. The alignment plate and supporting frame.

4.2.1 The hot plate assembly :

The main section of the hot plate assembly is the test section. The hot plate assembly was made of G.I. sheets having three different amplitudes of vee corrugation i. e, 10mm, 15mm, 25mm with total dimension of 456mm X 534mm . An asbestos cloth of 12mm thick was placed on the upper side of the lower corrugated plate to insulate it electrically from the electrical heaters placed on this asbestos cloth (Fig. 4.3). Another asbestos cloth was placed over the heaters to make the upper corrugated plates of the assembly well insulated from the sandwiched electrical heaters. There were three heaters on the hot plate assembly. One was used to heat the experimental test section and the other two heaters were used as end and side guard around the test section. These guard heaters were provided to reduce the end conduction losses from the

13

experimental hot plate to a minimum level. For this purpose these guard heater sections were separated from the experimental hot plate section by cutting the top corrugated plate into five pieces forming separate guard heater sections and the central experimental test section. The test section was 152mm X 230mm ; 152mm across the corrugation and 230mm along the corrugation.

The end and side guard heater sections were 152mm wide on all the sides of the experimental hot plate section. Thus the over all dimensions of the hot plate assembly was 456mm X 534mm. This hot plate assembly was placed inside a rectangular ring of 483 mm X 560 mm. The rectangular ring was made of 76mm wide and 19.05mm thick wooden strip. Details of the hot plate assembly have been shown in figure 4.3 and details of design and fabrication process of the heaters are given in the Appendix - A.

The outer surfaces of both the test section, end and side guard heater section were painted black with dull black plastic paint. The test section was separated from both the end and side guard section by asbestos powder to reduce conduction loss.

4.2.2   The Outer Guard Heater Assembly :

The main feature of the outer guard heater assembly is to isolate the test hot plate section thermally from the surrounding surface except from the top. This assembly mainly consisted of upper guard heater ring and lower guard heater box. The heat input was varied by using Variacs 4 , 5 and 6 to maintain the temperature difference between the test hot plate and its surrounding surfaces to zero. Under this condition all the heat input to the experimental hot plate section would be transferred by conduction , convection and radiation only to the cold flat plate which was placed above the hot plate.

4.2.2a.   The Upper Outer Guard Heater Ring :

The upper outer guard heater ring was a rectangular shaped structure which consisted of the following section :

      a.   Inner wooden rectangular ring
      b.   Inner asbestos rectangular ring
      c.   Outer asbestos rectangular ring
      d.   Outer wooden rectangular ring

The inner wooden rectangular ring in which the test section was placed having a dimension of 483mm X 564mm. The inner and outer wooden rings were held together with a 579mm X 660mm outside dimension. 12mm thick and 48mm wide wooden annular rings at the top of the upper guard heater assembly. The height of the upper guard heater assembly was 139mm. The inner and outer asbestos rectangular rings were fitted inside the annular space between the outer and inner rectangular wooden rings. The outer asbestos ring 127mm wide was fitted inside the outer wooden rings . The heater was made by wrapping 29 SWG Nichrome wire on the mica sheet sandwiched in between the inner and outer asbestos ring. The capacity of the heater was 105 Watt. A cross section of the upper outer guard heater assembly is shown in figure 4.4. Both the outside and inside surfaces of the upper guard heater ring was painted with dull black plastic aint.

14

4.2.2b. The Lower Outer Guard Heater Ring :

The lower outer guard heater ring was a rectangular shaped structure which consisted of the following section :

    a.   Inner wooden rectangular box
    b.   Inner asbestos rectangular box
    c.   Outer asbestos rectangular box
    d.   Outer wooden rectangular box

The wooden rectangular box over which the hot plate assembly was placed was of 483mm X 564mm X 16mm in inside dimension. The outer wooden box having outside dimension of 579mm X 660mm X 76mm was made of 12mm thick wooden strip. The outside dimension of the inner wooden box was 507mm X 588mm X 40mm. The outer asbestos box having dimension of 555mm X 636mm X 64mm was fitted the inner surface of the outer wooden rectangular box and the inner asbestos box having dimension of 531mm X 612mm X 52mm was fitted over the outer surface of the inner wooden box i.e. over the inner surface of the outer asbestos box. Two separate Nichrome heaters were sandwiched in between the inner and the outer asbestos rings, one was lower bottom guard heater and the other was lower side guard heater. A cross section of the lower outer guard heater assembly is shown in figure 4.5. The outer surfaces of the outer wooden rectangular box was painted black with dull black plastic paint.

4.2.3   The Cold Plate Assembly :

The cold plate assembly was a sealed 550mm X 470mm X 19.05mm rectangular box made of 3.175 thick mild steel plates painted with dull black plastic paint. Provision of water circulation was made from a reserve tank through inlet and outlet connections. The outlet and inlet connections were placed on the upper surface of this box. The flat bottom surface of this assembly , facing the corrugated plate was acting as a receiver of heat that was convected and radiated from the hot corrugated plate. The whole cold plate assembly was placed above the hot corrugated plate and held by the vertical clamps , fixed on the upper outer guard heater assembly. These clamps had arrangements to change the spacing between the hot corrugated plate and the cold flat plate from 19.5mm to 109.5mm in steps of 10mm. The cold plate assembly is shown in figure 4.6.

4.2.4   The Alignment Plate and Supporting Frame :

The hot and cold plate assembly along with the guard heaters were placed inside of a rectangular frame made of 38.1mm X 38.1mm X 6.35mm mild steel angle on the two side supports of this frame , each of them is attached with the plate assembly by means of two bolts. Another two bolts were fixed at the center of the two opposite longitudinal sides of the frame and passed through the holes of the side supports so that the frame and the plate assembly with the guard heaters could swivel about a horizontal axis i.e. the lateral axis of the hot plate through these bolts. The rectangular frame is shown in figure 4.7.

Two circular disc of mild steel having diameter of 102mm and thickness of 6.35mm namely as alignment plates were connected at the center of the two opposite lateral sides of the rectangular frame by means of two screws passed through 6.5mm diameter holes located on each disc at

40mm apart and the holes of the two 57mm X 57mm hanging side supports made of 6.35mm thick mild steel sheet that were welded with the supporting frame at its center. These discs had also several holes of diameter 6.5mm along a circle of radius 38mm. The angle of inclination of the test section was varied by means of these holes by changing the inclination angle from 0^0 to 90^0 in steps of 15^0. One of the alignment plate is shown in figure 4.8.

A supporting stand consisting of two pairs of legs 915mm apart connected by a flat mild steel bar. The height of this stand was 460mm. The rectangular frame along with the two alignment plates was connected with this stand at the top center of its legs by means of two bolts passed through the 16mm diameter central holes of the alignment plates and the two holes located at the center of the two lateral sides of the frame so that the frame and the plate assembly with the guard heaters could also swivel about a horizontal axis i.e. the longitudinal axis of the hot plate. The connection between the rectangular frame and the supporting stand is shown in figure 4.9.

The angle of inclination of the test section of the hot corrugated plate could set at a desired value by means of two screws passed through the corresponding peripheral holes of diameter 6.5mm of the alignment plates as mentioned above and the two holes 76mm apart located at the top of the two legs of the supporting stand. The supporting stand is shown in figure 4.10.

4.3 The Reserved Water Tank :

The reserve water tank was an overhead tank - a simple cylindrical drum made of galvanized iron sheet. The water level in the tank was kept constant during experiments by controlling the water flow using the inlet and outlet valves of this tank . The cold plate assembly was cooled by passing a steady flow of cooling water from this tank through rubber pipes of 12.5mm diameter.

4.4 Instrumentation :

There were provisions for measuring angle of inclination, air gap between the hot and the cold plates and the temperature at different points of the experimental set-up in the present investigation. There were five variacs and one stabilizer to supply regulated voltage at different sections of the experimental set-up. Each variac had graduated scale on it to measure the voltage supplied to the heaters. Also the voltage supplied and current by the stabilizer to the test section was measured by a precision Normameter MP-14 . Again the details of the instrumentation and measurement procedure is depicted in detail later on.

4.5. Temperature measurement :

The accuracy of the value of natural convection was dependent on the accuracy of the measurement of temperature and input power (voltage and current value). For this reason , precision instruments were used. Temperature at different sections of the experimental set-up were measured by Fortyone 36 SWG Chromel-Alumel thermocouples connected to a millivoltmeter of MP- 12 having a range of 50^0 C to 75^0 C [for K type] to show the temperature directly through two selector switches each having 24 points. Out of these , nine thermocouples of number 1 to 9 , were fixed on the bottom surface of the test section of the hot corrugated plate and five thermocouples of number 37 to 41 , were fixed on the bottom surface of the cold plate facing the corrugated plate and the rest were fixed on the guard heater sections. The position of the thermocouples are shown in figures 5.1 to 5.5 . These thermocouples were calibrated in

between 0^0C (melting ice temperature) and 100^0 C (saturated steam temperature).There was a maximum variation of 0.10 % between the actual and standard reading within the working range of the experiment . The calibration curve for thermocouple number 5 is shown in figure 5.6.

For greater accuracy the temperature of the exposed top surface of the experimental hot corrugated plate [T_{COR}] was determined after necessary conduction correction . Appendix B contains the outline of the procedure for calculating the conduction correction.

4.6. Heat Flux Measurement :

Amount of heat supplied per unit area of the test section through heater was the heat flux. Heat flux from the hot corrugated plate was calculated by measuring the current and voltage to the main heater.

A digital voltmeter of Model Normameter MP-14 was employed to measure the voltage across the stabilizer which supplied the necessary heat to the test section of the hot plate assembly. The voltmeter had the range of 0-750 volts.

A digital ammeter of Model Normameter MP-14 was employed to measure the current supplied to the test section of the hot plate. This ammeter had the range of 0 to 10 amps.

4.7. Test Procedure :

Three sets of vee corrugation having different amplitudes (H = 10mm , 15mm , 25mm) of vee corrugation were used. For all sets temperature difference [Δ T] , angles of inclination of the air layer [θ] and the air gaps [L] were measured. The experimental fluid was air at atmospheric pressure. Experiments were carried out under steady state condition. The experiment was carried out first using corrugation having H = 10mm , then on H = 15mm, and then on H = 25mm. The test was carried out according to the following procedures :

a. Before starting the experiment the room temperature was recorded for selecting T_{COR} to maintain a steady Δ T [say, $\Delta T = T_{COR} - T_{COLD} = 10^0$ C] since $T_{COLD} = T_{ROOM}$.

b. The spacing between the hot corrugated plate and the cold flat plate was measured as the distance between the bottom surface of the cold plate and the mid section of the troughs and crest of the corrugated plate (FIG. 4.2). The spacing L i.e. air gap of L = 35mm was kept by fixing the cold plate to the appropriate holes of the clamps fixed on the upper outer guard heater assembly.

c. Then the rig was aligned to horizontal position for angle of inclination θ = 0^0

d. Then all the heater circuits were switched on and at the same time , the water line of the cold flat plate and the reserve tank were opened.

e. To maintain the temperatures of thermocouples 1 to 36 at T_{COR} the voltages of test section and guard heater section were varied by stabilizer and variacs. The cold plate

was also maintained at the room temperature by controlling the water flow through it to maintain ΔT constant during a particular test run.

f. When steady state was reached i.e. $T_{COR} - T_{COLD} = 10^0$ readings of temperatures of thermocouples No. 1 to 9 and 37 to 41 were recorded. At the same time readings of ammeter and voltmeter connected to the test section of the hot plate was also noted, to obtain the heat input.

g. The procedures of steps (e) and (f) were repeated for inclination angles $\theta = 30^0$, 45^0, and 75^0 keeping air gap , L = 35mm constant throughout.

h. Then by changing the air gap , [L] to the other values of 55mm , 75mm , and 95mm operations from step [c] to step [g] were repeated.

i. Then for other values of ΔT i.e. for 26^0 C and 35^0 C all the operations described in steps [b] to [h] were repeated. Thus one full set of readings were completed .

For one full set of data , i.e. for H = 10mm forty eight (48) sets of readings were recorded. Similarly for H = 15mm and 25mm the procedures (a) to (i.) were repeated respectively. Thus total of 144 sets of readings were obtained. The ranges of parameters for different corrugation were as follows.

For H = 10mm

Rayleigh number	$Ra_L = 3.294 \times 10^4$ to 1.8814×10^6
Heat flux	$q'' = 59$ to 286 W/m^2
Temperature difference between hot and cold plate	$\Delta T = 10^0$ C to 35^0 C

Temperature of the hot plate,	$T_{COR} = 36^0$ C to 64^0 C
Inclination angle,	$\theta = 0^0$ to 75^0
Air gap	L = 35 mm to 95 mm

For H = 15mm

Rayleigh number	$Ra_L = 3.294 \times 10^4$ to 1.8814×10^6
Heat flux	$q'' = 60$ to 289 W/m^2
Temperature difference between hot and cold plate	$\Delta T = 10^0$ C to 35^0 C

Temperature of the hot plate,	$T_{COR} = 36^0$ C to 64^0 C
Inclination angle,	$\theta = 0^0$ to 75^0
Air gap	L = 35 mm to 95 mm

For H = 25mm

Rayleigh number	$Ra_L = 3.294 \times 10^4$ to 1.8814×10^6
Heat flux	$q'' = 62$ to 295 W/m^2
Temperature difference between hot and cold plate	$\Delta T = 10^0$ C to 35^0 C

Temperature of the hot plate, $T_{COR} = 36^0$ C to 64^0 C

Inclination angle, $\theta = 0^0$ to 75^0

Air gap $L = 35$ mm to 95 mm

4.8. Reduction of Data

Convective heat transfer co-efficient was calculated from convective heat flux. The heat flux, q" obtained from readings of voltmeter and ammeter was the combination of convective and radiative heat flux. So in calculating convective heat flux , the radiative heat flux was deducted from this measured heat flux. To find out the radiative heat Stefan-Boltzman equation for gray surface [equation 3.1] was used. The outline for obtaining the emissivity of the test section of the hot corrugated plate has been given in appendix-C , and the emissivity for the vee corrugated plates having opening angle of 60^0 has been considered to be 0.975

CHAPTER 5

RESULTS AND DISCUSSION

This experimental investigation deals with the steady state natural convection heat transfer from hot vee corrugated plates through air to a cold flat plate placed above and parallel to the hot corrugated plate. The assembly being inclined at various angles with respect to horizontal was carried out in a finite rectangular enclosure having adiabatic surroundings. Three types of corrugation having amplitudes, H = 10mm, 15mm, 25mm were used. Experiments covered a range of Rayleigh number from 3.2940 X 10^4 to 1.8814 X 10^6 and angle of inclination from 0^0 to 75^0. The temperature difference (ΔT) between the hot and cold plates kept constant at 10^0 C, 26^0 C, and 35^0 C.

The temperature distribution over the experimental hot corrugated plate and cold plate for different aspect ratios (A or L/H) and different inclination angles (θ) was found to be isothermal. The temperature distribution for a typical illustration for hot and cold plate is shown in figures 6.1 to 6.3 and figures 6.4 to 6.6 respectively.

The effect of aspect ratio (L/H) on heat transfer rate across rectangular regions for various angles of inclination (θ) and temperature difference (ΔT) for all types of corrugation, is shown in figures 6.7 to 6.10. Each figure is drawn for a particular θ with different values of ΔT and H. From graphs 6.7 to 6.10, it is observed that for both types of corrugation "h" increases with increasing of aspect ratio for a certain ΔT upto a certain limit and then decreases. But the limiting value of aspect ratio upto which, "h" increases are found to be different for different ΔT and for different corrugations. It is also observed from figures 6.7 to 6.10 that for same ΔT and θ , an increase in the amplitude of corrugation the value of 'h' increases upto a certain value of aspect ratio for each type of corrugation. But after that the values of aspect ratio, 'h' decreases with increasing in amplitude of corrugation and aspect ratios. The reason of such occurrence is that increasing of gap between the hot corrugated plate and the cold flat plate increases the aspect ratio and permits better mixing of the fluid leading to an enhancement of heat transfer rate. But this enhancement of heat transfer rate has got a certain limit and beyond this limit heat transfer coefficient are found to decrease with the increasing of aspect ratio. This is due to the fact that beyond these limiting values of 'A' the convective currents appear to be weak to reach the cold flat plate and transfer less heat after crossing a larger distance. As aspect ratio is the ratio of mean plate spacing to the amplitude of corrugation, so for same aspect ratio an increase in amplitude of corrugation the mean plate spacing increases. So the limiting value of aspect ratio was found to be different for different types of corrugations.

Figures 6.11 to 6.19 also show the variation of 'h' with aspect ratio (A), each of which was drawn for a particular value of ΔT and H. It is observed that for each value of aspect ratio with an increase in the value of inclination angle heat transfer coefficient decreases and it is maximum at 0^0. This is perhaps due to the fact that the Rayleigh number for breaking down of unstable situation in order to set convective motion within the fluid increases with the increasing of angle of inclination. Again the effect of fluid stagnation in the corrugation cavity at higher angle of

inclination may also not be ruled out as the fluid flow direction appears to be perpendicular to the corrugation channel.

Figures 6.20 to 6.22 shows that for $0^0 \leq \theta \leq 75^0$ and at constant ΔT, heat transfer coefficient increases with an increase of aspect ratio 'A' upto a certain value. But this limiting value of 'A' was found to be different for different amplitudes of corrugations. The limiting values of 'A' were -

for H = 10mm   A =   4 to 8
     H = 15mm   A = 2.35 to 5.0
     H = 25mm   A = 1.8 to 3.2

To show the effect of temperature potential on heat transfer rate for various angles of inclination (θ) and aspect ratio (A) for both types of corrugation, figures 6.23 to 6.26 were plotted which presents h vs ΔT for a particular 'L' with different values of θ. From these figures it is clear that average heat transfer coefficient increases more or less linearly with the increasing of temperature potential.

Figures 6.27 to 6.42 show the relationship between the Nusselt number and $Ra_L \cos\theta$ for different values of L and angle of inclination (θ). From these figures it is observed that for all types of corrugation, Nusselt number increases with increasing of Rayleigh number at a particular L and angle of inclination. This is due to the fact that at a constant L and angle of inclination, Rayleigh number increases with increasing of temperature potential (ΔT). Again increasing of Rayleigh number leading to the increase of Nu_L.

Results are presented in terms of Nusselt number and angle of inclination for a particular amplitude of corrugation (H) and at Rayleigh number $Ra_L = 0.4 \times 10^6$ in Fig. 6.43 as a typical illustration. From this it is observed that at a constant amplitude of corrugation and Rayleigh number, Nusselt number decreases with increasing angle of inclination. Nusselt number is also found to be maximum at $\theta = 0^0$ for all Rayleigh numbers. This is due to the fact that at a constant gap between the hot and the cold plates, the convective fluid particles in inclined position have to cross larger vertical distance in transferring heat energy than in horizontal.

Comparison :

Figures 6.7 to 6.22 show the variation of average heat transfer coefficient on aspect ratio for different ΔT and angle of inclination. The convective heat transfer coefficient for H = 25 mm is the highest and that for H = 10 mm is the lowest for same value of ΔT and θ. From Fig. 6.43 it is observed that, the value of Nusselt number is greater for H = 25 mm, than that for H = 15mm, and H = 10mm. That is an increase in amplitude 'H' shows higher heat transfer performance. This is due to the fact that better clearance between the adjacent ribs of corrugation may permit better clearance for inflow and outflow of convecting fluid.

Figures 6.44 and 6.45 shows the comparison of Nusselt number of the present study with the

Nusselt number of the works of Kabir (1988), Feroz (1992) and Saiful (1995). From Fig. 6.44 ,for lower Rayleigh number i.e. for $Ra_L = 0.4 \times 10^6$, when the values of Nusselt number for vee corrugation of H = 25mm are compared with those of above works, it is shown that Kabir's (Sinusoidal corrugated) are lower by 12%, Feroz's (Trapezoidal corrugated) are lower by 22%, Feroz's (Rectangular corrugated) are lower by 28% and Saiful's (Square corrugated) are lower by 40%. Here in Saiful's investigation on square corrugation it was experimentally found that at horizontal position of corrugated plates the maximum values of average natural convective heat transfer coefficients were to be 2.215 Watt/m^2 K for H = 25 mm , 2.143 Watt/m^2 K for H = 15 mm , and 2.059 Watt/m^2 K for H = 10 mm. But from this investigation the maximum values of average natural convective heat transfer coefficients were found to be 3.121 Watt/m^2 K for H = 25 mm, 3.027 Watt/m^2 K for H = 15 mm, and 2.962 Watt/m^2 K for H = 10 mm. All these values were obtained at horizontal position of the corrugated plates.

It is also observed from Fig. 6.45 that for higher Rayleigh number ($Ra_L = 1.0 \times 10^6$) this difference in value of Nusselt number of present study is higher than other related works mentioned earlier. This is happening due to the fact that the surface area for vee corrugation is less than Kabir's Sinusoidal corrugation, Feroz's Trapezoidal corrugation, Feroz's Rectangular corrugation and Saiful's Square corrugation. The surface area for vee corrugations of these experimental test sections are approximately 74% less than the those surface area of square corrugations.

The Nusselt number of this investigation for $Ra_L = 0.4 \times 10^6$ and at H = 25 mm was greater by 0.6% than the values of Chinnappa (1970), who was performed an experimental investigation across air layers bounded by a horizontal vee corrugated and flat plates, which can observed from figure 6.44. This is due to the fact that the absorptance of a vee corrugated surface for several plan long- wave emissivities varies with the projected angle of incidence . It was considered in this experiment that the value of the hemispherical emissivity of vee corrugated plate having opening angle of 60^0 was 97.5 . May be the experiment was carried out by Chinnappa with considering the emissivity of vee corrugated was different from 0.975. For that reason the convective heat transfer of this experiment might be higher than Chinnappa's investigations.

From present study it is also shown that the value of Nusselt number for H = 25mm is higher than that of H = 15mm by 8% and of H = 10mm by 15%.

Correlation :

In earlier studies of Kabir (1988), Feroz (1992) and Saiful (1995) correlations were formulated in the form of

$$Nu_L = C \, (Ra_L \cos \theta)^n \, (A)^m.$$

Kabir (1988) and Feroz (1992) determined the exponents 'n' and 'm' by plotting Nu_L vs ($Ra_L \cos\theta$) and $Nu_L / (Ra_L \cos \theta)^n$ vs A respectively. The value of constant 'C' was determined from the graphical representation of Nu_L vs ($Ra_L \cos \theta$)^n (A)^m.

This graphical method for determining the value of exponents and constant has some inherent errors because the measurement of slope was done manually from the curves. So the above method was not used in this study. The values of exponents and constant were determined by a computer programming which uses the least square method of curve fitting to fit all the data.

The values of 'C', 'n' and 'm' were found to be as follows

$C = 0.276$, $n = 0.294$, $m = 0.331$.

So all the experimental data for vee corrugation were correlated by the following equation to within $\pm 12\%$.

$Nu_L = 0.276 \, (Ra_L \cos \theta)^{0.294} \, (A)^{-0.331}$;

where, $3.294 \times 10^4 \leq Ra_L \leq 1.8814 \times 10^6$

$1.4 \leq A \leq 9.5$

$0^0 \leq \theta \leq 75^0$

This is shown graphically in Fig.6.46.

CHAPTER 6

CONCLUSIONS AND RECOMMENDATIONS

This chapter includes the conclusions that can be drawn from the experimental investigation of natural convection of hot vee corrugated plates to cold plates. The recommendations for which the present investigation can be extended are presented here.

6.1 Conclusions :

1.   In all the three sets of vee corrugation the natural convective heat transfer coefficient (h) was found to be dependent on temperature potential (ΔT), angle of inclination (θ) and aspect ratio (A).

2.   It was found that the average natural convective heat transfer coefficient increases with increasing of aspect ratio upto a certain limit and then has a tendency to decrease with further increasing of aspect ratio. This implies that for each set of corrugation there is a optimum value of aspect ratio for which the value of 'h' is maximum.

3.   The dependency of average natural convective heat transfer coefficient (h) on temperature potential (ΔT) is found to be more or less linear for all the three types of corrugation.

4.   In all these three sets of corrugation the convective heat transfer coefficient decreases with the increasing of angle of inclination.

5.   From this investigation the maximum values of average natural convective heat transfer coefficients were found to be 3.121 Watt/m^2 K for H = 25 mm, 3.027 Watt/m^2 K for H = 15 mm, and 2.962 Watt/m^2 K for H = 10 mm. All these values were obtained at horizontal position of the corrugated plates.

6.   It is also observed that the average Nusselt number decreased with increasing of angle of inclination. The maximum values of average Nusselt number were experimentally found to be 10.6343 for H = 25 mm, 10.2586 for H = 15 mm, and 9.7799 for H = 10 mm. All these values were also found at horizontal position of the corrugated plates. Besides this it is observed that the value of Nusselt number decreases with decreasing amplitude of corrugation (H).

7.   All the data for vee corrugations were correlated by the following correlating equation to within ± 12 %.

$$Nu_L = 0.276 \, (Ra_L \cos \theta)^{0.294} \, (A)^{-0.331} \; ;$$

where, $3.294 \times 10^4 \leq Ra_L \leq 1.8814 \times 10^6$

$$1.40 \leq A \leq 9.50$$

$$0^0 \leq \theta \leq 75^0$$

$$10^0 C \leq \Delta T \leq 35^0 C$$

9. The Nusselt number of this investigation for $Ra_L = 0.4 \times 10^6$ and at $H = 25$ mm was greater by 0.6% than the values of Chinnappa (1970), who was performed an experimental investigation across air layers bounded by a horizontal vee corrugated and flat plates

10. For lower Rayleigh number i.e. for $Ra_L = 0.4 \times 10^6$, the values of Nusselt number for vee corrugation of $H = 25$mm are compared with Kabir's Sinusoidal corrugation, Feroz's Trapezoidal corrugation, Feroz's Rectangular corrugation and Saiful's Square corrugation, it is shown that Kabir's (Sinusoidal corrugated) are lower by 12%, Feroz's (Trapezoidal corrugated) are lower by 22%, Feroz's (Rectangular corrugated) are lower by 28% and Saiful's (Square corrugated) are lower by 40%. It is also observed from the figure that for higher Rayleigh number ($Ra_L = 1.0 \times 10^6$) this difference in value of Nusselt number of present study is higher than other related works mentioned earlier.

6.2 Recommendations :

1. The effect of Prandtl number on the natural convection heat transfer can be investigated by performing similar experiments with other fluids e.g., water, silicon oil etc.

2. A comprehensive investigation of natural convection heat transfer of the similar type may be carried out over a wider range of Rayleigh number.

3. The entire investigation can be carried out by interferometric techniques for confirming the flow pattern of the convective fluid within the region.

4. An experimental investigation can be performed with very high temperature potential i.e. $\Delta T \gg 35^0 C$ and also the velocity field can be investigated.

5. This investigation can be repeated with changing the vee angle i.e. greater or less than the vee angle of 60^0.

6. Numerical simulation of natural convection heat transfer from hot corrugated plates to a cold flat plate can also be predicted.

7. The entire investigation can be repeated by using hot vee corrugated plates with flush heat sources.

REFERENCES

Arnold, J.N.,Catton, I., and Edwards, D.K. 1976. "Experimental investigation of Natural Convection in Inclined Rectangular Regions of Differing Aspect Ratios" J. Heat Transfer, Vol. 98, pp. 67-71.

Ayyaswamy, P.S., and Cotton, I., 1974, "Natural Convection Flow in a Finite Rectangular Slot Arbitrarily Oriented with Respect to the Gravity Vector", International Journal of Heat and Mass Transfer, Vol. 17, pp. 173-184.

Ayyaswamy, P.S., and Catton, I., 1973, "The Boundary Layer Regime for Natural Convection in a Differentially Heated, Tilted Rectangular Cavity", J. Heat Transfer, Trans. ASME Series C, Vol. 95, pp. 543-545.

Buchberg, H.,Catton, I., and Edwards, D.K., 1976 "Natural Convection in Enclosed spaces; A Review of Application to Solar energy Collection." J. Heat Transfer, Vol. 98, No.2, pp. 182-188.

Burmeister, L.C., 1983, "Convective Heat Transfer", John Wiley and Sons. Inc.

Channdrasekhar, S., 1961, " Hydrodynamic and Hydromagnetic Stability", Clarendon Press, Oxford.

Chinnappa, J.C.V., 1970 "Free Convection in Air Between a 60^0 Vee-Corrugated Plate and Flat Plate", International Journal of Heat and Mass Transfer, Vol. 13, pp. 117-123.

Chu,T.Y., and Goldstein, R. J., 1973, "Turbulent Convection in a Horizontal Layer of Water", Journal of Fluid Mechanics, Vol. 60, pp. 141-159.

Chu,T.Y., and Goldstein, R.J., 1969,"Thermal Convection in a Horizontal Layer of Air", Prog. Heat and Mass Transfer, Vol. 2, pp.55-75,

David, P.Dewitt, and Frank, P.Incropera, 1985, "Introduction to Heat Transfer".

De Graff, J.C.A., and Van Der Held, F.E.M., 1953, "The Relation Between the Heat Transfer and the Convection Phenomena in Enclose Plane Air Layers", Appl. Sci. Res. A., Vol 3, pp. 393-409.

Difederico, I., and Foradoschi, F.P., 1966, "A Contribution to the Study of Free Convection in a Fluid layer heated from Below", International Journal of Heat and Mass Transfer, Vol. 9, pp.1351-1360.

Dropkin, D., and Somerscales, F., 1966, "Experimental Investigation of the Temperature Distribution in a Horizontal Layer of Fluid Heated from below", International Journal of Heat and Mass Transfer, Vol. 9, pp. 1189-1204.

Dropkin, D., and Somerscales, F., 1965, "Heat Transfer by Natural Convection in Liquids Confined by Two parallel Plates which are Inclined at Various Angles with Respect to the Horizontal", Journal of Heat Transfer. Series C, Vol. 87, pp. 77-81.

Dropkin D., and Globe, Se.E., 1959 "Natural Convection in Liquids Confined by Two Horizontal Plates and Heated from Below", Journal of Heat Transfer,Vol. 87, Series C, pp. 24-28.

Eckert, E.R.G., and Carison. W.O., 1969 , "Natural Convection in an Air Layer Enclosed Between Two Vertical Plates with Different Temperatures," International Journal of Heat and Mass Transfer, Vol. 2, pp. 102-120.

Emery, A., Chu, N.C., 1969, "Heat Transfer Across Vertical Layers", ASME Journal of Heat Transfer, Vol. 91, pp. 391.

Feroz, C.M.,1992,"Natural Convection from Hot Corrugated Plates to a Cold Flat plate", M.Sc.Engineering(Mechanical) Thesis, BUET.

Gryzagoridis, J., 1971, "Natural Convection from a Vertical Plate in Low Grashof Number Range", International Journal of Heat and Mass Transfer, Vol. 14, pp. 162-164.

Hart, J., 1971, "Stability of the Flow in a Differentially heated Inclined Box," Journal of Fluid Mechanics,Vol. 47, pp. 547-576.

Herring, J.R., 1965, "Investigation of problems in Thermal Convection", Journal Atoms Sci. Vol. 20. p. 325.

Herring, J.R., 1964, "Investigation of problems in Thermal Convection: Rigid Boundaries", Journal Atoms Sci. Vol. 21. p. 227.

Hollands, K.G.T., Unny, T.E., Raithby, G.D. and Konicek, L., 1976. "Free Convective Heat Transfer Across Inclined Air Layers", Journal of Heat Transfer, Vol. 98, No. 2, pp. 189-193.

Hollands, K.G.T., Raithby, G.D. and Konicek, L., 1975. "Correlation Equations for Free Convection Heat Transfer in Horizontal Layers of air and Water", International Journal of Heat and Mass Transfer, Vol. 18, pp. 879-884.

Hollands, K.G.T., and Konicek, L., 1973, " Experimental Study of the Stability of Differentially Heated Inclined Air Layers", International Journal of Heat and Mass Transfer, Vol. 16, pp. 1467-1476.

Hollands, K.G.T., 1965, " Convectional Heat Transfer Between Rigid Horizontal Boundaries after Instability", Physics Fluids, Vol.8 , pp. 389-390.

Hollands, K.G.T., 1963, "Directional Selectivity, Emittance and Absorptance properties of Vee-Corrugated Surfaces", Solar Energy, Vol. 7, pp. 108-116.

Holman, J.P.1981, "Heat Transfer", Fifth Edition, McGraw-Hill Book Company.

Jakob, M., 1949 "Heat Transfer", Vol. 1, John Wiley and Sons, Inc.N.Y.

Jakob. M., 1946, Trans. ASMRE, Vol. 68. pp. 189.

Jeffreys, H., 1928, "Some Cases of Instability in Fluid Motion", Proc. Roy. Soc. (London), (A), Vol. 118, p. 195.

Kabir Humayun, 1988, "An Experimental Investigation of Natural Convection Heat Transfer from a Hot Corrugated Plate to a Flat Plate", M.Sc.Engineering (Mechanical) Thesis, BUET.

Low,A.R., 1929, "On the Criterion for Stability of a Layer of Viscous Fluid Heated from Below", Proc. Roy. Soc. (London), (A), Vol. 125, p. 180.

Malkus, W.V.R., 1963, "Outline of a Theory of Turbulent Convection", Theory and Fundamental Research in Heat Transfer, Edited by J.A.Clark, Pergamon Press, New York, pp. 203-212.

Mull W., and Reiher H., 1930, "Experimental Investigation of Free Convection Heat Transfer in Horizontal Air Layers".Gesundh-lng. 28(1), pp. 1-28.

McAdams, W.H., 1949, "Heat Transmission",Third Edition, McGraw-Hill Book Company, Inc.

Ostrach, S., 1957, "Convective phenomenain Fluids Heated from Below", Trans. ASME, Vol. 79, pp. 299-305.

O'Toole, J.L., and Siveston, P.L., 1961, "Correlations of Convective Heat Transfer in Confined Horizontal Layers", A.I.Ch.E. Chem.Engg. Prog. symp. Ser. Vol. 57(32), pp. 81-86.

Ozoe, H., Sayma, H., and Churchill, S.W., 1975, "Natural Convection in an Inclined Rectangular Channel at Various Aspect Ratios and Angles: Experimental Measurements." International Journal of Heat and Mass Transfer, Vol. 18, pp. 1425-1431.

Randall, K.R. et. al., "Interferometeric investigation of Convection in Slat-Flat Plate and Vee-Corrugated Solar Collectors", Solar Energy International Progress, pp. 447-460.

Rayleigh, L., 1916, "On Convection Currents in a Horizontal Layer of Fluid when the Higher Temperature is on the underside", Phil. Magh. Vol. 32 p. 529.

Rossby, H.T., 1969, "A Study of Benard Convection with and without Rotation", Journal of Fluid Mechanics, Vol. 36(2), pp. 309-335.

Schluter, A., Lortz, D., Busse, F., 1965,"On the Stability of Steady Finite Amplitude Convection ," Journal of Fluid Mechanics, Vol. 23, pp. 129-144.

Schmidt, R.J., and Silveston, P.L., O.A., 1959, "Natural Convection in Horizontal Liquid Layers", Chem. Engg. Prog. Symp. Ser 29, Vol. 55, pp. 163-169.

Schmidt, R.J., and Saunders, O.A., 1938, "On the Motion of Fluid Heated from Below", Proc. Roy. Soc. (London), (A), Vol. 165. pp. 216-218.

Sterling, C.V., and Scriven, L.E., 1964, Journal of Fluid Mechanics, Vol. 19, p . 321.

Thomson, J.J., 1882, Proc. Glasgow Phil. Soc., Vol. 13. pp. 464.

APPENDIX - A

DESIGN OF THE TEST RIG

During the design of the test rig the following two aspects were considered :

    (1)   Heat Transfer Calculations
    (2)   Electrical heater design.

A1.   Heat Transfer Calculations :

All the heat transfer calculations included estimation of the steady state heat transfer rates from different exposed heated surfaces of the experimental rig under different designed operating conditions as given below :

[1]   Calculation of rate of heat transfer from the hot corrugated plate to the cold flat plate by convection and radiation.

[2]   Calculation of rate of heat transfer from the exposed surfaces of the upper guard heater assembly to the ambient air by convection and radiation.

[3]   Calculation of rate of heat transfer from the exposed surfaces of the lower guard heater assembly to the ambient air by convection and radiation.

For proper design the above three items were estimated for two extreme design temperatures namely the maximum and minimum design temperatures. From the previous available experimental data it was observed that maximum heat transfer will occur when the rig is horizontal , and mean plate spacing is minimum and the temperature of the test rig is maximum. Similarly minimum heat transfer will occur when the rig is vertical , mean plate spacing is maximum and the temperature of the test rig is minimum.

A1.1   Calculation of Rate of Heat Transfer from the Hot Corrugated Plate to the Cold Flat Plate :

Heat transfer from the hot corrugated plate to the cold flat plate takes place by two different modes (conduction is negligible) ;
(a) Natural convection and   (b) Radiation.

A1.1a   Calculation of Natural Convection Heat Transfer :

For design purpose it was assumed that the corrugated plate was a flat one. For computing heat transfer co-efficient approximately the following correlating equations by Jakob [1949] for horizontal [fig. A.1] and vertical [Fig. A.2] positions of the test rig heated from below were used .

For Horizontal Position :

$$Nu_L = 0.195 \ [\ Gr_L \ ]^{1/4}, \quad 10^4 < \ Gr_L \ < 4 \times 10^5 \ \text{------------------------------------}[1]$$

$$Nu_L = 0.068 \ [\ Gr_L \ ]^{1/3}, \qquad Gr_L \ < 4 \times 10^5 \ \text{-------------------------------------}[2]$$

For Vertical Position :

$$Nu_L = 1 \ , \qquad\qquad Gr_L \ < 2000 \ \text{---}[3]$$

$$Nu_L = 0.18 \ [\ Gr_L \ ]^{1/4} \ [\ H/L]^{-1/9} \ , \quad 2 \times 10^3 < \ Gr_L \ < 2 \times 10^5 \ \text{----------------------}[4]$$

$$Nu_L = 0.065 \ [\ Gr_L \ ]^{1/3} \ [\ H/L]^{-1/9} \ , \quad 2 \times 10^5 < \ GrL \ < 11 \times 10^6 \ \text{---------------------}[5]$$

After knowing Nu_L convective heat transfer co-efficient was found by using the following equation :

$$h = Nu_L \ . \ K/L \ \text{--}[6]$$

And finally convective heat transfer rate was calculated by using the following equation :

$$q_{CONV} = A_{COR} . \ h \ [\ T_{COR} - T_{COLD}] \text{---}[7]$$

A1.1b   Calculation of Radiation Heat Transfer :

For estimating the radiation heat transfer rate following assumptions were made :

(i.)   Interior surfaces i.e. the hot corrugated plate and cold flat plate behaved like black bodies.

(ii)   Heat transfer by convection was not taken into account.

(iii)   Side walls of the test rig were adiabatic.

Generally radiation from surface is due to reflection and emission. Since the interior surfaces as mentioned above were assumed to be black, the radiation emitted was absorbed without any reflection. Defining q_{i-j} as the rate at which radiation was emitted by a black surface i. and was intercepted by black surface j , [figure A.3] i.e.

$$q_{i-j} = [\ A_i \ J_j \ ] \ F_{ij} \text{---}[8]$$

Since radiosity equals emissive power for a black surface [$J_i = E_{bj}$] , hence

$$q_{i-j} = A_i \ F_{ij} \ E_{bi} \ \text{---}[9]$$

$$q_{j-i} = A_j \ F_{ji} \ E_{bi} \ \text{--}[10]$$

The net radiation exchanged between two black surfaces :

$q_{ij} = q_{i \cdot j} - q_{j \cdot i}$

or, $q_{ij} = A_i F_{ij} E_{bi} - A_j F_{ji} E_{bi}$ --[11]

By reciprocity , $A_j F_{ji} = A_i F_{ij}$ --[12]

According to Stefan - Boltzman Law :

$E_{bi} = \sigma T_i^4$ --[13]

$E_{bj} = \sigma T_j^4$ --[14]

Now from equations [11], [12], [13] and [14] :

$q_{ij} = A_i F_{ij} \sigma [T_i^4 - T_j^4]$ --[15]

Considering surfaces i. and j as corrugated and flat plate respectively and assuming that the radiation emitted by the corrugated surface was intercepted by the cold flat plate [$F_{ij} = 1$] , the equation [15] took the following form :

$q_{rad} = A_{COR} \sigma [T_{COR}^4 - T_{COLD}^4]$ --[16]

From equation [16] the radiation heat transfer was estimated.

A1.2   Calculation of Rate of Heat transfer from the Exposed surfaces of the Upper Guard heater Assembly to the Ambient Air by Convection and Radiation :

When the experimental rig was kept horizontal , the exposed surfaces of the upper guard heater assembly consisted of two pairs of parallel vertical plane surfaces facing outward having dimensions of 660mm x 127mm and 579mm x 127mm.

When the experimental rig was kept vertical , one of the pairs of dimensions 660mm x 127mm of the exposed surfaces of the upper guard heater assembly became horizontal ; one facing upward and another facing downward. But the other pair of the exposed heated surfaces of dimension 579mm x 127mm remained vertical facing outward.

For design the following correlations were used to estimate the rate of heat transfer from the exposed surfaces of the upper guard heater assembly :

[I]   For computing convective heat transfer co-efficient approximately the following correlating equation recommended by Gyrzagoridis (1971) for vertical heated surfaces of height H(Figure A.4) was used.

$Nu_H = 0.555 [Gr_H Pr]^{1/4}$, $10 < Gr_H < 10^9$ --[17]

Where ,
Nu_H and Gr_H are based on length of the vertical surface.

[ii] For computing convective heat transfer co-efficient approximately for heated horizontal surfaces (Figure A.5 and A.6) of characteristic length $L_C = \sqrt{(\text{Area of the plate})} = A_P$ the following correlating equations recommended by McAdams (1949) were used.

$$Nu_{Lc} = 0.54 \, [\, Gr_{Lc} \, .Pr \,]^{1/4} \, , \quad 10^5 < Gr_{Lc} < 2 \times 10^7 \, , \quad [\text{ For upward facing}] \text{-----------------------}[18]$$
$$= 0.14 \, [\, Gr_{Lc} \, .Pr \,]^{1/3} \, , \quad 2 \times 10^7 < Gr_{Lc} < 3 \times 10^{10}$$

$$Nu_{Lc} = 0.27 \, [\, Gr_{Lc} \, .Pr \,]^{1/4} \, , \quad 3 \times 10^5 < Gr_{Lc} < 3 \times 10^7 \, , \quad [\text{ For downward facing}] \text{-----------------}[19]$$

Where, Nu_{Lc} and Gr_{Lc} are based on the characteristic length L_C of the plane as mentioned above.

The radiation heat transfer from these exposed heated surfaces were estimated by the following equation :

$$q_{rad} = A_S \, .\varepsilon_S . \sigma \, [\, T_g^4 - T_s^4 \,] \text{---}[20]$$

A1.3 Calculation of Rate of Heat Transfer from the Exposed Surfaces of the Lower Guard Heater Assembly to the Ambient Air by Convection and Radiation :

When the experimental rig was kept horizontal , the exposed surfaces of the lower guard heater assembly consisted of two pairs of parallel vertical plane surfaces facing outward having dimension of 660mm x 64mm and 579mm x 64mm and the bottom surface 660mm x 579mm facing downward.

When the experimental rig was kept vertical , one of the pairs of surface having the dimensions 660mm x 64mm of the lower guard heaters assembly became horizontal ; one facing upward and another facing downward . But the other pair of the exposed heated surfaces of dimensions 579mm x 64mm remained vertical facing outward . The bottom face became vertical.

For estimating both convective and radiative heat transfer rate from the exposed surfaces of the lower guard heater assembly the correlating equation were the same as described in the preceding section [A1.2].

For both the lower and upper guard heater assembly the sum of the heat convected and radiated from the exposed surfaces must be equal to the amount of heat conducted from guard heaters through asbestos and wooden strip layers. But during the design the exposed surface temperature (T_S) of the guard heaters assembly was not known . So T_S was assumed and estimation of conduction heat transfer was made. Then by using this surface temperature the amount of convective and radiative heat transfer were calculated. The iterative solution was continued until the conduction heat transfer rate became equal to the sum of convective and radiative heat transfer. The equation used for estimating conduction heat transfer rate is given below :

$$q_{Cond} = A_S . \Sigma_{j=i}^{2} \, K_j / L_j \, [\, T_g - T_s \,] \text{---}[21]$$

K_1 = The thermal conductivity of asbestos cloth = 0.192 w / m ^{0}K

K_2 = The thermal conductivity of wooden strip = 0.130 w / m ^{0}K

33

L_1 = The thickness of the asbestos cloth = 12 mm
L_2 = The thickness of the wooden strip = 12 mm
T_S = Temperature of the guard heating element = T_{COR}

Now by substituting the above values into equation (21) the conduction heat transfer rate was found to be :

$$q_{Cond} = 26.833 \, A_S \cdot [\, T_g - T_S \,] \text{---[22]}$$

The present experimental investigation was carried out with a rectangular rig that was made by Kabir (1988) . So the results of the heat transfer calculations for rig design were taken from Kabir's work.

A2.   Heater Design :

The total number of heaters were six in the experimental setup. Among the heaters one heater was used in the experimental test section and the other five heaters acted as guard heaters. Each of the heaters had separate controlling variac through which power input to the heaters were controlled during experiment. Power required for each heater was estimated from heat transfer calculations shown in A1.

The details of the heater design are given below :

Power (P) taken by the electric heater of resistance R can be determined by the following equation :

$$P = I_{safe}^{\,2} \, x \, R \text{ --[23]}$$

If r be the resistance of the heating wire per meter of length , then for a heater of power P the length of the heating wire will be :
$$L = R/r \text{ --[24]}$$

By knowing I_{safe} and power (P) taken by each electric heater the required resistance (R) was calculated from equation (23) . For particular heating wire , internal resistance 'r' is fixed. So , by putting the values of R and r into equation (24) required length for each heater was determined.

The ratings of the heating wires were as follows :

Type 1 : Resistance , r = 39.37 ohms/m
           Current carrying capacity = 0.75 amps

Type 2 : Resistance, r = 26.25 ohms/m
           Current carrying capacity = 1.5 amps.

The particulars of the heating arrangement that were used are given in following tabular forms :

Heater Number and Name	Maximum Power Requirement (Watt)	Type	Length of wire (cm)	Location	Variac Connected with Heater	
					Safe Installed Capacity (Watt)	Safe Voltage (Volt)
Experimental hot corrugated plate heater.	12.50	1-Nicrome Wire	97.40	Experimental test section Figure 4.3	22.5	30
Outer side guard heater.	83.40	1-Nicrome Wire	376.60	Longitudinal sides of the test section Figure 4.3	22.5	30
Outer end guard heater	20.79	1-Nicrome Wire	93.87	Lateral sides of the test section Figure 4.3	90	120
Upper outer guard heater.	97.60	1-Nicrome Wire	165.24	Upper guard heater ring Figure 4.4	180	120
Bottom guard heater	113.02	1-Nicrome Wire	510.34	Lower guard heater ring Figure 4.4	90	120
Lower outer guard heater	43.17	1-Nicrome Wire	194.93	Lower guard heater ring Figure 4.5	45	60

APPENDIX - B

CONDUCTION CORRECTION

One dimensional fourier conduction equation is :

$$q'' = K. \Delta T_C / \Delta x \ [\text{ For one layer of conduction zone }] \text{ ---[1]}$$

$$= T_C / \sum (\Delta x_i / k_j) \ [\text{ For two or more layers of conduction zone }] \text{ ----------------------------[2]}$$

According to the present investigation it is observed that under steady state heat conduction the resistance to the heat conduction will consist of the resistance offered by the upper asbestos cloth layer upper corrugated plate (G.I. Sheet).

The thermal conductivity of asbestos cloth, $K_1 = 0.157 \ W / m^0 k.$

The thermal conductivity of G.I. sheet, $\quad K_2 = 70 \ W / m^0 k.$

The thickness of asbestos cloth, $\quad X_1 = 2.15052 \times 10^{-3} \ m.$

The thickness of asbestos cloth, $\quad X_2 = 7.9375 \times 10^{-4} \ m.$

(The above values were taken from M. Sc. Engineering thesis of Saiful, 1995)

It is assumed that there is no temperature difference at the interface of the lower corrugated plate and the interface of the lower guard heater box. So that the heat only goes up toward the cold plate. It is also assumed that the temperature at the bottom surface of the lower corrugated plate is equal to the temperature at the interface of the two asbestos cloth.

Now by substituting the above values into equation [2] the conduction correction in temperature measurements were found to be -

$$\Delta T_C = 0.0137089 \ q'' \text{ --[3]}$$

Where, q" will be taken as electrical heat input (W/m^2) per unit projected surface area of the experimental section of the hot corrugated plate.

APPENDIX - C

DETERMINATION OF EMISSIVITY OF THE CORRUGATED SURFACE

As the accuracy in predicting the radiation heat transfer from the experimental hot corrugated plate to the cold flat plate largely depends on the precise determination of the long wave emmisivity and hemispherical emmisivity of the corrugated surface, so the emmisivity of vee corrugated plates were determined as accurate as possible.

Both the three sets of vee corrugated plates were painted by dull black plastic paint. Hollands (1963) developed the method of determination of the hemispherical emissivities of the vee corrugated surfaces using the emmisivity of the plane surface. When a plane G.I. sheet is uniformly painted to dull black with black paint, its emmisivity can be taken as the emmisivity of the black paint. From table 3.6 of "Journal of Solar Energy" , H.P. Gray; Vol. 1 , John Wiley and Sons Ltd. (1982) the emmisivity of the black paint was found to be 0.94. The emmisivity of the G.I. corrugated (painted black) plate was assumed to be the same as that of plane G.I. sheet (painted black). Considering this value of the emissivity, the hemispherical emmisivity of vee corrugated plate having opening angle of 60^0 was 97.5 (using figure C.2).

APPENDIX - D

D.1   Correlation of natural convection heat transfer in an inclined rectangular region :

Difedevico and Foraboschi (1966) carried out experimental investigation on natural convection heat transfer in an inclined rectangular region with different convective fluids and developed correlation in the following form :

$$Nu = C (Ra)^n (Pr)^m \text{---[1]}$$

Kabir (1988) carried out an experimental investigation of natural convection heat transfer across air layer from a hot sinusoidal corrugated plate to a flat plate enclosed in a rectangular region inclined at various angle with respect to horizontal for various aspect ratios (A) and developed the following correlation :

$$Nu_L = 0.0132 (Ra_L \cos\theta)^{0.51} (A)^{-0.35} \text{---[2]}$$

$$5.56 \times 10^3 \leq Ra_L \leq 2.34 \times 10^6$$

Feroz (1992) carried out an experimental investigation of natural convection heat transfer across hot trapezoidal and rectangular corrugated plates to a cold flat plate enclosed in a rectangular region included at various angle with respect to horizontal for various aspect ratios (A) and developed the following correlations.

$$Nu_L = 0.0112 (Ra_L \cos\theta)^{0.521} (A)^{-0.4546} \text{--[3]}$$

$$Nu_L = 0.0102 (Ra_L \cos\theta)^{0.530} (A)^{-0.4423} \text{--[4]}$$

Where,

$$9.84 \times 10^4 \leq Ra_L \leq 2.29 \times 10^6$$

$$0^0 \leq \theta \leq 75^0$$

$$2.60 \leq A \leq 5.22$$

$$10^0 C \leq \Delta T \leq 35^0 C$$

Saiful (1995) carried out an experimental investigation of natural convection heat transfer across hot square corrugated plates to a cold flat plate enclosed in a rectangular region included at various angle with respect to horizontal for various aspect ratios (A) and developed the following correlations.

$$Nu_L = 0.295 (Ra_L \cos\theta)^{0.265} (A)^{-0.442} \text{--[5]}$$

Where,

$$3.294 \times 10^4 \leq Ra_L \leq 1.881 \times 10^6$$

$$0^0 \leq \theta \leq 75^0$$

$$1.4 \leq A \leq 9.5$$

$$10^0 C \leq \Delta T \leq 35^0 C$$

D.2 Correlation of natural convection heat transfer from a hot corrugated plate to a cold flat plate ;

The present study was an experimental investigation of natural convection from hot vee corrugated plates to a cold flat plate. Only vee corrugated plates of different amplitudes were used. The required correlation was derived by considering the effect of the following factors :

D.2a. Effect of fluid properties :

The most commonly used dimensionless parameters which include the effect of fluid properties in natural convection are :

$$Pr = \mu C_P / k \text{ and}$$

$$Ra_L = g.\beta . \Delta T. L^3 / \nu . \alpha$$

The present experimental investigation was carried out with only one convective fluid (air) , so Pr was assumed as constant property in the correlating equation. Therefore Nusselt number (Nu), which measures the thermal convective property of the fluid mainly depends on Rayleigh number (Ra_L) . It was experimentally found that Nusselt number increases with the increasing of Rayleigh number. For analysis of natural convection from inclined surface because of buoyancy force, Ra_L is generally substituted by its vertical component i.e. $Ra_L \cos\theta$. So $Ra_L \cos\theta$ should include the contribution of the fluid property in natural convection. Let correlation of the following form be assumed :

$$Nu_L \propto (Ra_L \cos\theta)^n \text{ ---[5]}$$

In this case all the data of three sets of corrugation were solved by FORTRAN Programme of curve fittings. From the best fit curve of linear regression model the correlation obtained was,

$$Nu_L \propto (Ra_L \cos\theta)^{0.189}$$

39

D.2b   Effect of spacing between hot and cold plates :

Kabir (1988), Feroz (1992) and Saiful (1995) suggested the following dimensionless group to describe the contribution of plate spacing between hot corrugated plate and cold flat plate in natural convection in a rectangular enclosure heated from below :

$$A = L/H \text{--[6]}$$

In equation (6) "L" is mean plate spacing and "H" is amplitude of corrugation. It was experimentally observed that average convective heat transfer coefficient for both types of corrugation increases upto a certain limit with the increase of aspect ratio (A). So, this dimensionless number also should include the contribution of spacing between hot and cold plates in free convection.

By including this dimensionless group the correlating equation was also obtained by similar FORTRAN Programme of curve fitting. From the best fit curve the correlating equation containing aspect ratio 'A' was found to be

$$Nu_L = 0.276 \ (Ra_L \cos \theta)^{0.294} \ (A)^{-.0331} \ ;$$

where, $3.294 \times 10^4 \ \leq \ Ra_L \ \leq 1.8814 \times 10^6$

$$1.40 \ \leq A \ \leq 9.50$$

$$0^0 \ \leq \theta \ \leq 75$$

$$10^0 C \ \leq \ \Delta T \ \leq \ 35^0 C$$

The graphical representation of the correlation is shown in figure 6.46.

The correlation correlates almost all data to $\pm 12\%$

APPENDIX - E

UNCERTAINTY ANALYSIS

E.1   GENERAL

Errors will creep into all experiments regardless of the care being exerted. If the experimenter knew what the error was, he would correct what would be no longer an error. But in most situations, the experimenter cannot talk very confidently about what the error in a measurement is. He can only talk about what it "might be" , about the limits that he feels bound the possible error. The term "uncertainty" is used to refer to a possible value that an error may have. Kline and McClintock (48) attributed this definition and it still seems an appropriate and valuable concept.

According to Thasher and Binder (78) for single sample measurement it is proposed that the experimenter describes the uncertainty of his measurement in terms of what he believes would happen if the measurement were repeated a larger number of times. In this way one can estimate the standard error and the uncertainty interval and can give odds that the error would be less than the uncertainty interval. The reliability of a result described in this manner is indicated by the size of the uncertainty interval and the magnitude of the odds.

This chapter is devoted to determine the interval around each measured parameter within which its true value is believed to lie and it will lead to the ultimate goal, that is, to estimate how great an effect of uncertainties in the individuals measurements have on the calculated results. An uncertainty estimate is only as good as the equation(s) it is based on. If those equations are incomplete and do not acknowledge all the significant factors that affect the results then the analysis will either underestimate or overestimate the uncertainty in the results. In the present experiment the uncertainty of calculation in average natural heat transfer coefficient and Nusselt number is influenced by variation of heat input, measurement in temperature, aspect ratio, area of the test section, angle of inclination and geometry of the enclosure.

E.2   BASIC MATHEMATICS

In this experiments, each test point is run only once, and hence they are single sample experiments. A precise method of single sample uncertainty analysis has been described in the engineering literature by the works of Kline and McClintock (48) and Moffat (59).

If a variable x_1, has a known uncertainty U_1, then the form of representing this variable and its uncertainty is,

$$x_1 = x_1 \text{ (measured)} \pm U_1 \qquad \text{---[E2.1]}$$

This statement should be interpreted to mean the following :
- The best estimate of x_1 is x_1 (measured)
- There is an uncertainty in x_1 that may be as large as $\pm U_1$
- The odds are 20 to 1 against the uncertainty of being larger than $\pm U_1$

It is important to note that such specification can only be made by the experimenter based on the total laboratory experience. Let us suppose, a set of measurements is made and the uncertainty in each measurement may be expressed with the same odds. These measurements are then used to calculate some desired result R using the independent variables $x_1, x_2, x_3, \ldots\ldots x_n$, where,

$$R = R(x_1, x_2, x_3, \ldots\ldots x_n) \quad\text{---[E2.2]}$$

If $U_1, U_2, U_3, \ldots\ldots U_n$ be the uncertainties in the independent variables given with the same odds, then the uncertainty U_R in the result having these odds is given in Kline and McClintock (48) as,

$$U_R = [\{(\partial R / \partial x_1) U_1\}^2 + \{(\partial R / \partial x_2) U_2\}^2 + \ldots\ldots + \{(\partial R / \partial x_n) U_n\}^2]^{1/2} \quad\text{--------------[E2.3]}$$

Where, the partial derivative of R with respect to x_i is the sensitivity coefficient for the result R with respect to the measurement x_i. In most situations, the overall uncertainty in a given result is dominated by only a few of its terms. Terms in the uncertainty equation that are smaller than the largest term by a factor of 3 or more can usually be ignored. This is a natural consequence of the Root-Sum-square (RSS) combination : Small terms have very small effects.

Sometimes the estimate is required as a fraction of reading, rather than in engineering units. While this can always be calculated using equation [E2.3] , it is also possible to do the calculation of relative uncertainty directly. In particular, whenever the equation describing the result is a pure product form such as equation [E2.4], than the relative uncertainty can be found directly .

That is, if $\quad R = x_1{}^a \; x_2{}^b \; x_3{}^c \ldots\ldots\ldots x_m{}^n \quad\text{---[E2.4]}$

then, $U_R / R = [\{a (U_1/x_1)^2 + b (U_2/x_2)^2 + \ldots\ldots\ldots +n (U_m/x_m)^2 \}] \quad\text{----------------------[E2.5]}$

E.3   UNCERTAINTY FOR AVERAGE NATURAL HEAT TRANSFER COEFFICIENT MEASUREMENT

Let the experimental investigation deals with the steady state natural convection heat transfer through air at atmospheric pressure from hot vee corrugated plates to a cold flat plate placed above and parallel to it, where the surroundings were maintained at constant temperature. Different amplitudes of corrugation i.e., H = 10mm, 15mm, 25mm were used. Let the heat q'' was transferred through hot vee corrugated plate to cold flat plate by using a heater then the mathematical equations for total heat will be

$$q'' = VI \cos\phi / A_{COR} \quad\text{---[E3.1]}$$

that is the total heat flux from the hot vee corrugated plate was calculated by measuring the current and voltage supply of the main heater.

Average natural heat transfer coefficient will be

$$h = [q'' - q_r''] / [T_{COR} - T_{COLD}] \quad\text{---[E3.2]}$$

Where, q_r'' is the heat transfer by radiation. In case of a fixed temperature potential the radiative heat flux becomes constant and the convective heat transfer varies on aspect ratio and angle of inclination of the enclosure. For calculating the uncertainty of natural convective heat transfer coefficient the equation may be written in the following way with ignoring the effect of estimated uncertainty for fixed radiative heat flux, because the amount of total radiative heat flux was 15 to 20% of the total heat flux was found from experiment which was considered as a small quantity compared to the total convective heat flux. So the average natural convective heat transfer coefficient will be -

$$h = [q''] / (T_{COR} - T_{COLD}) = (VI \cos \phi) / \{A_{COR}(T_{COR} - T_{COLD})\}$$

Where V and I is the supply voltage and current to the hot corrugated plate, A_{COR} is the area of the hot test section, $T_{COR} - T_{COLD}$ is the temperature of the test section and cold plate which was measured through fourteen Chromel Alumel thermocouples. Let us suppose the enclosure is deviated by an angle β from the horizontal and different angle of inclination due to wrong adjustment. Then the measured natural convective heat transfer coefficient will be

$$h = \{(VI \cos \phi) \cos\beta\} / \{A_{COR}(T_{COR} - T_{COLD})\} \text{-----------------------------------[E3.3]}$$

Now differentiating both the sides of equation [E3.3] with respect to V, I , A_{COR} ,($T_{COR} - T_{COLD}$), β respectively, we get ;

$$\partial h / \partial V = \{(I \cos \phi) \cos\beta\} / \{A_{COR}(T_{COR} - T_{COLD})\} \text{-----------------------------[E3.4]}$$

$$\partial h / \partial I = \{(V \cos \phi) \cos\beta\} / \{A_{COR}(T_{COR} - T_{COLD})\} \text{----------------------------[E3.5]}$$

$$\partial h / \partial A_{COR} = -\{(VI \cos \phi) \cos\beta\} / \{A_{COR}^2 (T_{COR} - T_{COLD})\} \text{----------------------[E3.6]}$$

$$\partial h / \partial (T_{COR} - T_{COLD}) = -\{(VI \cos \phi) \cos\beta\} / \{A_{COR}(T_{COR} - T_{COLD})^2\} \text{----------[E3.7]}$$

$$\partial h / \partial \beta = -\{(VI \cos \phi) \sin\beta\} / \{A_{COR}(T_{COR} - T_{COLD})\} \text{------------------------------[E3.8]}$$

Let U_h be the uncertainty in the result and U_V ,U_I ,U_{ACOR} ,$U_{(TCOR - TCOLD)}$ and U_β be the uncertainty in the voltage, current, area of the test section and temperature of the hot and cold plate reading and angle of deviation of the enclosure respectively. So, from equation [E2.5] we get,

$$U_h = [\{(\partial h / \partial V) U_V\}^2 + \{(\partial h / \partial I) U_I\}^2 + \{(\partial h / \partial A_{COR}) U_{ACOR}\}^2 + [\{\partial h / \partial (T_{COR} - T_{COLD})\} U_{(TCOR - TCOLD)}]^2 + \{(\partial h / \partial \beta) U_\beta\}^2]^{1/2} \text{---[E3.9]}$$

Putting the values of partial derivatives , the above equation can be written as follows :

$$U_h = [[U_V^2[\{(I \cos \phi) \cos\beta\} / \{A_{COR}(T_{COR} - T_{COLD})\}]^2 + U_I^2[\{(V \cos \phi) \cos\beta\} / \{A_{COR}(T_{COR} - T_{COLD})\}]^2 + U_{ACOR}^2 [\{(VI \cos \phi) \cos\beta\} / \{A_{COR}^2 (T_{COR} - T_{COLD})\}]^2 + [U_{(TCOR - TCOLD)}^2[\{(VI \cos \phi) \cos\beta\} / \{A_{COR}(T_{COR} - T_{COLD})^2\}]^2 + U_\beta^2[\{(VI \cos \phi) \sin\beta\} / \{A_{COR}(T_{COR} - T_{COLD})\}]^2]^{1/2} \text{---[E3.10]}$$

$$= [\{(VI \cos \phi) \cos\beta\} / \{ A_{COR} (T_{COR} - T_{COLD})\}] [(U_V/V)^2 + (U_I/I)^2 + (U_{ACOR}/A_{COR})^2$$
$$+ \{U_{(TCOR - TCOLD)}/ (T_{COR} - T_{COLD})\}^2 + U_\beta^2 \tan^2\beta]^{1/2} \quad \text{-----------------------------------[E3.11]}$$

Dividing equation [E3.11] by equation [E3.3], we get;

$$U_h/h = [(U_V/V)^2 + (U_I/I)^2 + (U_{ACOR}/A_{COR})^2 + \{U_{(TCOR - TCOLD)}/ (T_{COR} - T_{COLD})\}^2$$
$$+ U_\beta^2 \tan^2\beta]^{1/2} \quad \text{---[E3.12]}$$

For room temperature, 27.8 ± 1^0C and atmospheric pressure, 14.7 psi, we have ;

$$V = 750 \pm 0.1$$
$$I = 10 \pm 0.01$$
$$A_{COR} = 34,960 \text{ mm}^2 \pm 382 \text{ mm}^2 \text{ [Nominal dimension } (152 \pm 1) \times (230 \pm 1) \text{]}$$
$$(T_{COR} - T_{COLD}) = 35^0C \pm 0.006^0C$$
$$\beta = 0^0 \pm 3^0$$

So, $U_h/h = [(0.1 / 750)^2 + (0.01 / 10)^2 + (382 / 34960)^2 + (0.006 / 35)^2 + (3 \pi/180)^2 \tan^2 3^0]^{1/2}$

$$= [(0.0000000178) + (0.000001) + (0.0001194) + (0.0000000274) + (0.00000753)]^{1/2}$$

$$= 0.011312$$

$$= 1.1312 \%$$

E.4   UNCERTAINTY FOR AVERAGE NUSSELT NUMBER

Let $Nu_L = (h L) / K$ ---[E4.1]

Where, Nu_L = Average nusselt number
       h = Average natural heat transfer coefficient
       L = Mean plate spacing
       K = Thermal conductivity of air

So, $\partial Nu_L / \partial h = L / K$ ---[E4.2]
      $\partial Nu_L / \partial L = h / K$ ---[E4.3]

If U_{NuL}, U_h and U_L be the uncertainty of Nu_L, h and L respectively, we get from equation [E2.5] :

$$U_{NuL} = [\{(\partial Nu_L / \partial h) U_h\}^2 + \{(\partial Nu_L / \partial L) U_L\}^2]^{1/2} \quad \text{-------------------------------[E4.4]}$$

$$= [\{ (hL/K) (U_h / h) \}^2 + \{(h L/K) (U_L/ L) \}^2]^{1/2}$$

$$= hL/K \ [(U_h \ / \ h)^2 + (U_l / L)^2]^{1/2} \ \text{------------------------------[E4.5]}$$

So , dividing equation [E4.5] by equation [E4.1], we have

$$U_{NuL} \ / \ Nu_L = [(U_h \ / \ h)^2 + (U_l / L)^2]^{1/2} \ \text{------------------------------[E4.6]}$$

For room temperature, 27.8 ± 1^0C and atmospheric pressure,14.7 psi, we have ;

$L = 95 \ mm \pm 0.5mm$
$U_h /h = 0.011312$

So , $U_{NuL} \ / \ Nu_L = [(0.011312)^2 + (0.5 / 95)^2]^{1/2}$

$$= [0.0001279 + 0.0000277]^{1/2}$$

$$= 0.012477$$

$$= 1.2477 \ \%$$

FIGURE

$\theta = 0^0 - 75^0$
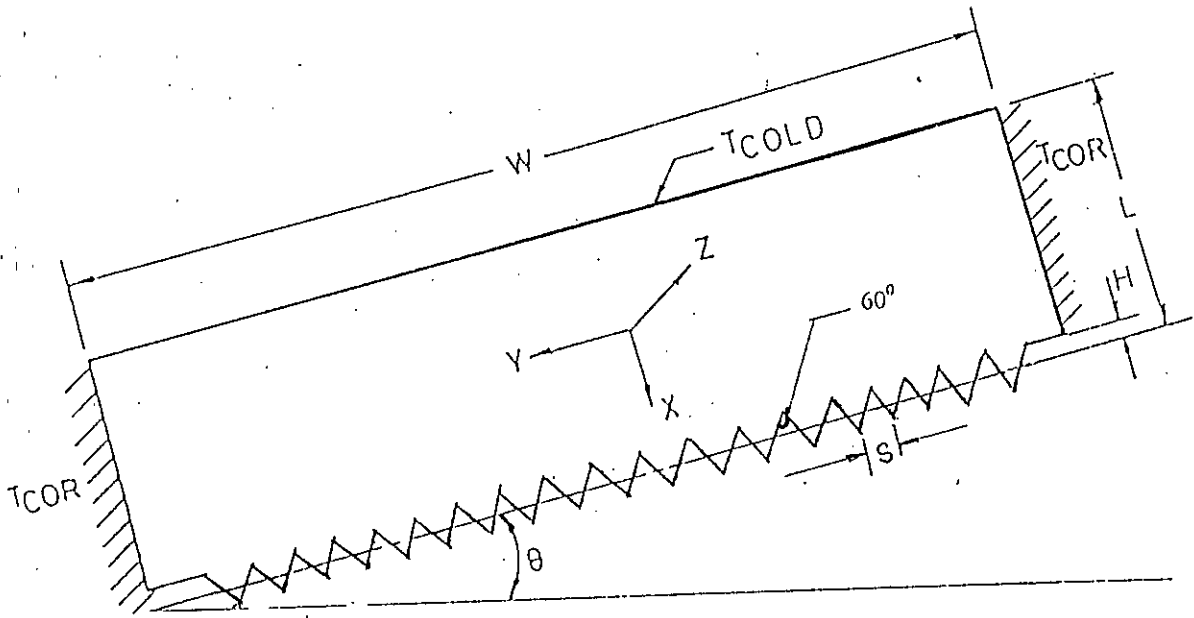
L = 35 mm - 95 mm

H = 10 mm, 15mm, 25mm

S = 23 mm, 34.6mm, 57.73mm

W = 63.5 mm

Vee angle = 60^0

FIG. 3.1 SKETCH OF THE INCLINED AIR LAYER BOUNDED BY VEE CORRUGATED PLATE AND FLAT PLATE
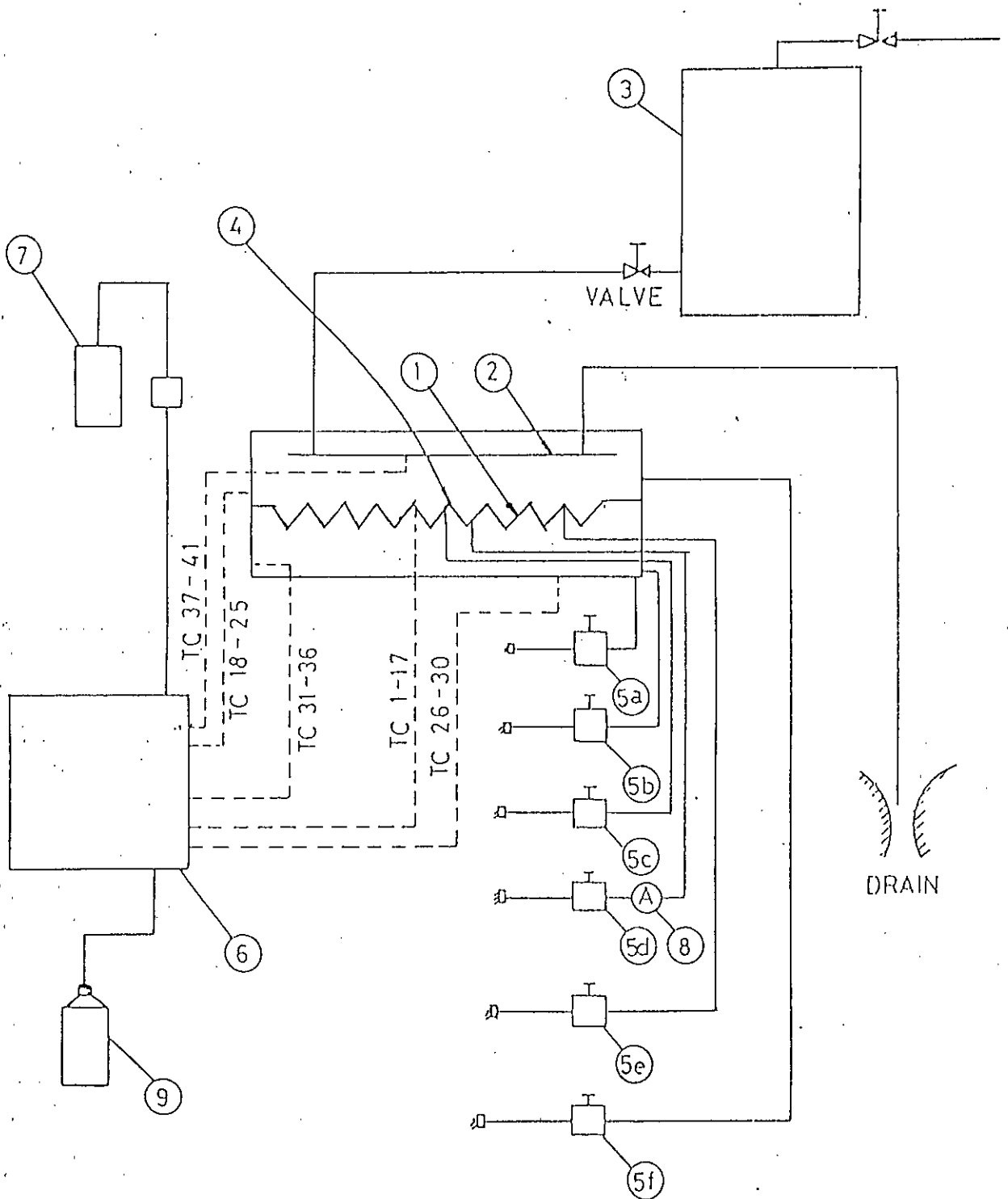
1. EXPERIMENTAL HOT PLATE
2. COLD PLATE
3. CONSTANT HEAD WATER DRUM
4. TEST SECTION
5a. VARIAC FOR HEATER-5
5b. VARIAC FOR HEATER-6
5c. VARIAC FOR HEATER-3
5d. STABILIZER FOR HEATER-1

5e. VARIAC FOR HEATER-2
5f. VARIAC FOR HEATER-4
6. THERMOCOUPLE SELECTOR SWITCH
7. DIGITAL MILIVOLT METER
8. DIGITAL AMMETER
9. COLD JUNCTION

FIG:4.1 SCHEMATIC DIAGRAM OF THE EXPERIMENTAL SET-UP.
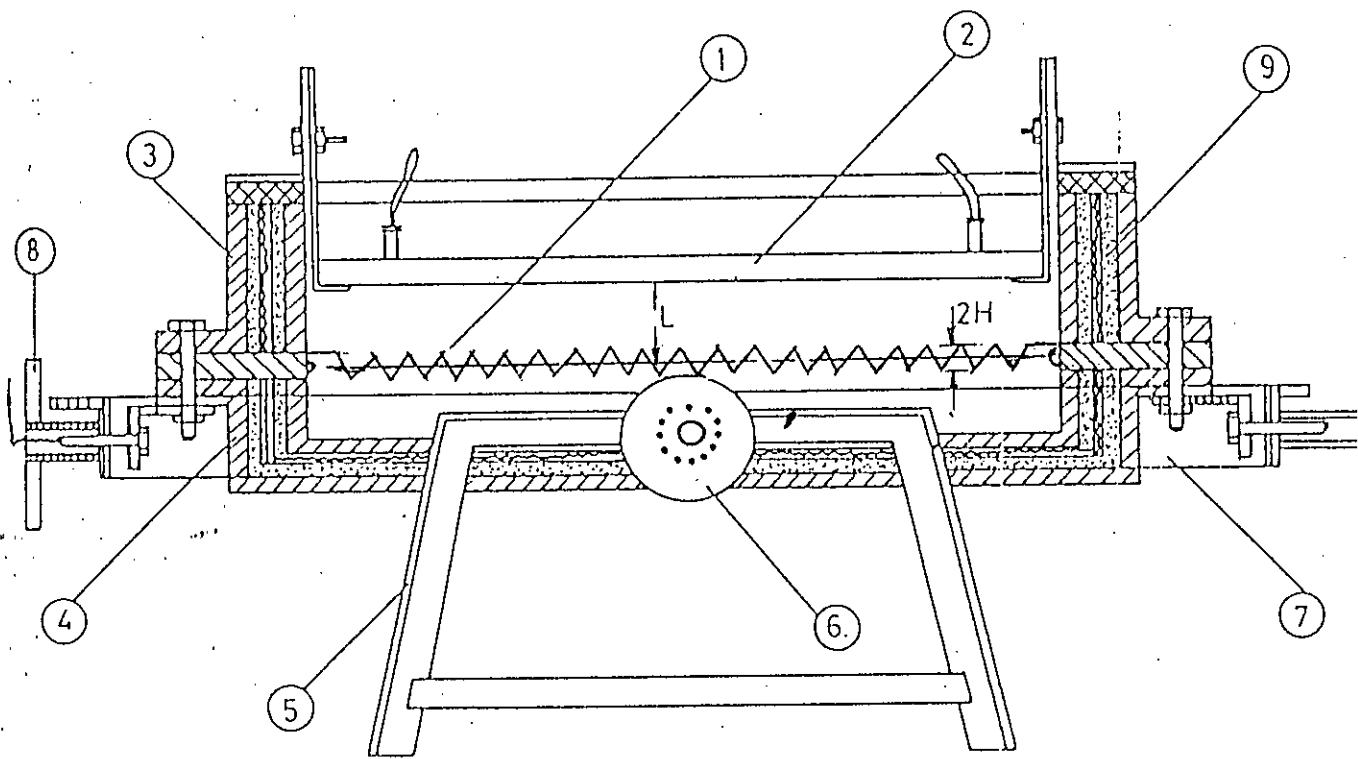
1. HOT PLATE ASSEMBLY
2. COLD PLATE
3. UPPER GUARD HEATER
4. LOWER GUARD HEATER
5. END RIG HOLDER
6. ALIGNMENT PLATE
7. SIDE RIG HOLDER
8. ALIGNMENT INDICATOR
9 NICHROME HEATERS

FIG. 4.2 DETAILS OF THE TEST SECTION FOR VEE CORRUGATION
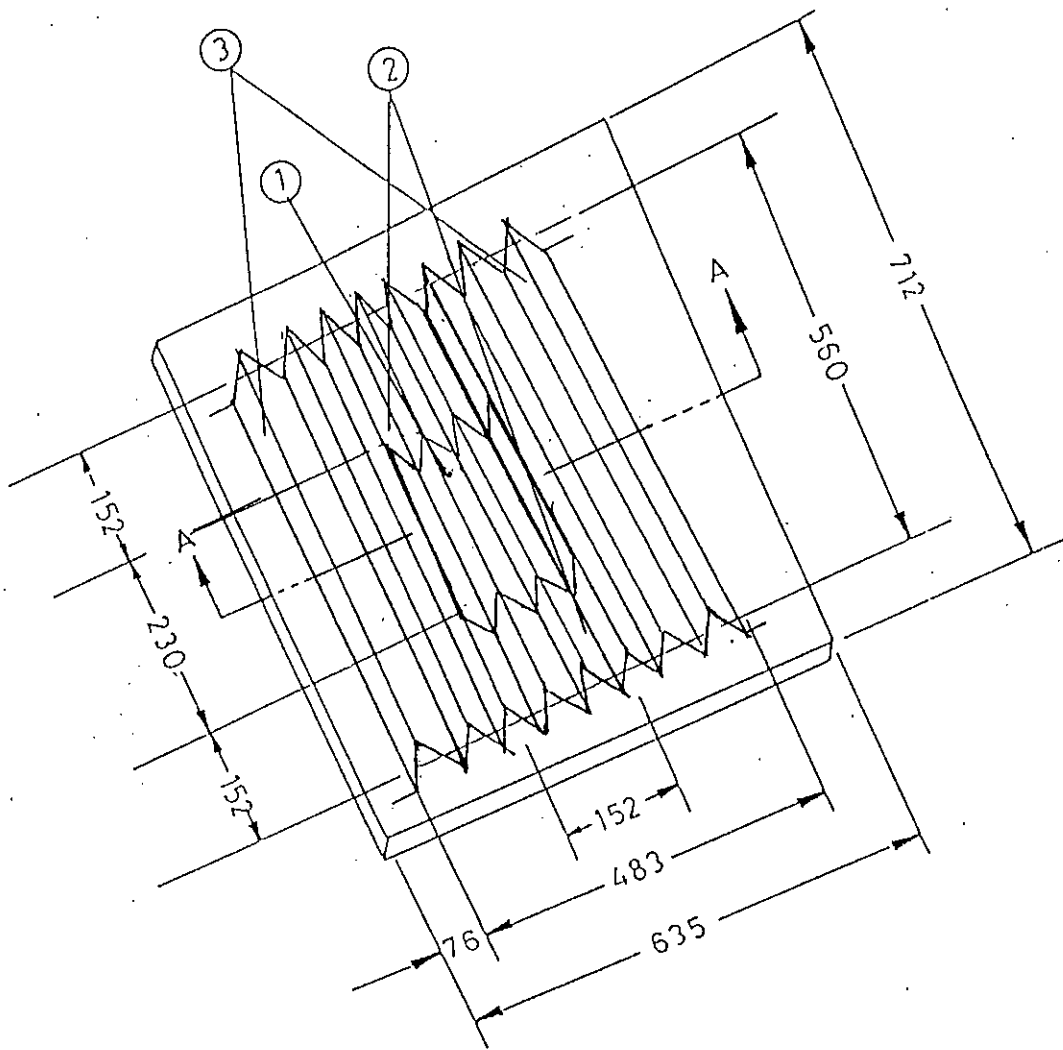
1. EXPERIMENTAL HOT PLATE.
2. OUTER END GUARD HEATER.
3. OUTER SIDE GUARD HEATER.
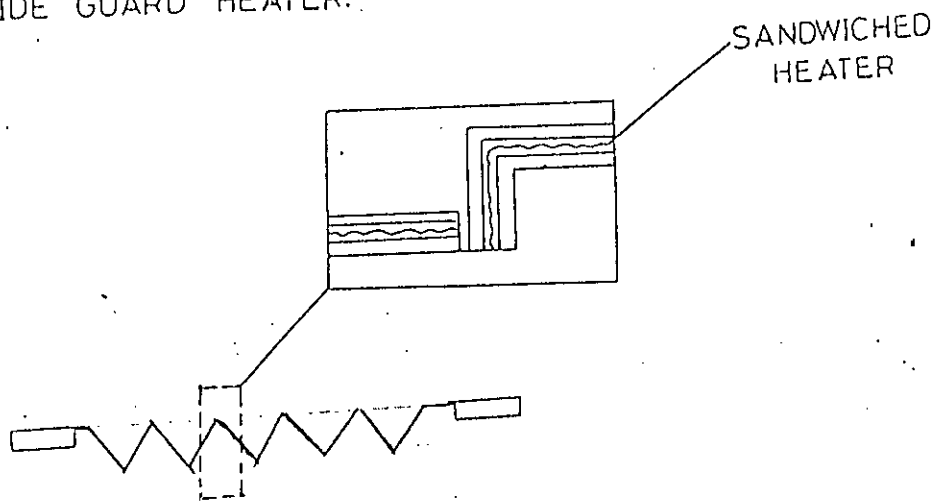
FIG:4.3 DETAILS OF HOT PLATE ASSEMBLY.
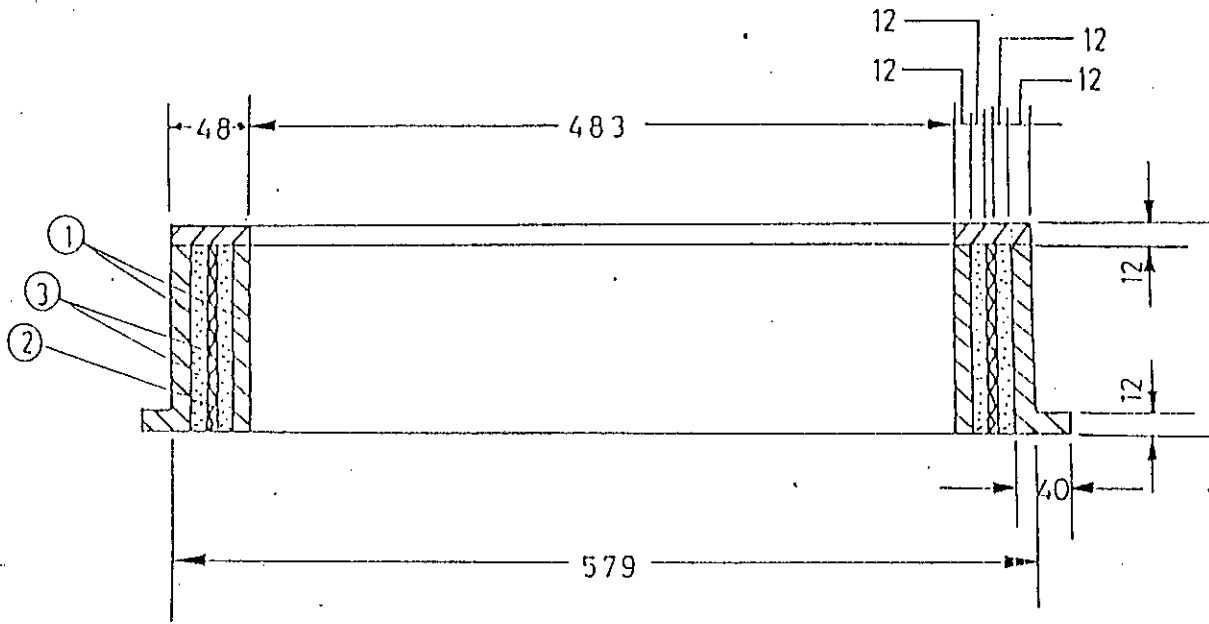
1. INNER AND OUTER WOODEN RING.
2. UPPER OUTER GUARD HEATER.
3. INNER AND OUTER ASBESTOS RING.

FIG:4.4 DETAILS OF UPPER GUARD HEATER RING.
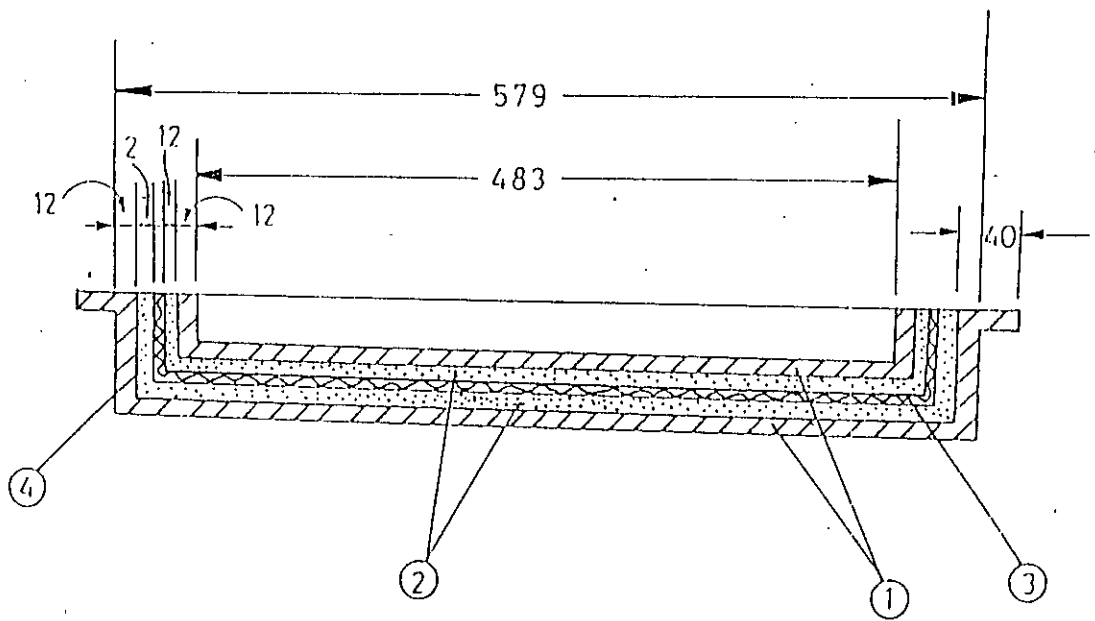
1. INNER AND OUTER WOODEN BOX.
2. ASBESTOS INSULATION.
3. BOTTOM GUARD HEATER.
4. LOWER OUTER GUARD HEATER. RING

FIG.4.5 DETAILS OF LOWER OUTER GUARD HEATER BOX.
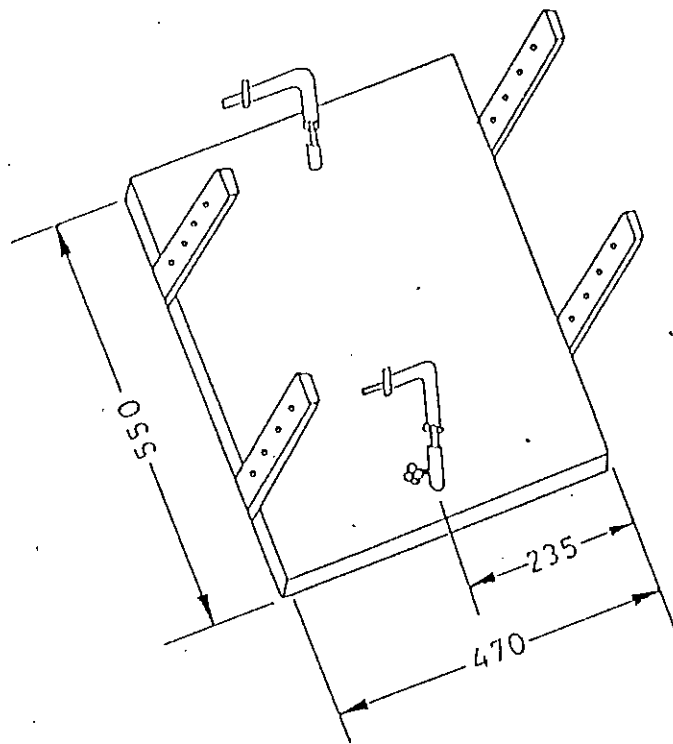
FIG:4.6 DETAILS OF THE COLD PLATE ASSEMBLY
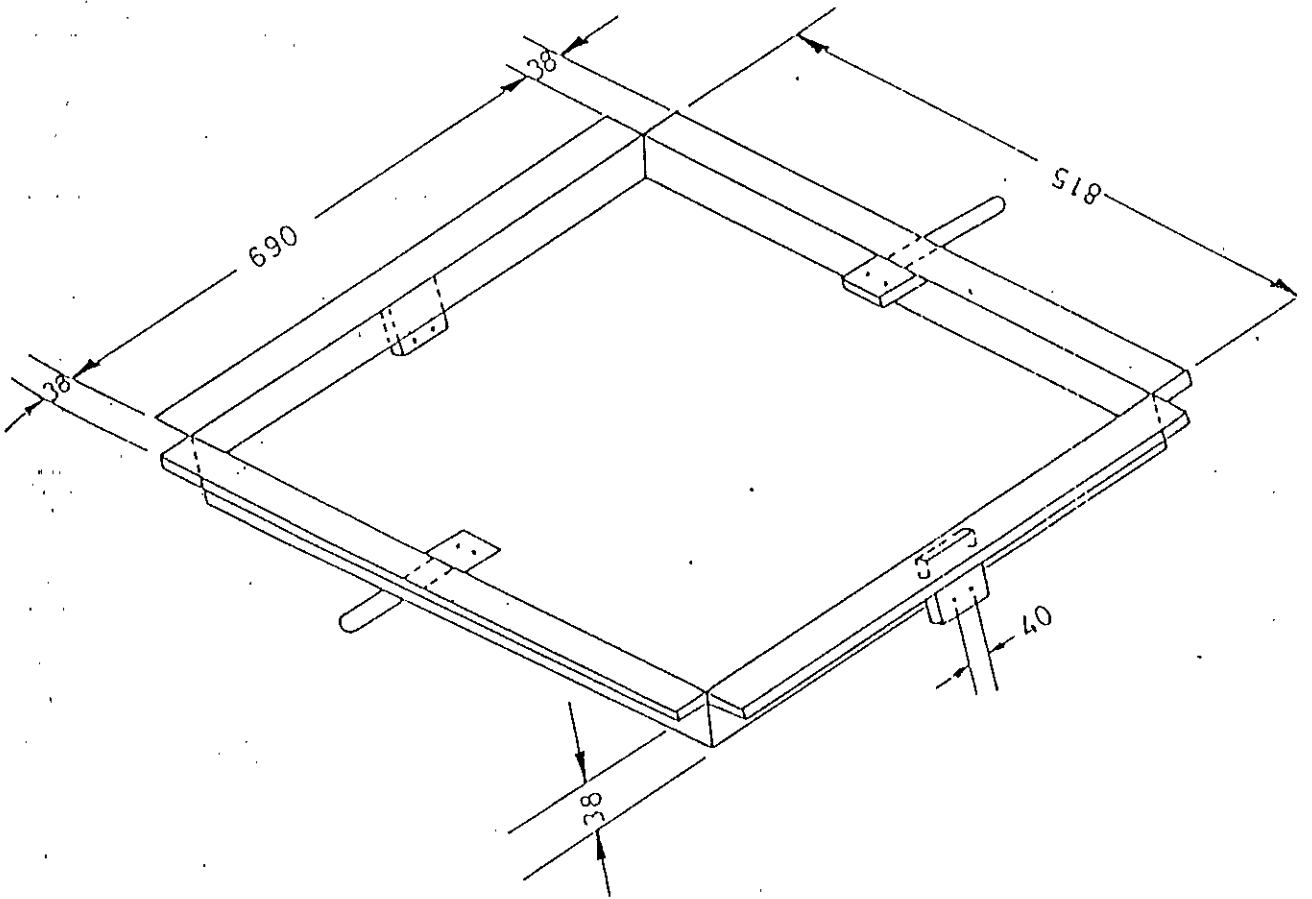
FIG: 4.7   THE RECTANGULAR SUPPORTING FRAME
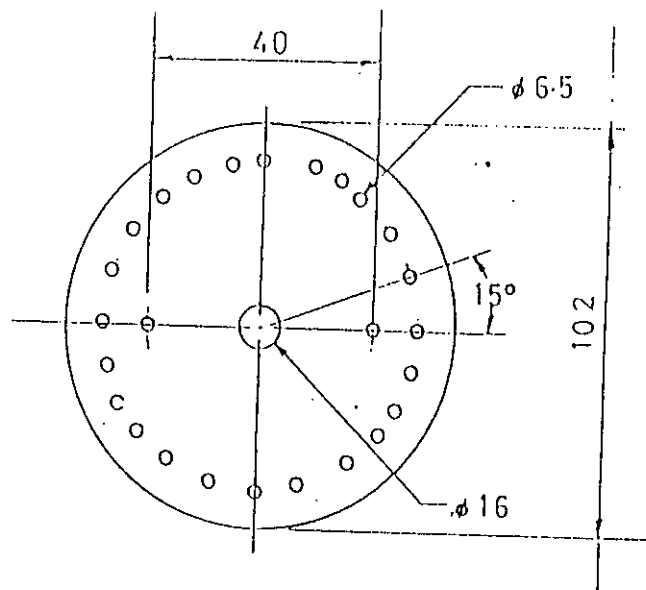
FIG.4.8 ALIGNMENT PLATE
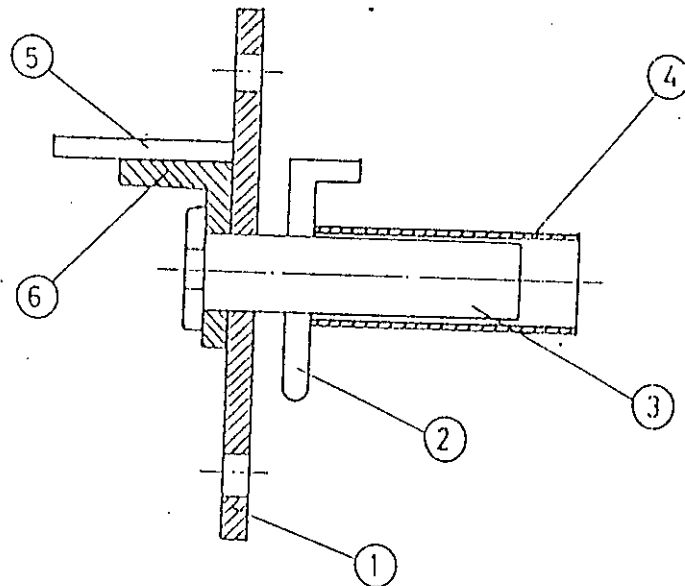
1. ALIGNMENT PLATE
2. SUPPORTING STAND
3. SUPPORTING BOLT
4. SUPPORTING BOLT HOLDER
5. SUPPORTING FRAME
6. OVER HANGING SIDE SUPPORT

FIG4.9 CONNECTING ASSEMBLY OF RECTANGULAR SUPPORTING
FRAME AND SUPPORTING STAND.
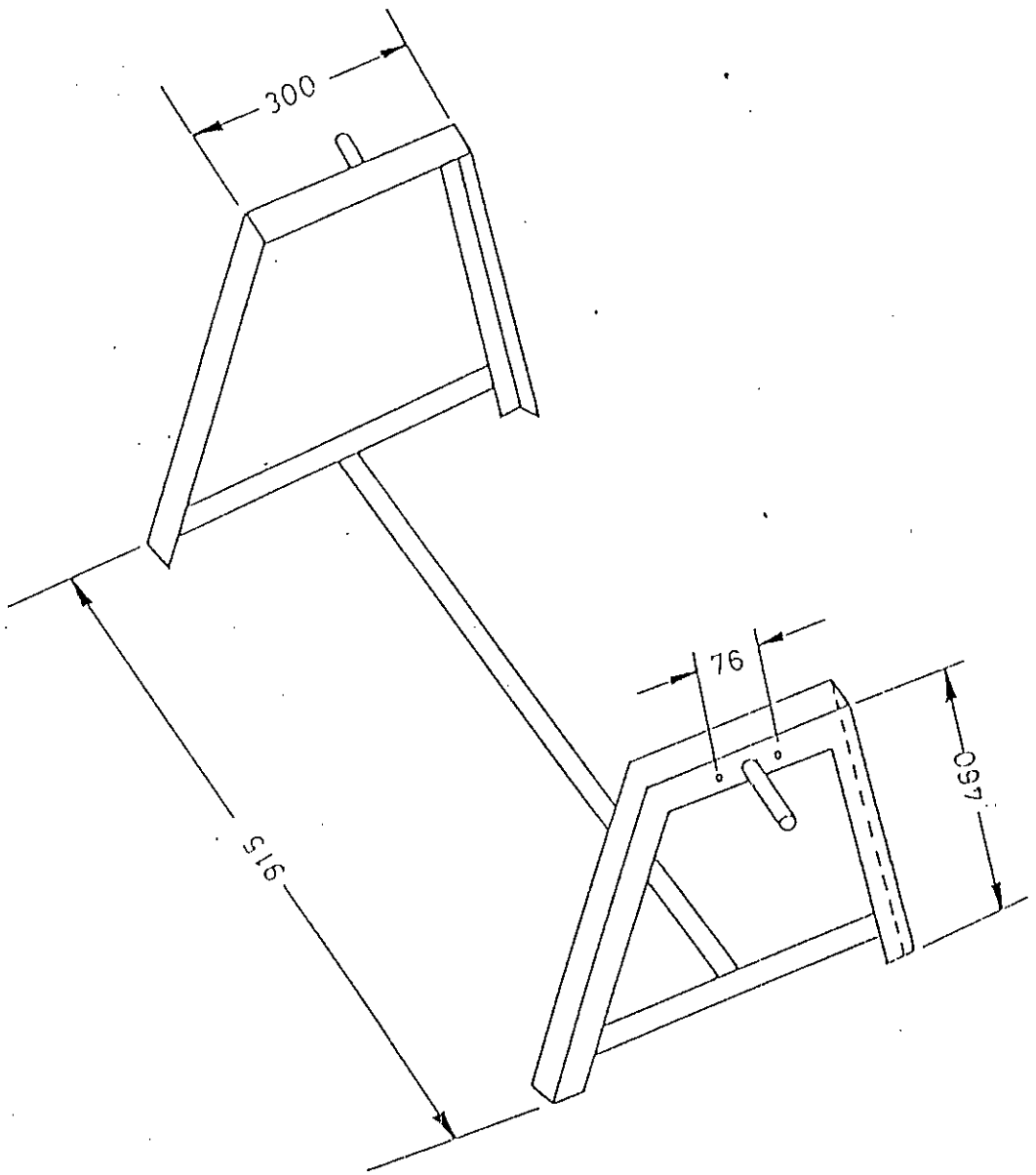
FIG:4.10 THE SUPPORTING FRAME
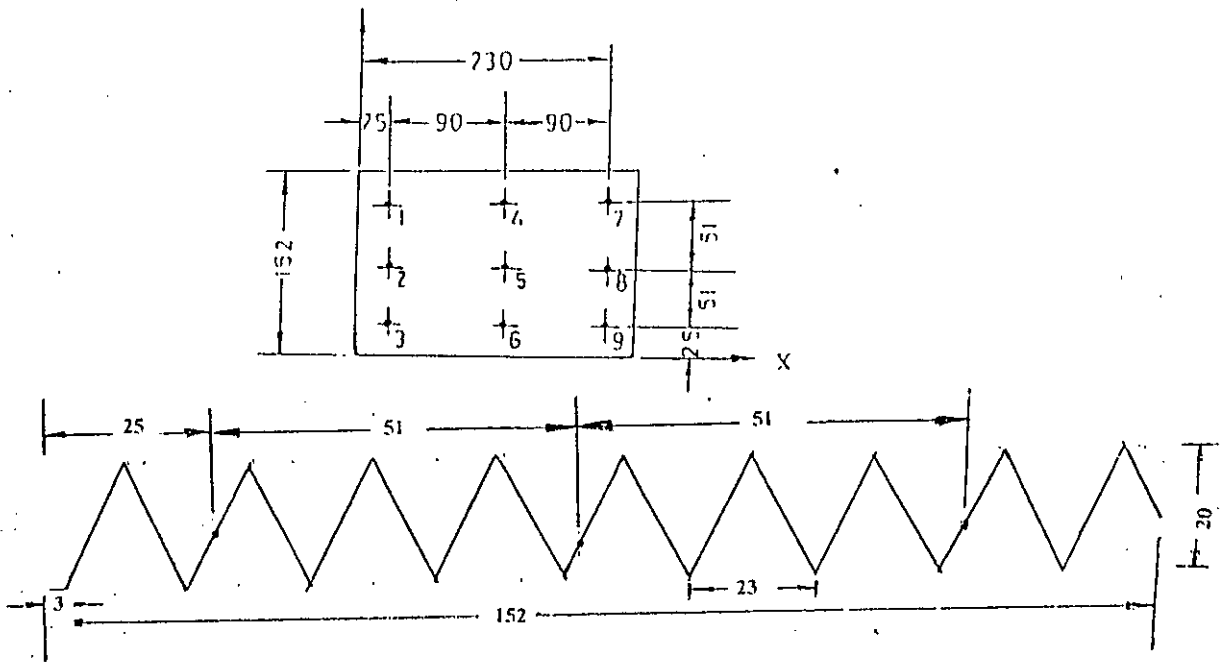
POSITION OF THERMOCOUPLES IN THE TEST SECTION OF THE HOT VEE CORRUGATED PLATE OF H = 10 MM
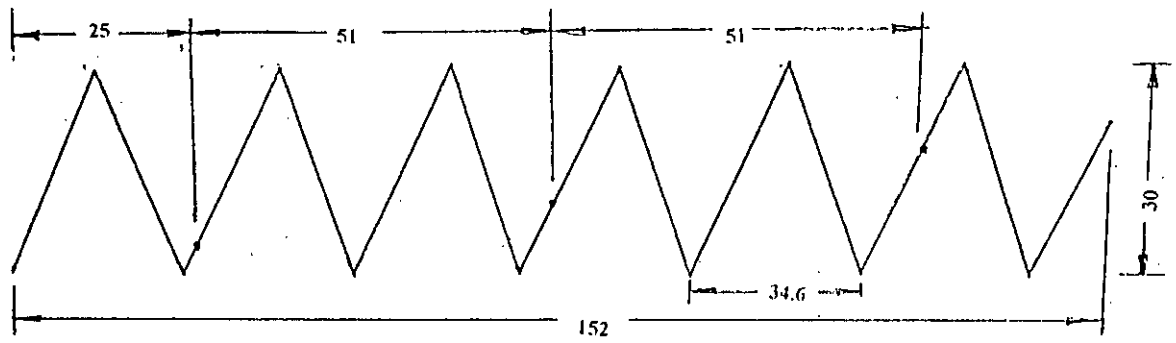
POSITION OF THERMOCOUPLES IN THE TEST SECTION OF THE HOT VEE CORRUGATED PLATE OF H = 15 MM
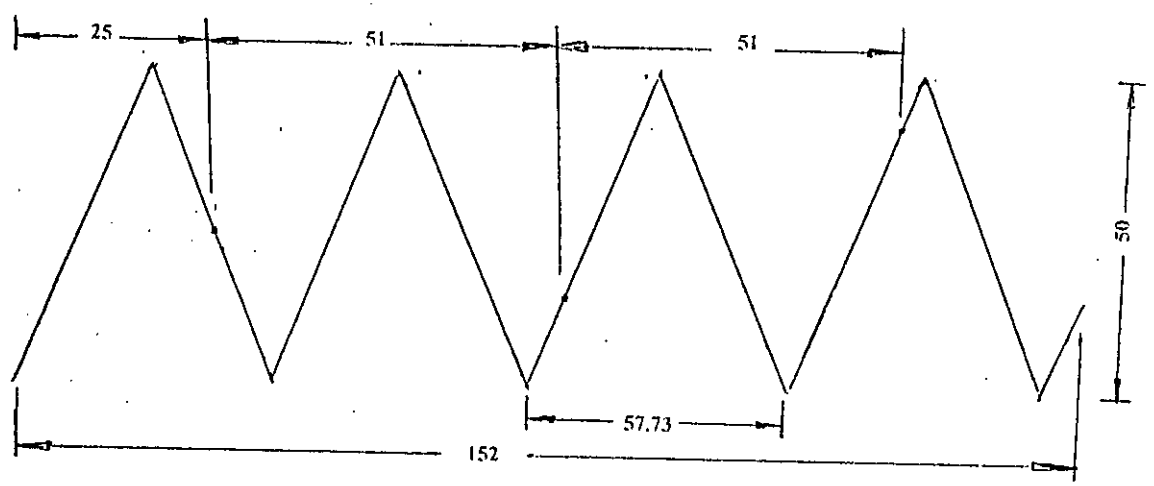
POSITION OF THERMOCOUPLES IN THE TEST SECTION OF THE HOT VEE CORRUGATED PLATE OF H = 25 MM

FIG. 5.1 : POSITION OF THERMOCOUPLES IN THE TEST SECTION OF HOT PLATE
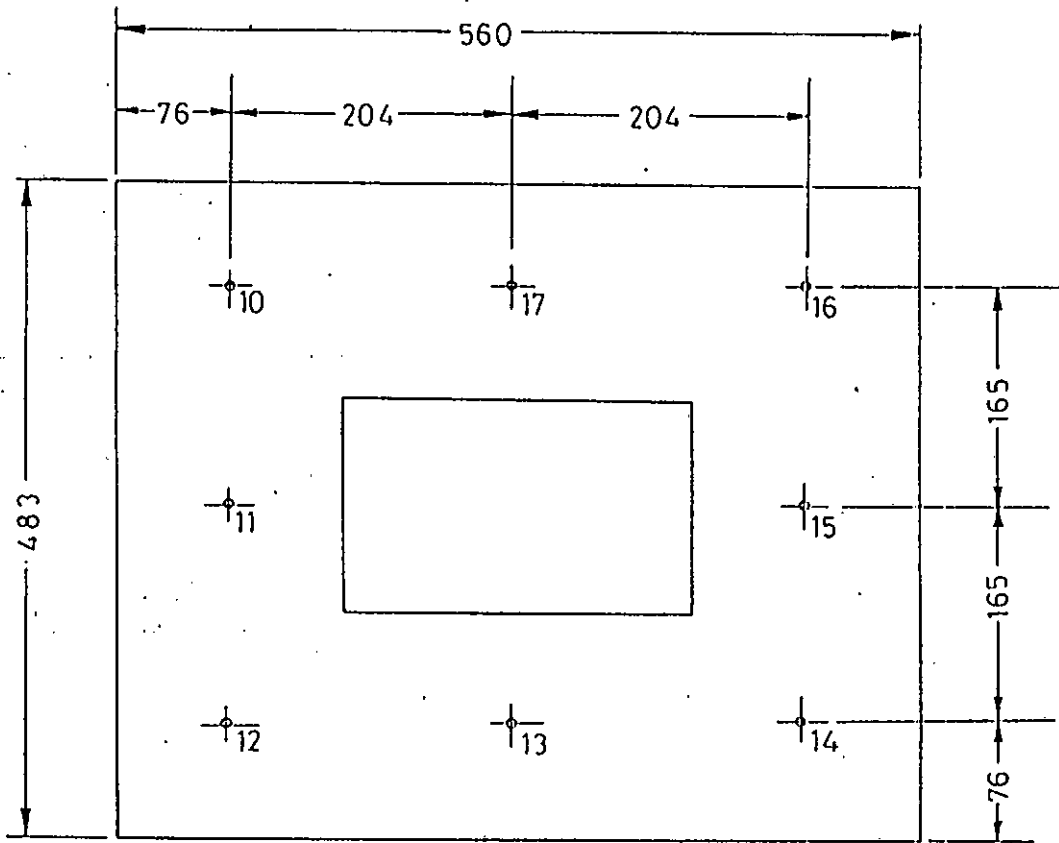
FIG:52 POSITION OF THERMOCOUPLES IN OUTER END AND
SIDE GUARD HEATER SECTIONS

FIG:5.3 POSITION OF THERMO COUPLES IN UPPER
OUTER GUARD HEATER RING.
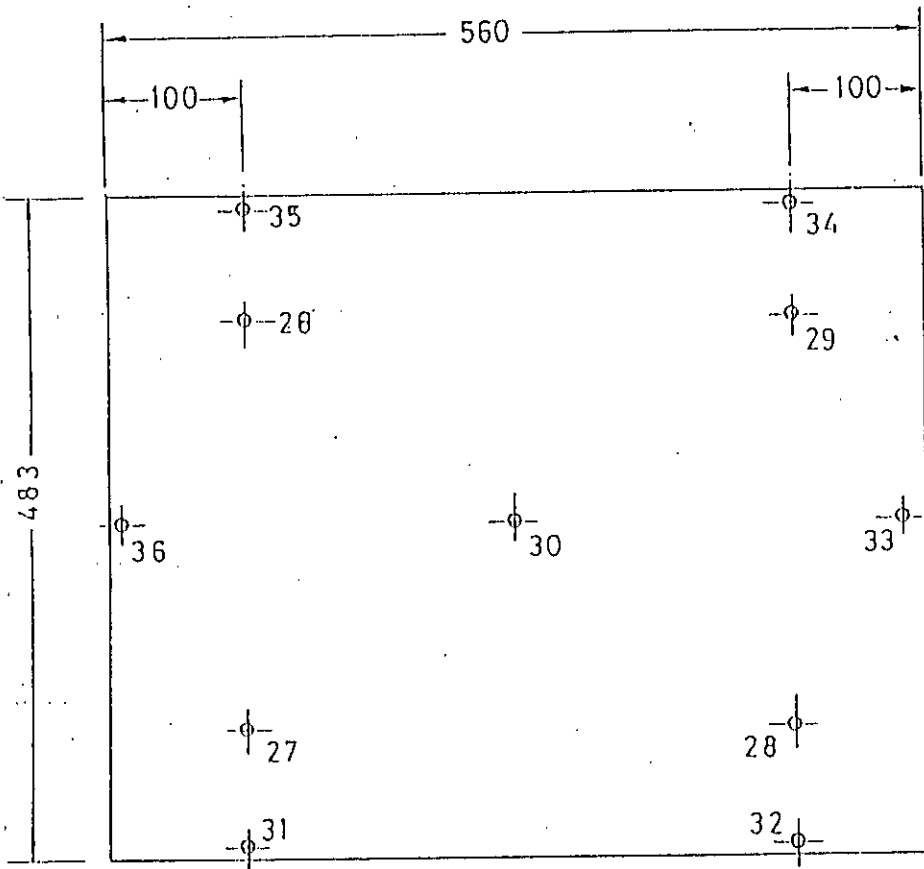
FIG.54 POSITION OF THERMOCOUPLES IN LOWER OUTER-GUARD HEATER BOX
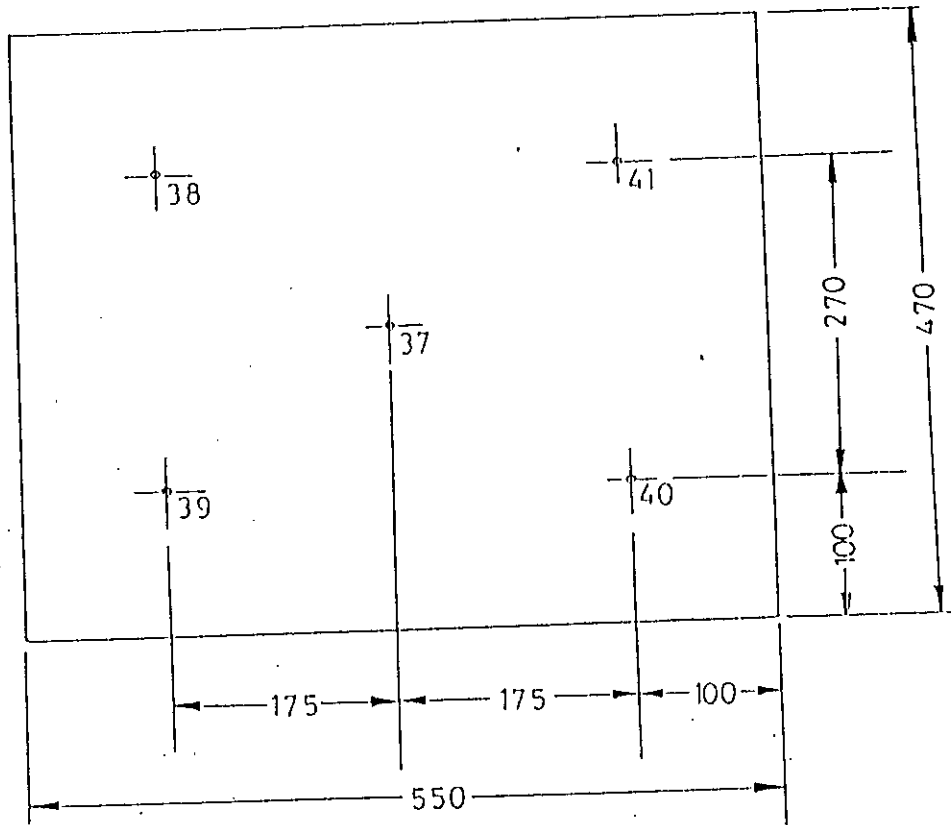
FIG:5.5 POSITION OF THERMO COUPLES IN
COLD FLAT PLATE.
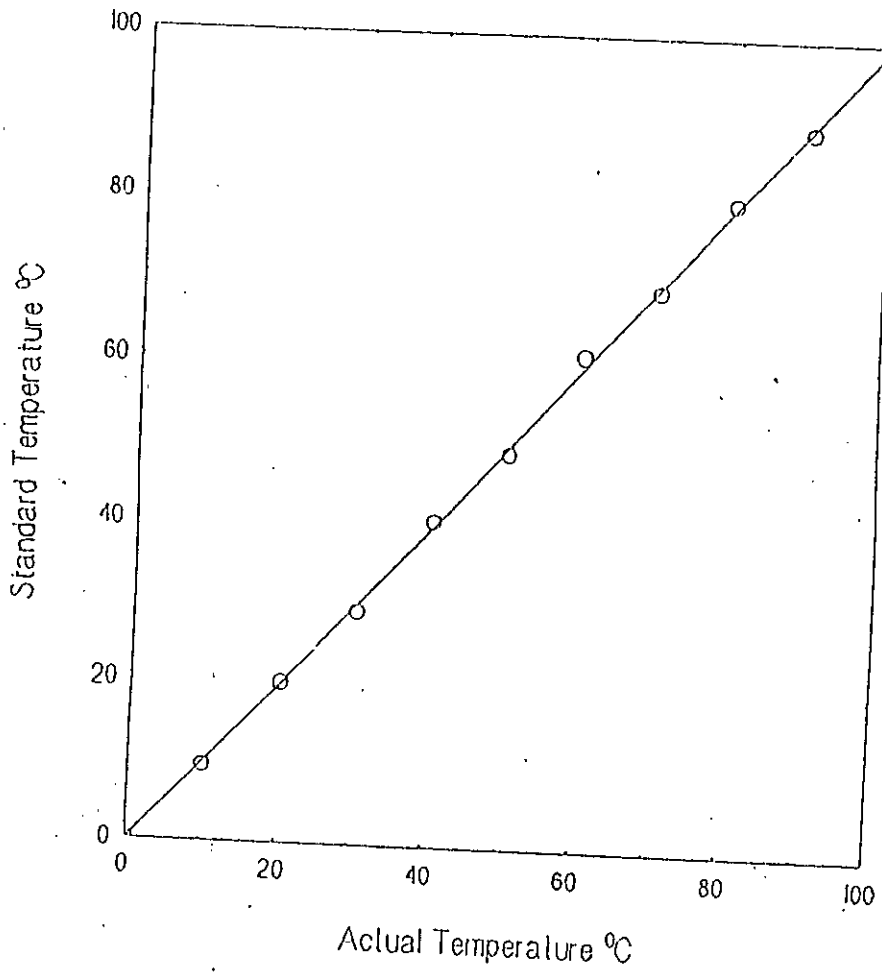
FIG. 5.6:   THERMOCOUPLE   CALIBRATION   CURVE   FOR
THERMOCOUPLE NO. 5.
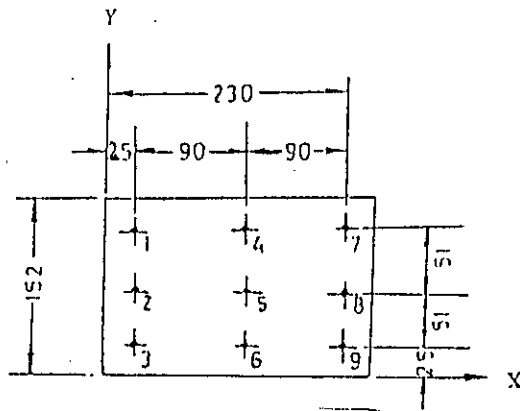
POSITION OF THERMO COUPLES IN THE TEST
SECTION OF THE HOT VEE CORRUGATED PLATE

H = 10mm, θ= 0⁰

Y_{COR} = 127 mm

X_{COR} = 205 mm

Y_{COR} = 76 mm

X_{COR} = 115 mm

Y_{COR} = 25 mm

X_{COR} = 25 mm

TEMPERATURE ⁰C

X_{COR}

Y_{COR} mm
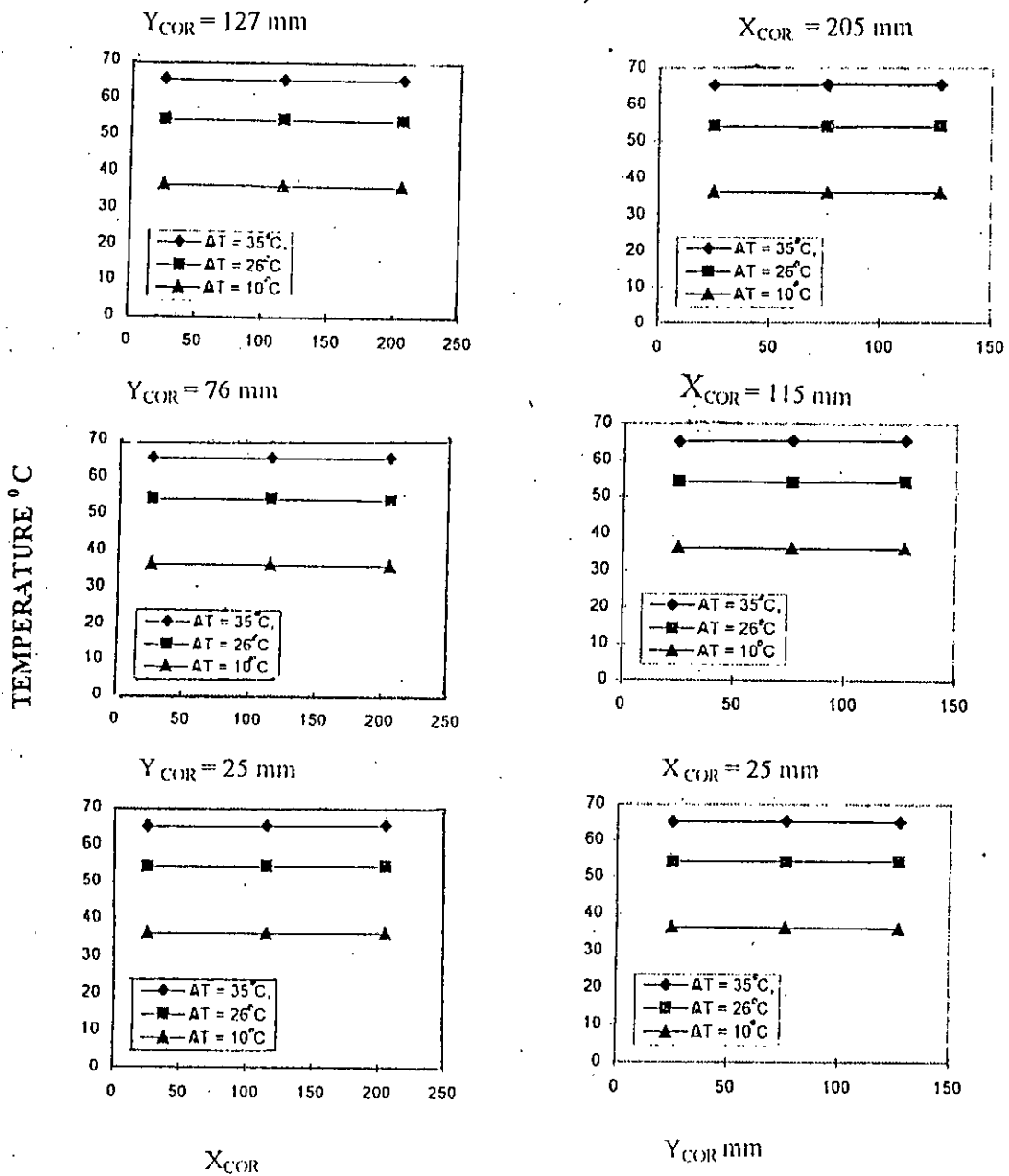
FIG. 6.1 : TEMPERATURE DISTRIBUTION OVER THE TEST SECTION OF THE HOT VEE CORRUGATED
PLATE FOR H = 10 mm.
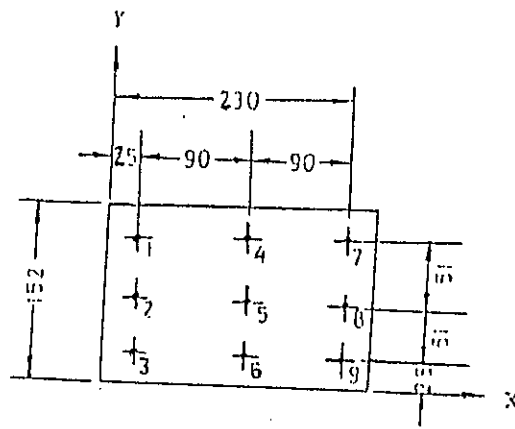
POSITION OF THERMO COUPLES IN THE TEST
SECTION OF THE HOT VEE CORRUGATED PLATE

$$H = 15mm, \theta = 0^0$$
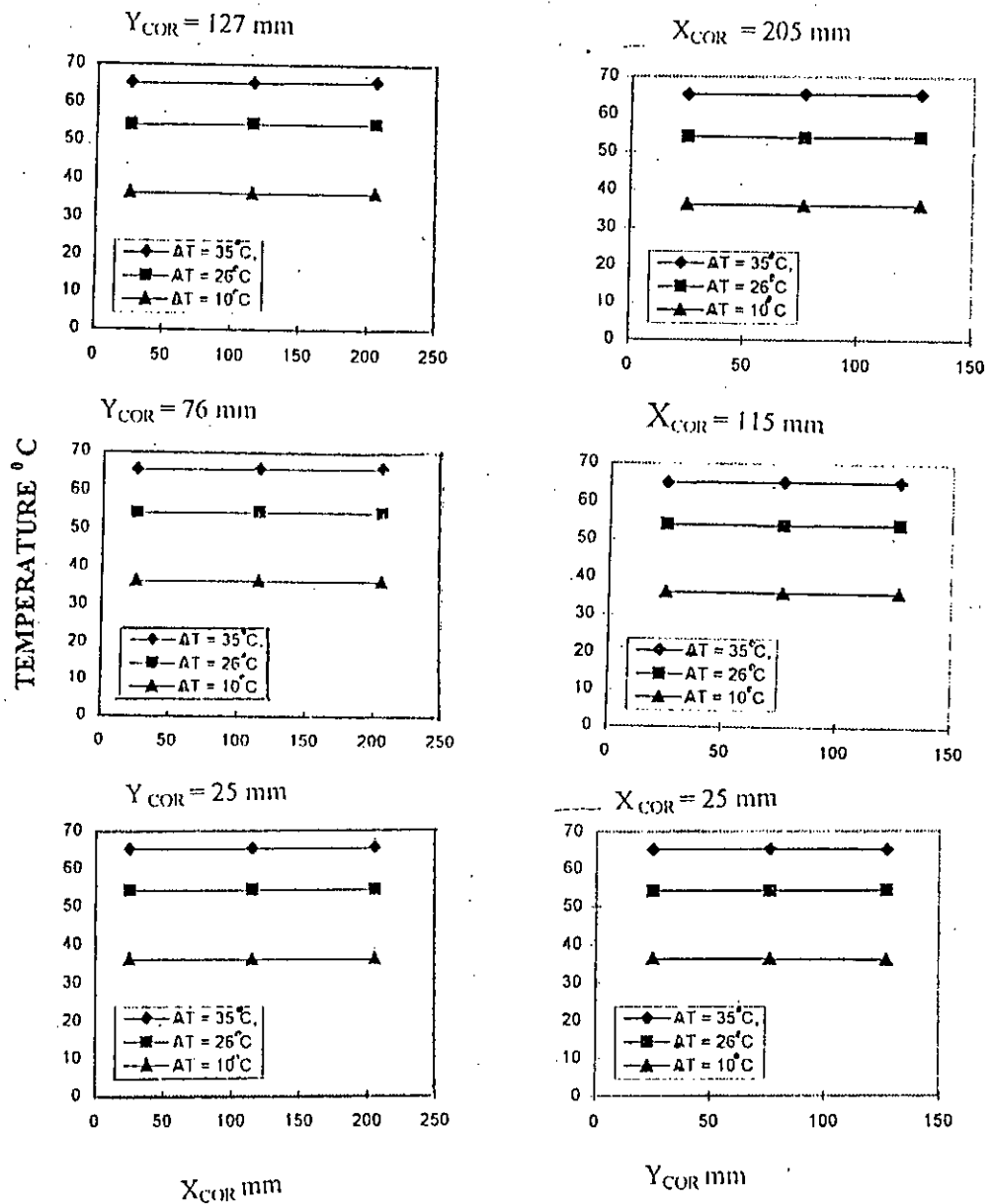
FIG. 6.2 : TEMPERATURE DISTRIBUTION OVER THE TEST SECTION OF THE HOT VEE CORRUGATED
PLATE FOR H = 15 mm.
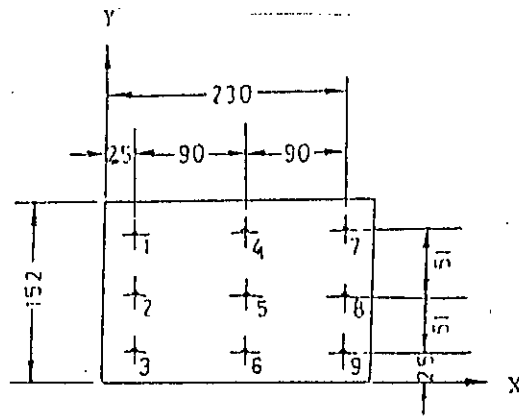
POSITION OF THERMO COUPLES IN THE TEST
SECTION OF THE HOT VEE CORRUGATED PLATE

$$H = 25mm, \theta = 0^0$$
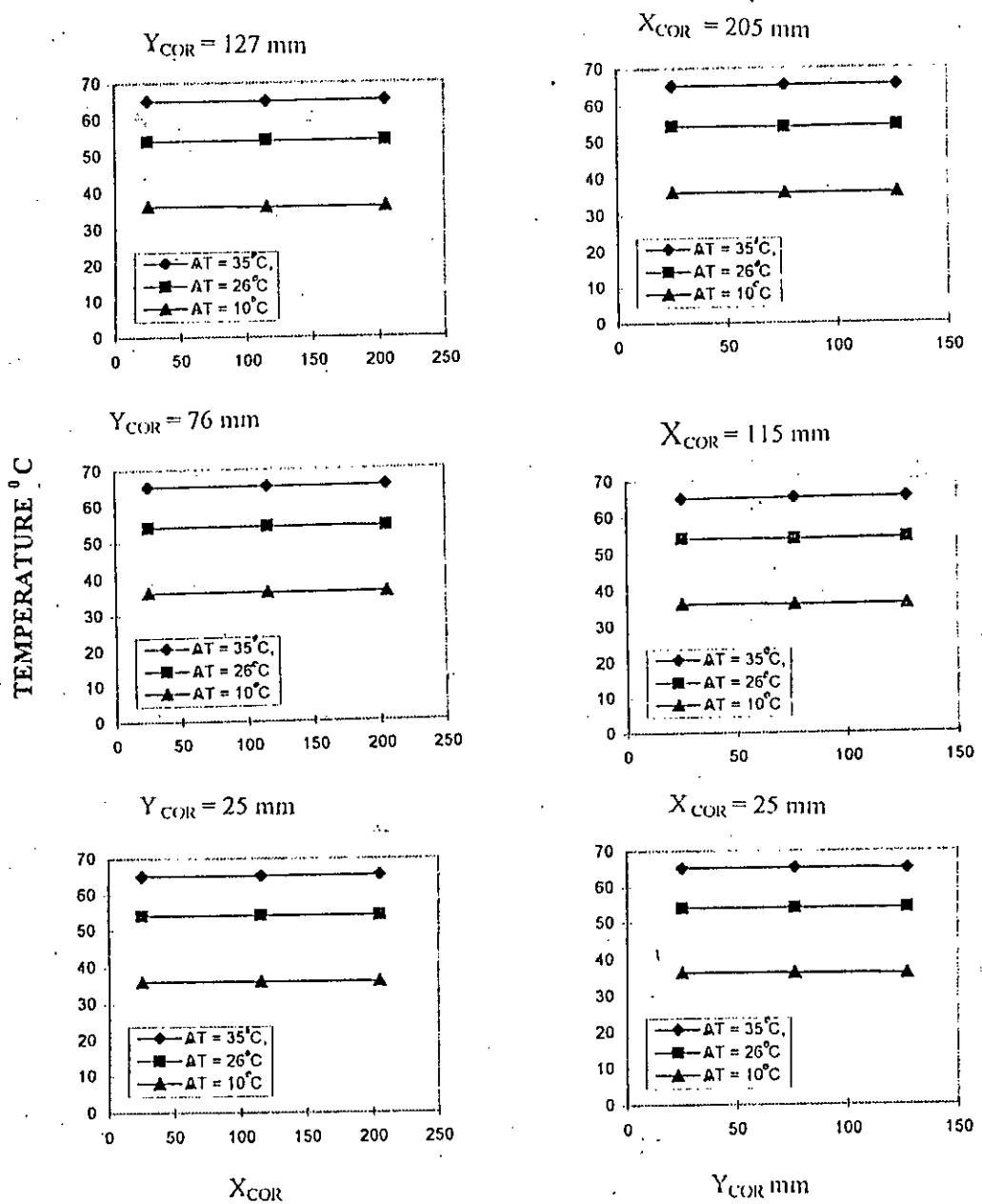
FIG. 6.3 : TEMPERATURE DISTRIBUTION OVER THE TEST SECTION OF THE HOT VEE CORRUGATED
PLATE FOR H = 25 mm.
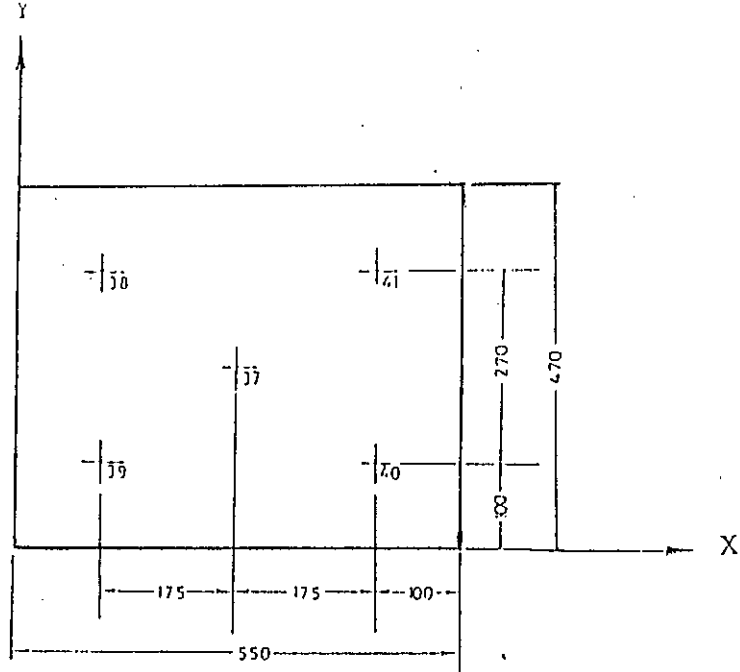
POSITION OF THERMO COUPLES IN COLD FLAT PLATE.

$$H = 10mm, \theta = 0^0$$
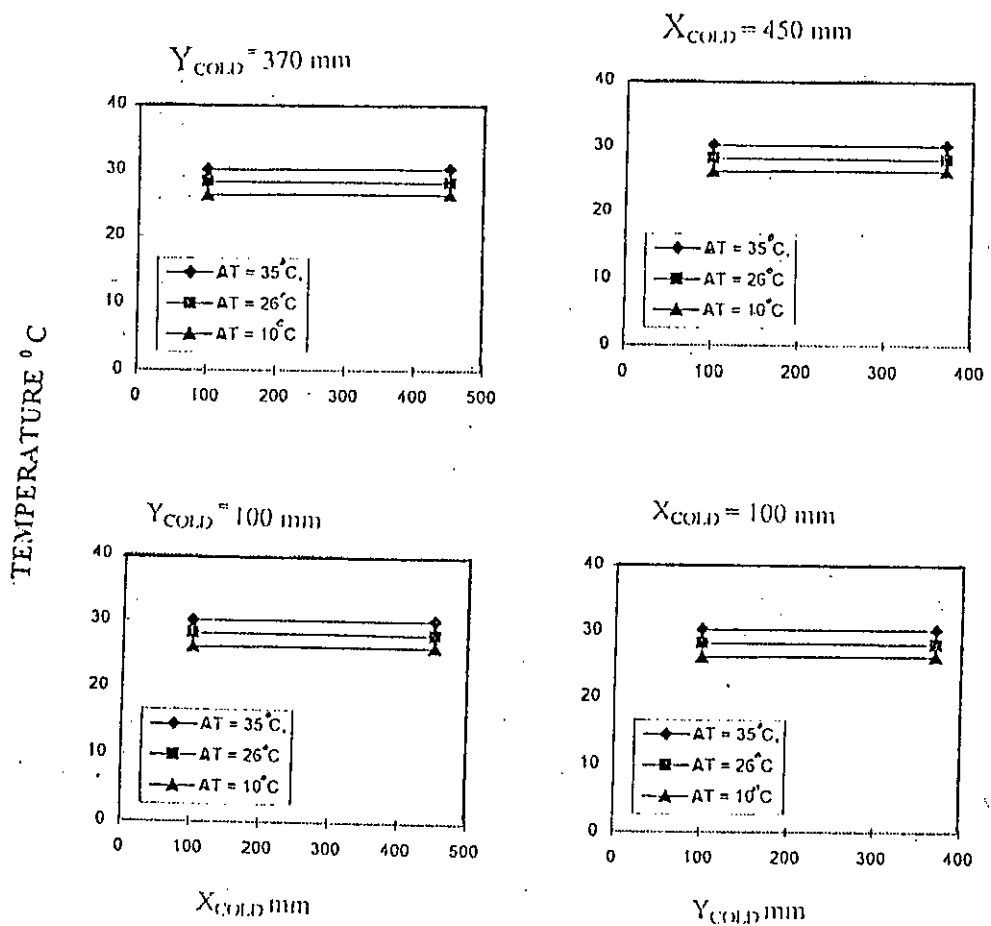
FIG. 6.4 : TEMPERATURE DISTRIBUTION OVER THE COLD FLAT PLATE FOR H = 10 mm.

POSITION OF THERMO COUPLES IN COLD FLAT PLATE

$$H = 15mm, \theta = 0^0$$
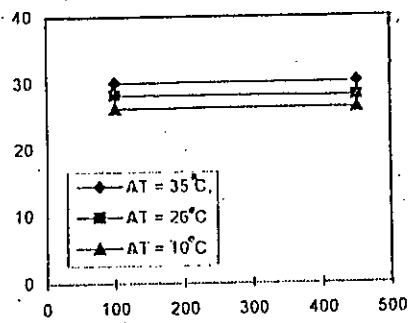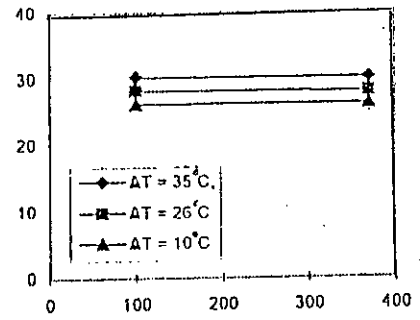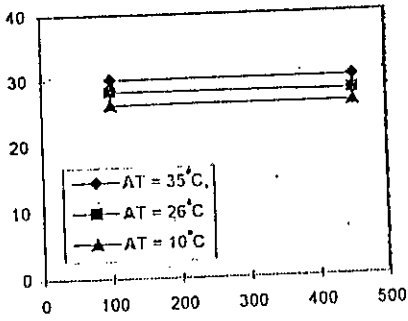
FIG. 6.5 : TEMPERATURE DISTRIBUTION OVER THE COLD FLAT PLATE FOR H = 15 mm.

POSITION OF THERMO COUPLES IN COLD FLAT PLATE

$H = 25mm, \theta = 0^0$

$Y_{COLD} = 370$ mm

$X_{COLD} = 450$ mm

AT = 35°C
AT = 26°C
AT = 10°C

$Y_{COLD} = 100$ mm

$X_{COLD} = 100$ mm

AT = 35°C
AT = 26°C
AT = 10°C

TEMPERATURE °C

X_{COLD} mm

Y_{COLD} mm
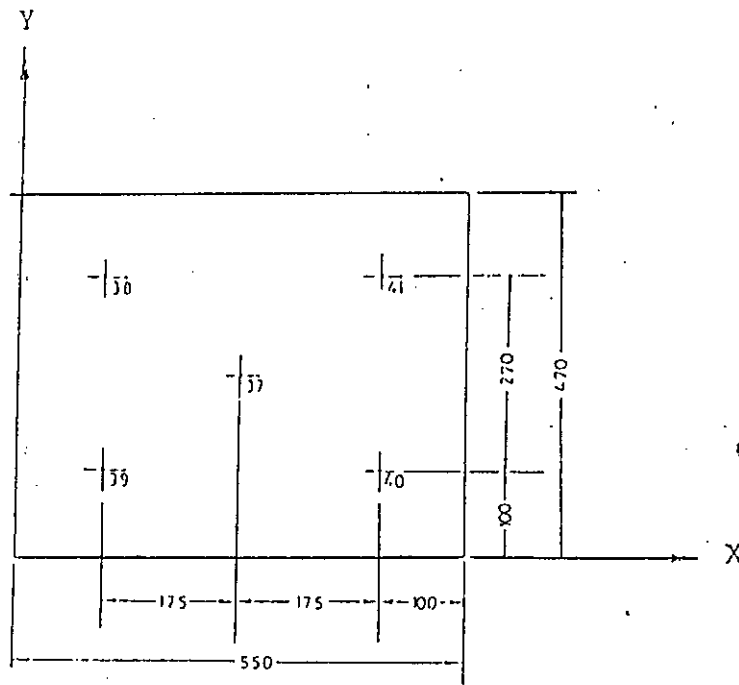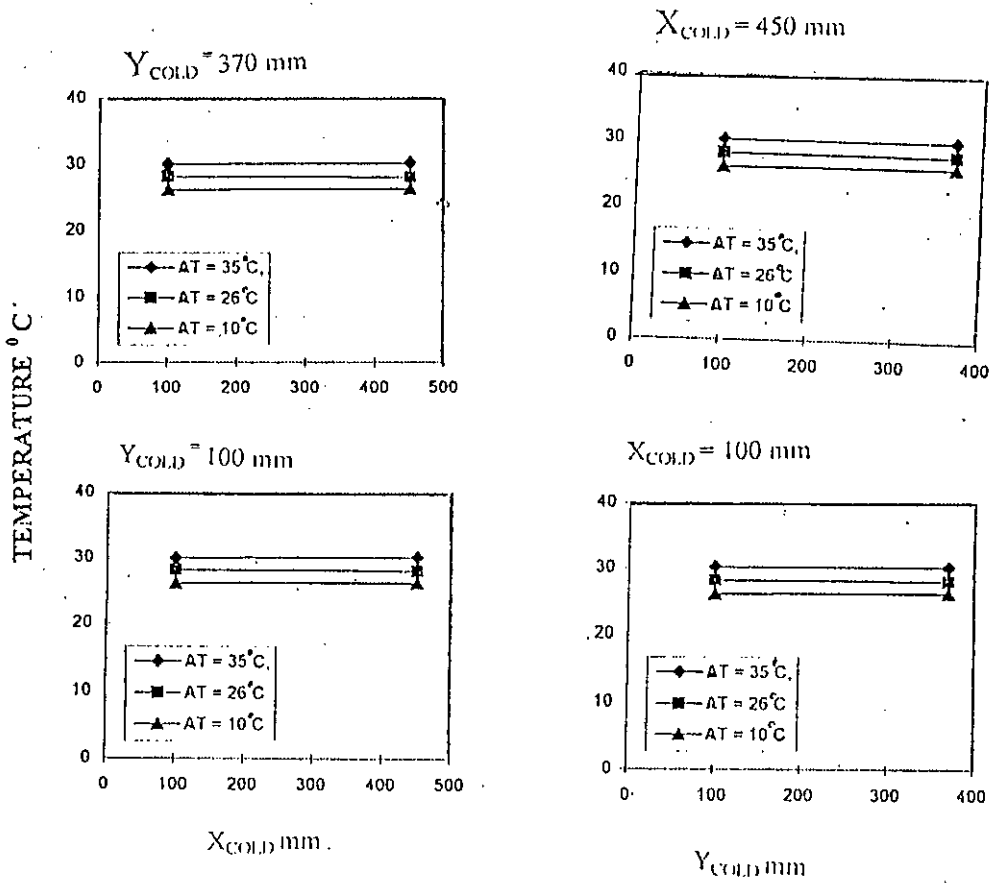
FIG. 6.6 : TEMPERATURE DISTRIBUTION OVER THE COLD FLAT PLATE FOR H = 25 mm.
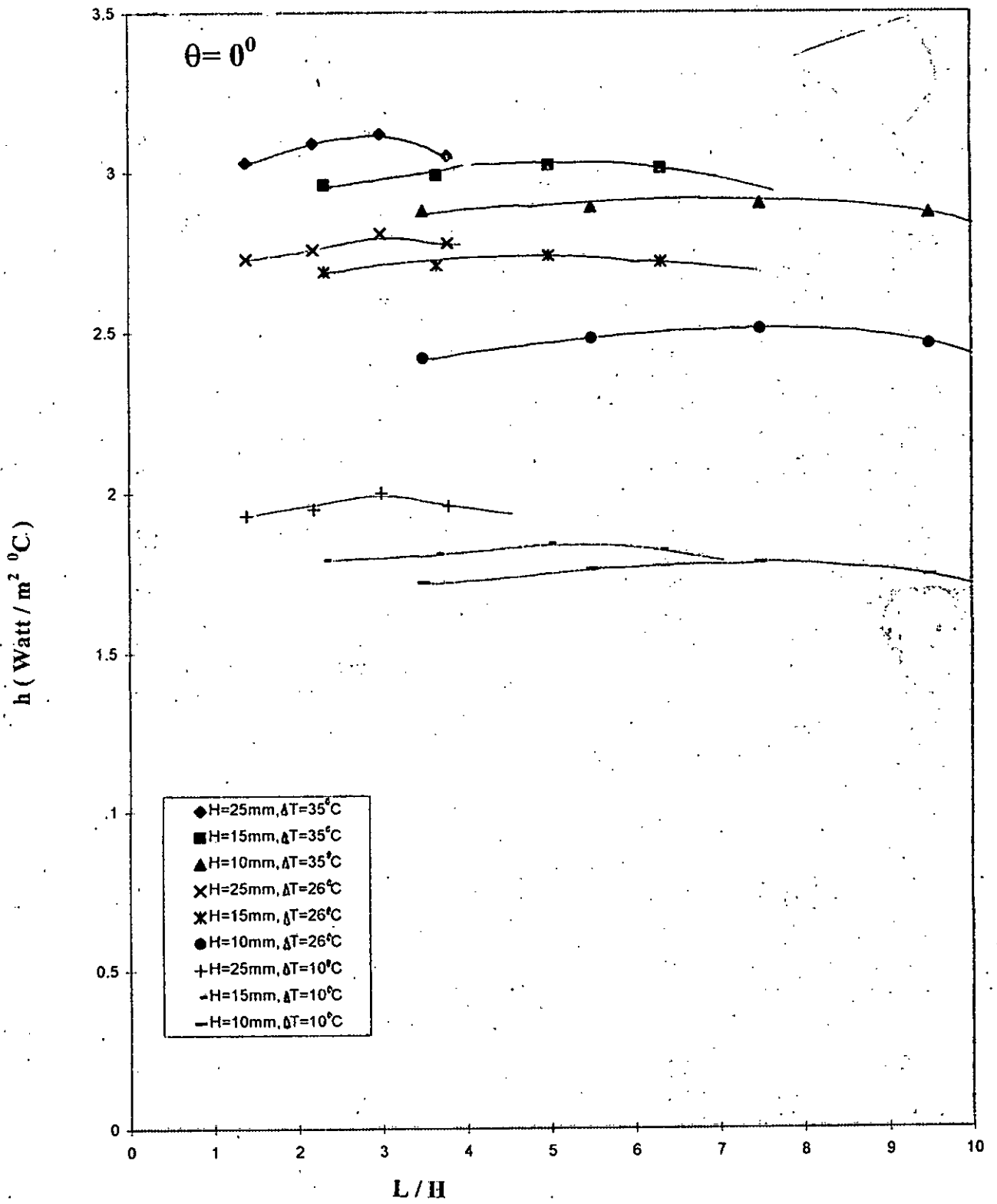
FIG 6.7 : EFFECT OF ASPECT RATIO (A) ON AVERAGE HEAT TRANSFER COEFFICIENT FOR θ = 0°.
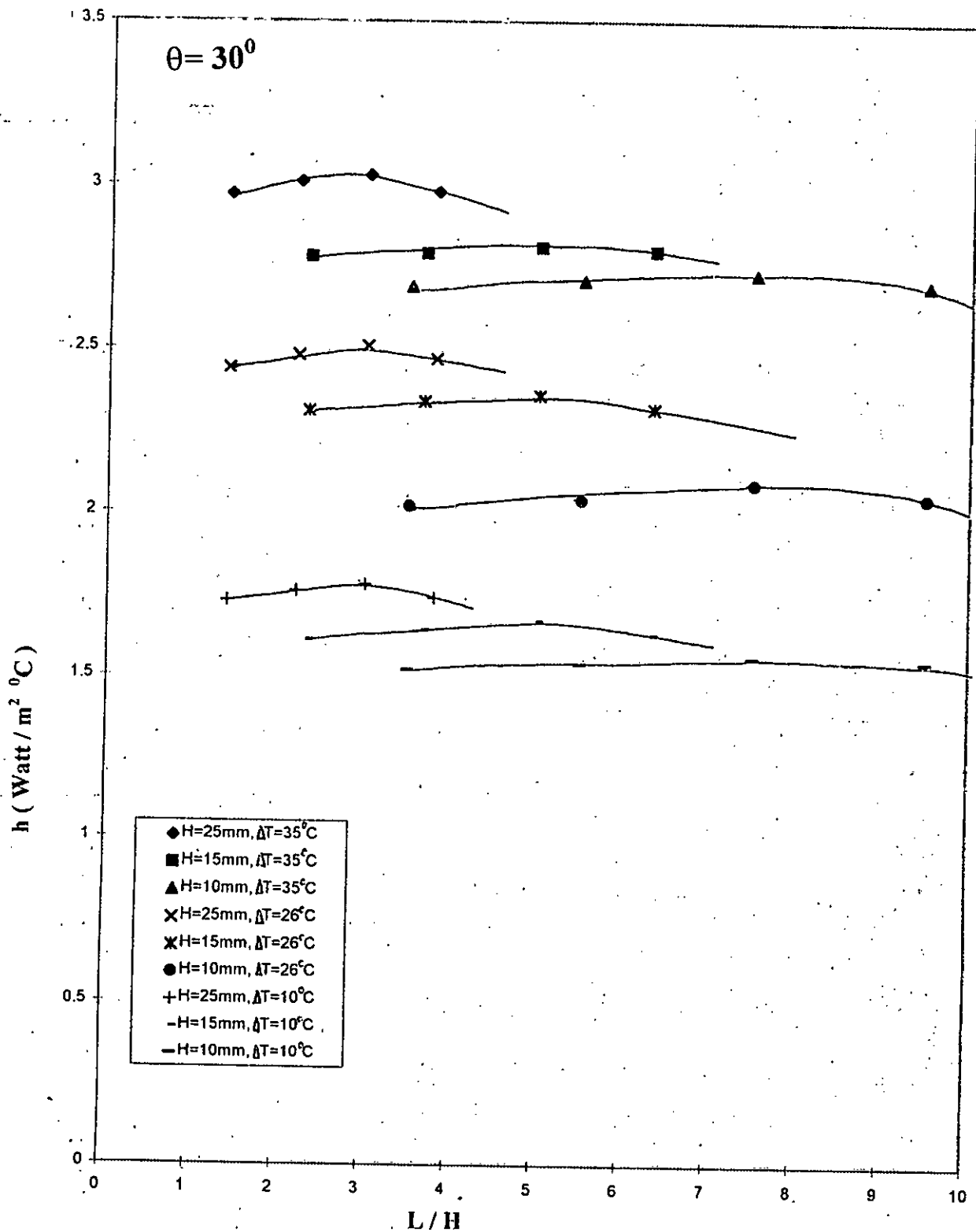
FIG 6.8 : EFFECT OF ASPECT RATIO (A) ON AVERAGE HEAT TRANSFER COEFFICIENT FOR $\theta = 30^0$

$\theta = 45^0$

Legend:
◆ H=25mm, ΔT=35°C
■ H=15mm, ΔT=35°C
▲ H=10mm, ΔT=35°C
✕ H=25mm, ΔT=26°C
✱ H=15mm, ΔT=26°C
● H=10mm, ΔT=26°C
+ H=25mm, ΔT=10°C
⌐ H=15mm, ΔT=10°C
— H=10mm, ΔT=10°C

y-axis: h (Watt / m² °C)

x-axis: L / H
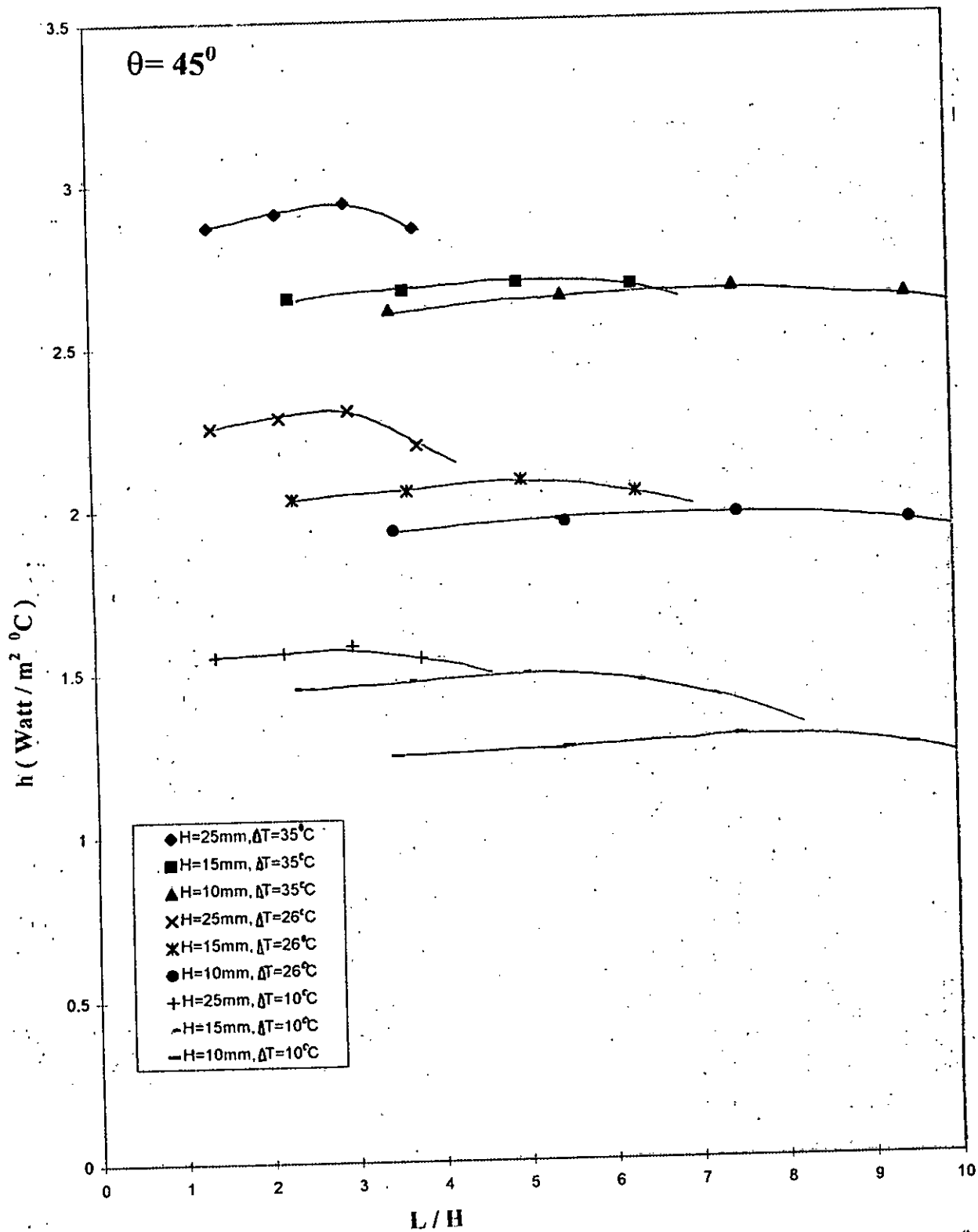
FIG 6.9 : EFFECT OF ASPECT RATIO (A) ON AVERAGE HEAT TRANSFER COEFFICIENT FOR θ =45".
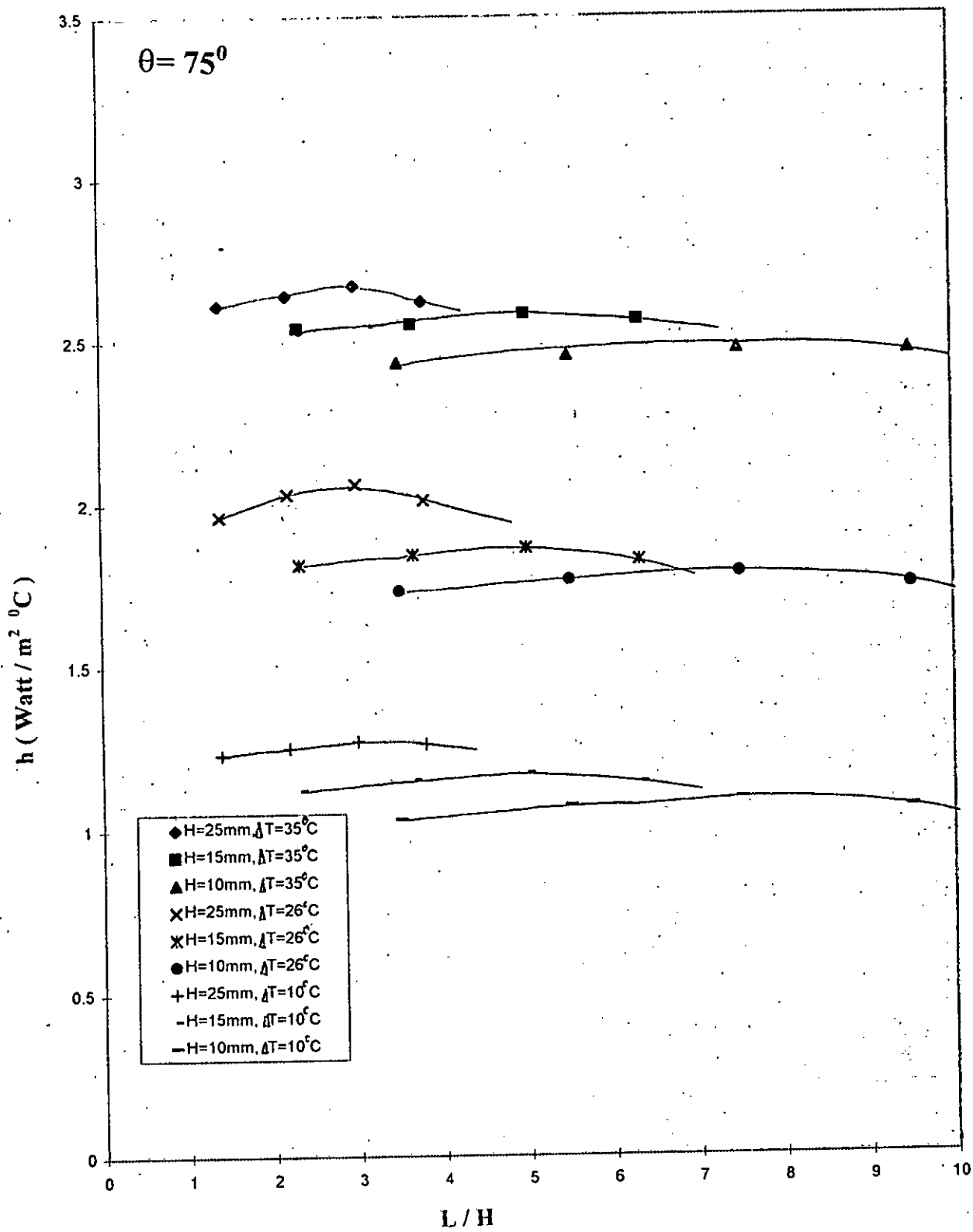
FIG 6.10 : EFFECT OF ASPECT RATIO (A) ON AVERAGE HEAT TRANSFER COEFFICIENT FOR θ =75"
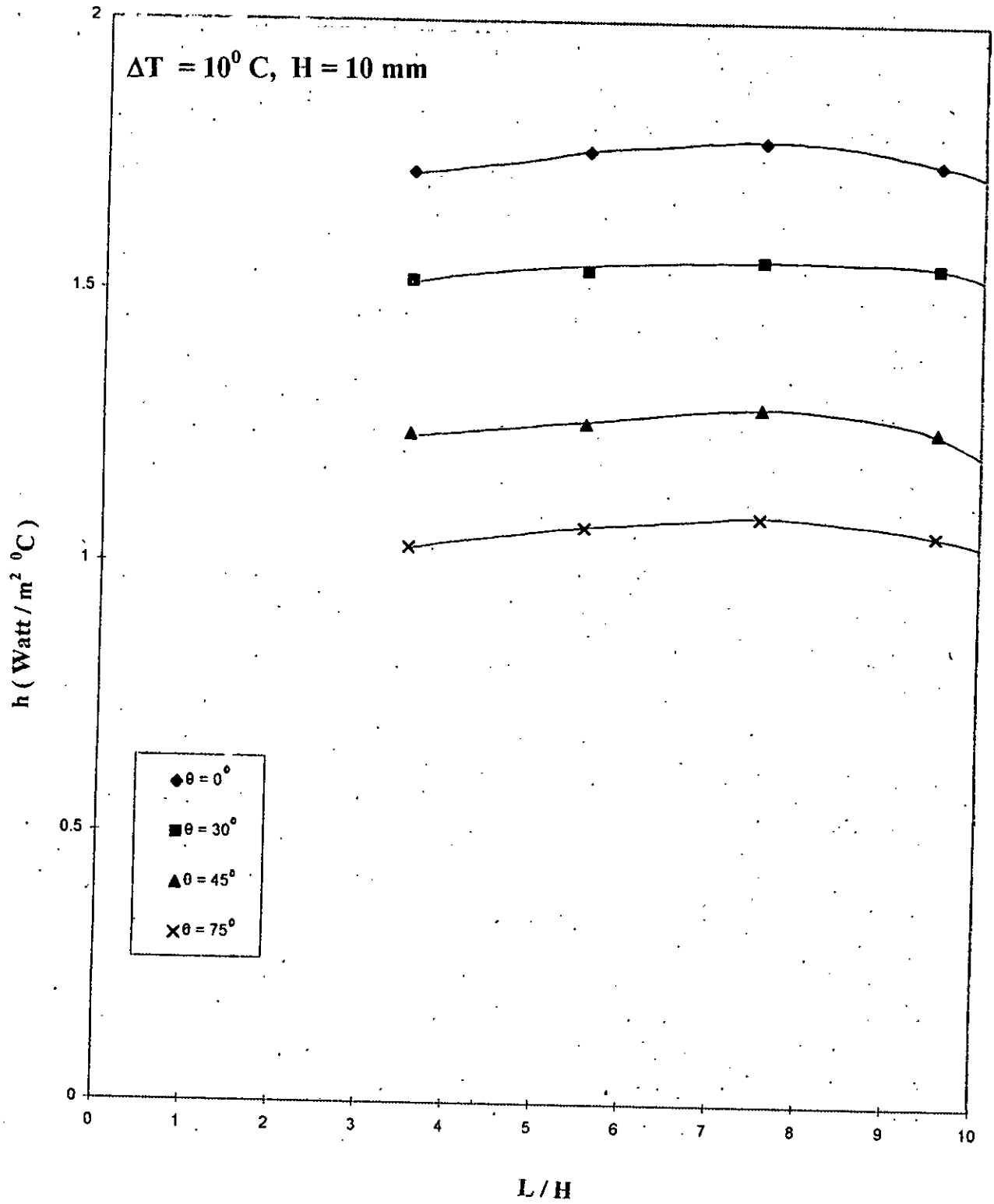
FIG 6.11 : EFFECT OF ASPECT RATIO (A) ON AVERAGE HEAT TRANSFER COEFFICIENT FOR DIFFERENT ANGLES OF INCLINATION (θ)
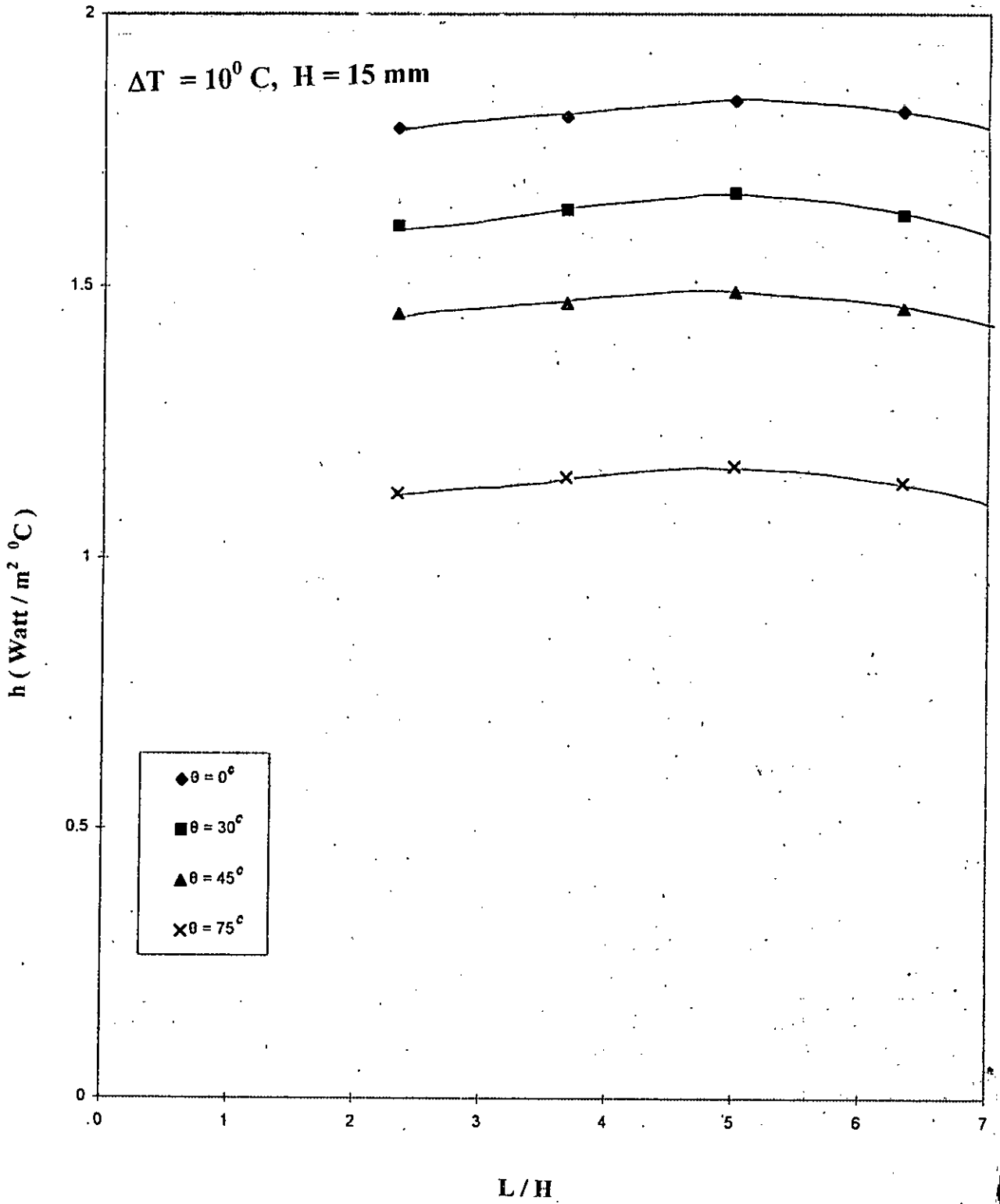
FIG 6.12 :   EFFECT OF ASPECT RATIO (A) ON AVERAGE HEAT TRANSFER COEFFICIENT FOR
DIFFERENT ANGLES OF INCLINATION (θ)
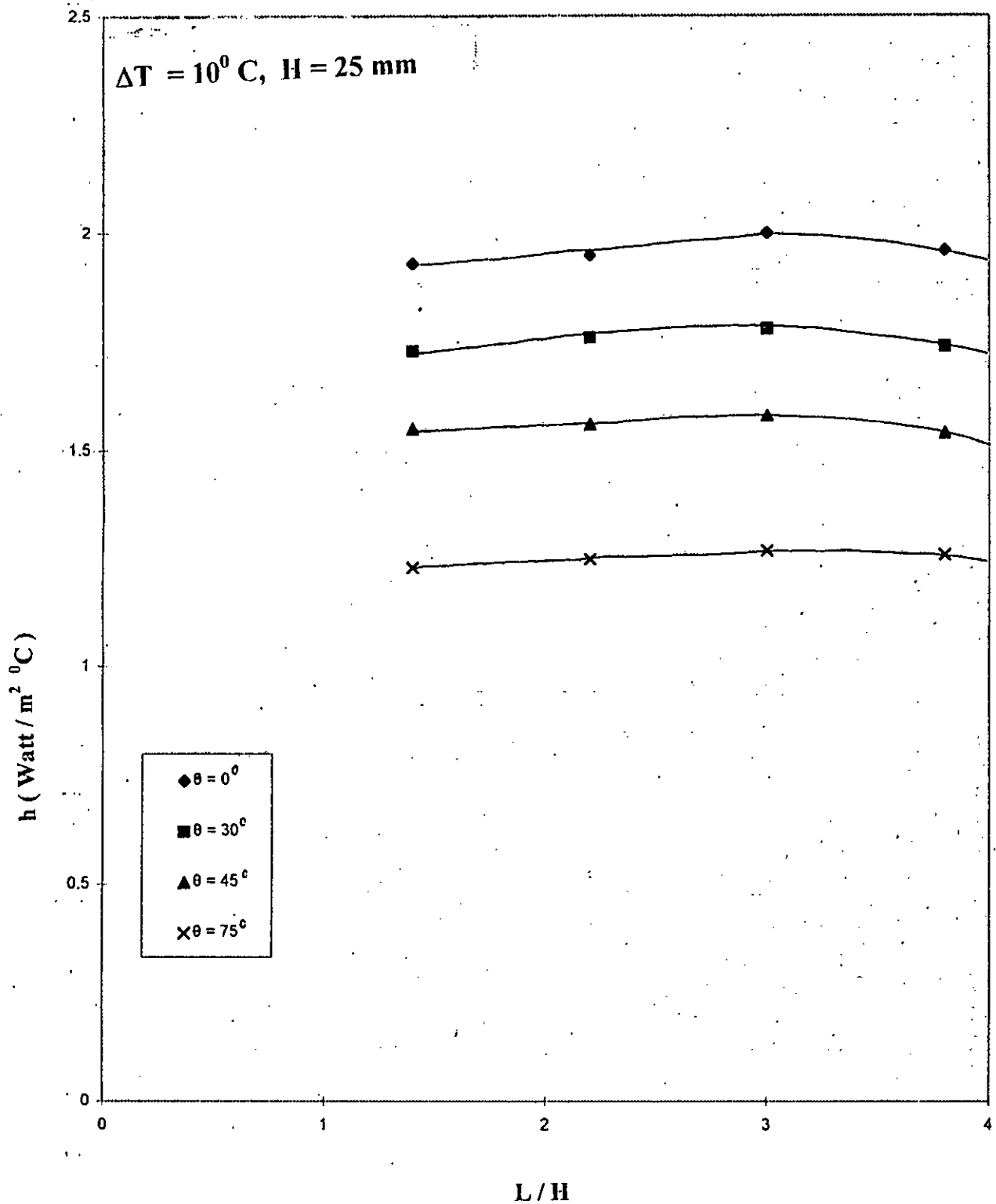
FIG 6.13 : EFFECT OF ASPECT RATIO (A) ON AVERAGE HEAT TRANSFER COEFFICIENT FOR DIFFERENT ANGLES OF INCLINATION (θ)
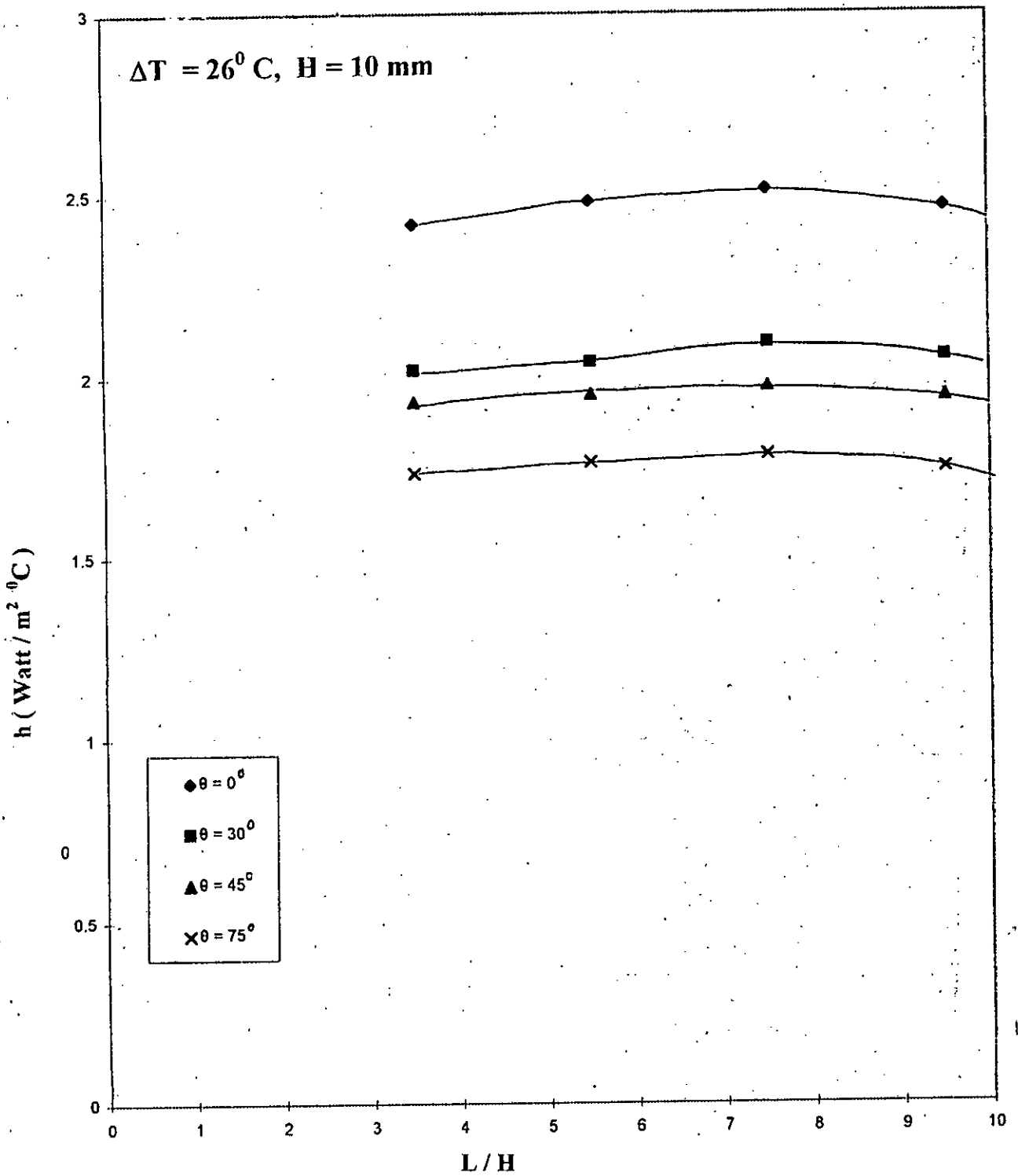
FIG 6.14 : EFFECT OF ASPECT RATIO (A) ON AVERAGE HEAT TRANSFER COEFFICIENT FOR DIFFERENT ANGLES OF INCLINATION (θ)
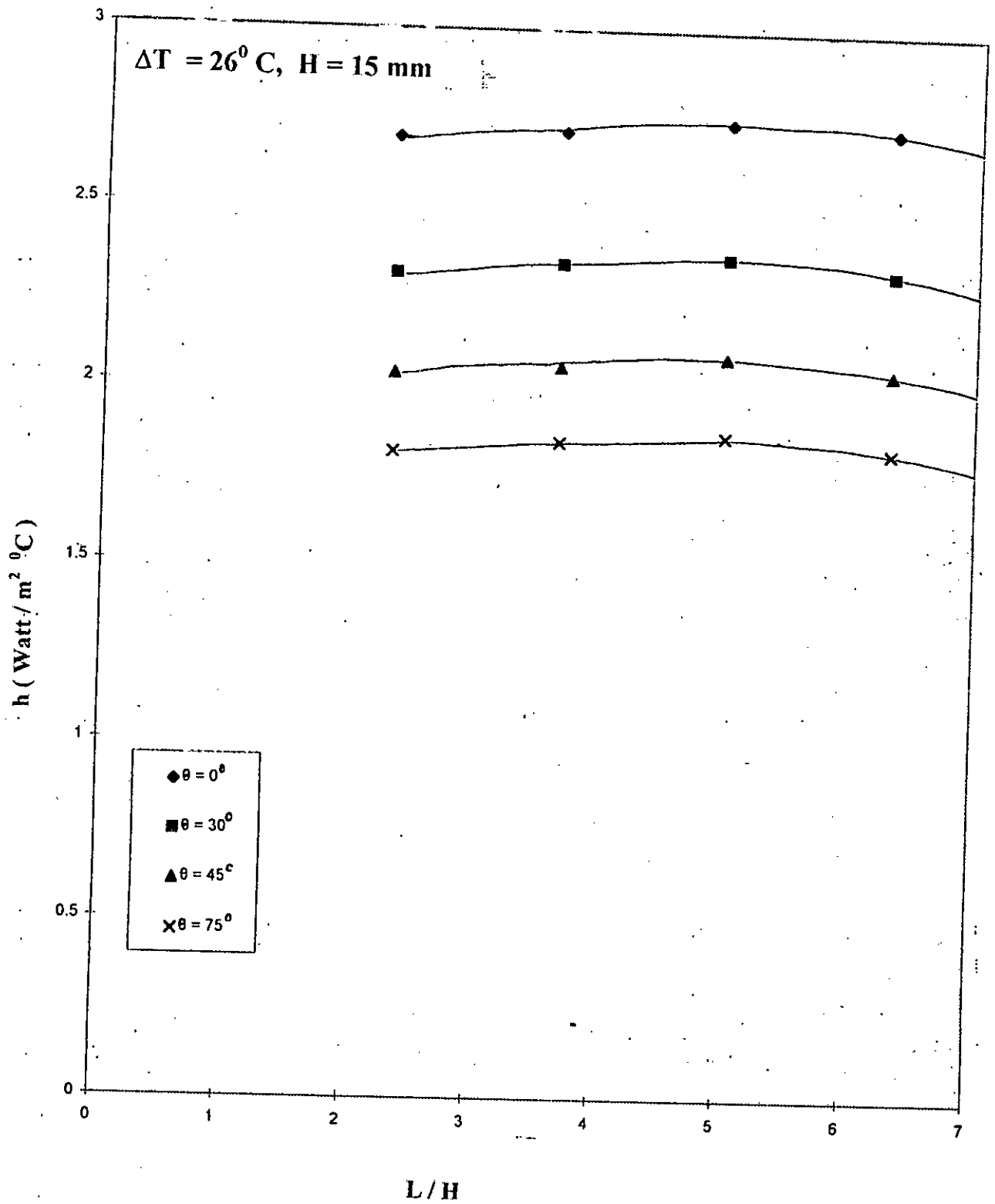
FIG 6.15 : EFFECT OF ASPECT RATIO (A) ON AVERAGE HEAT TRANSFER COEFFICIENT FOR
DIFFERENT ANGLES OF INCLINATION (0)

$$\Delta T = 26^0 C, \quad H = 25 \text{ mm}$$

Legend:
- ◆ θ = 0°
- ■ θ = 30°
- ▲ θ = 45°
- × θ = 75°

Y-axis: h (Watt / m² °C)

X-axis: L / H
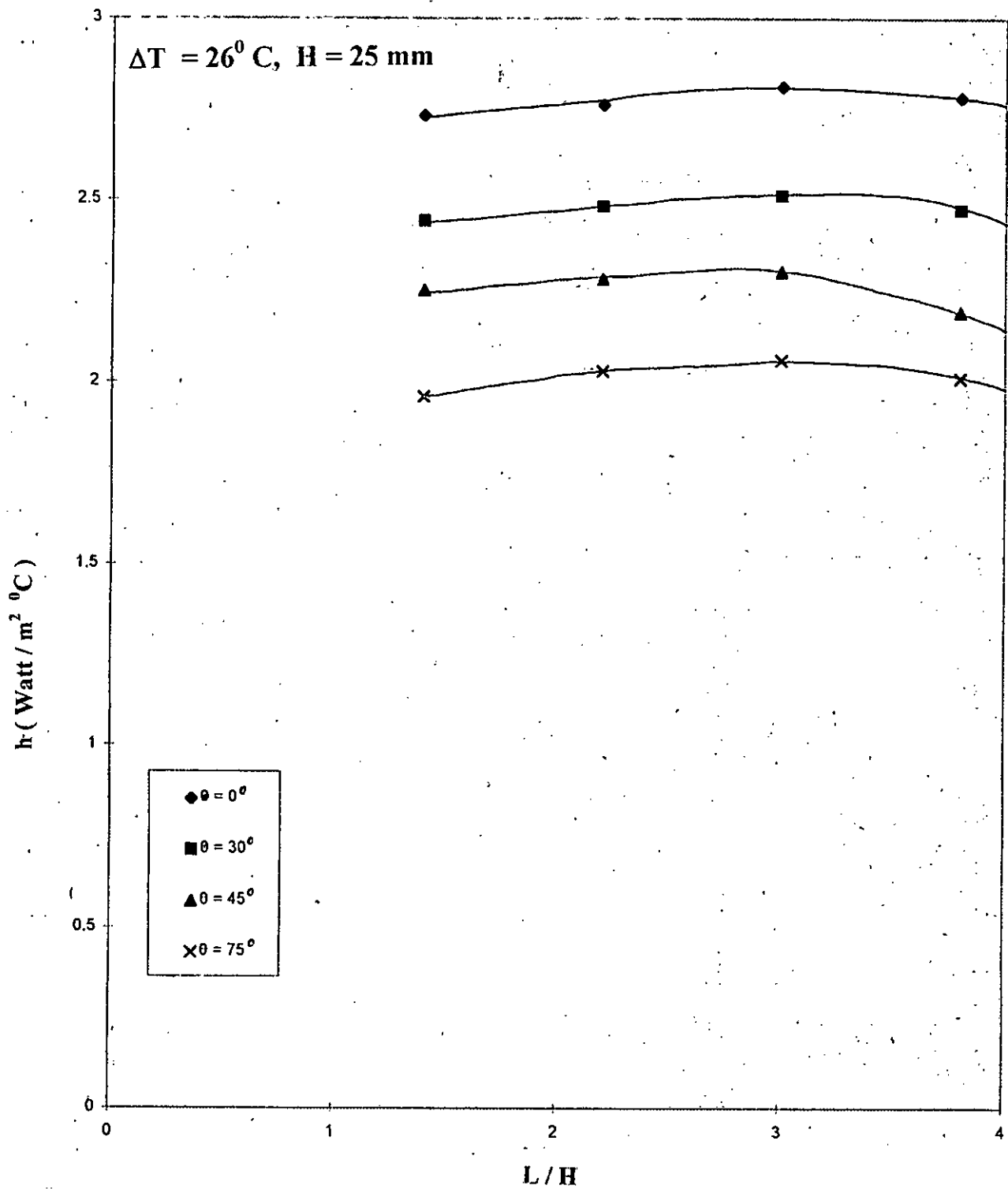
FIG 6.16 :   EFFECT OF ASPECT RATIO (A) ON AVERAGE HEAT TRANSFER COEFFICIENT FOR DIFFERENT ANGLES OF INCLINATION (θ)
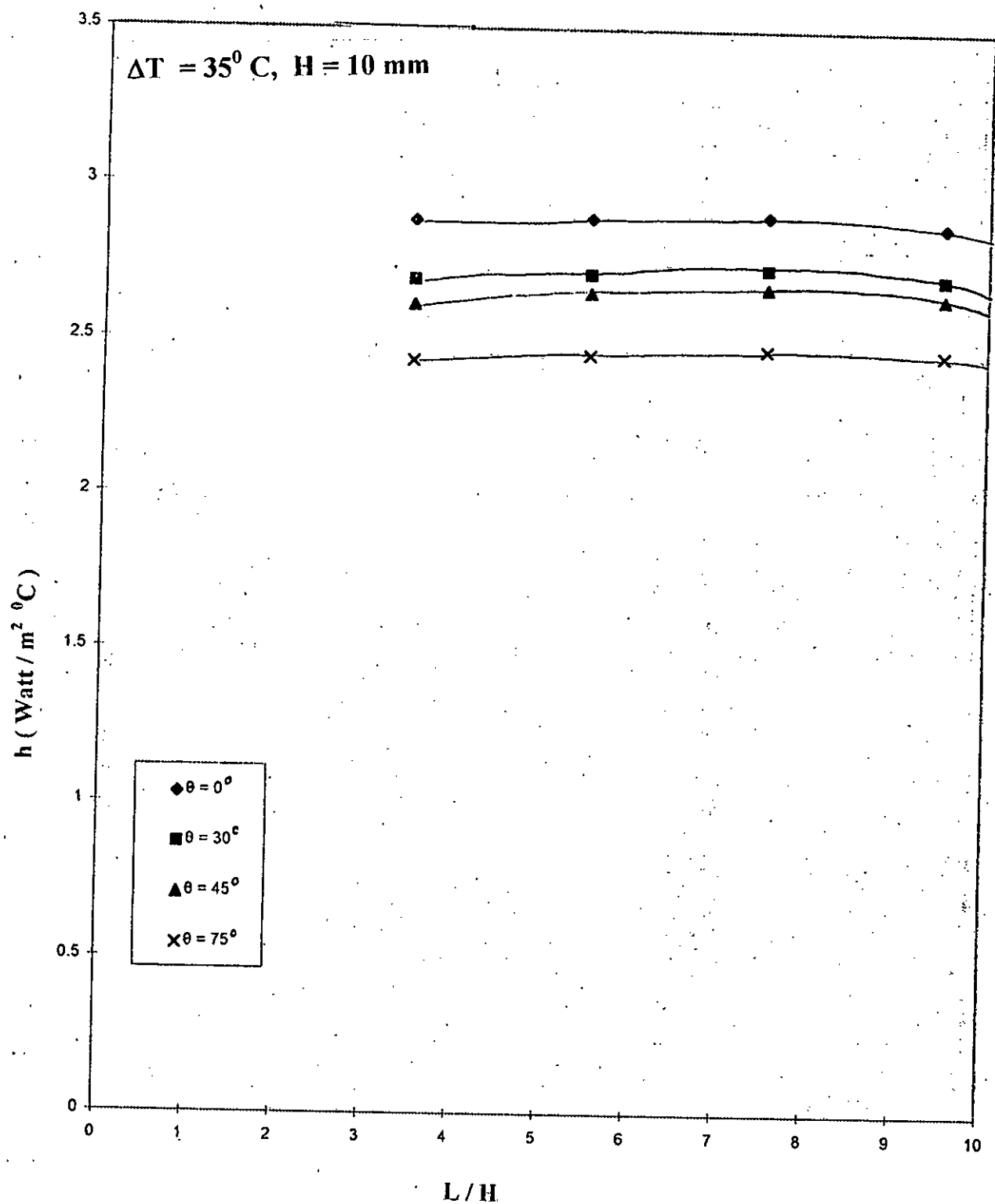
FIG 6.17 : EFFECT OF ASPECT RATIO (A) ON AVERAGE HEAT TRANSFER COEFFICIENT FOR DIFFERENT ANGLES OF INCLINATION (θ)
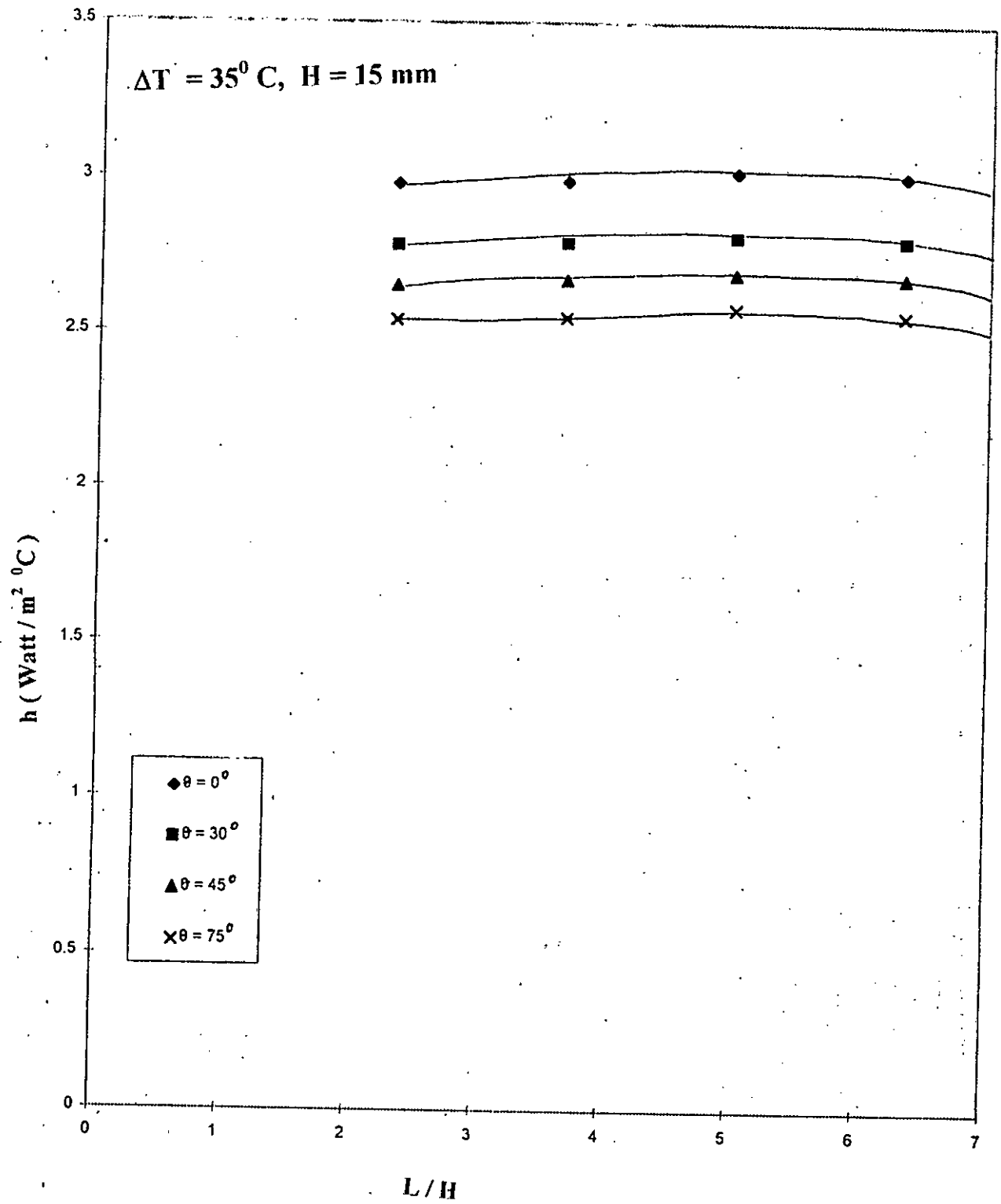
FIG 6.18 : EFFECT OF ASPECT RATIO (A) ON AVERAGE HEAT TRANSFER COEFFICIENT FOR DIFFERENT ANGLES OF INCLINATION (θ)

FIG 6.19 : EFFECT OF ASPECT RATIO (A) ON AVERAGE HEAT TRANSFER COEFFICIENT FOR DIFFERENT ANGLES OF INCLINATION (θ)

ΔT = 10⁰C

$\Delta T = 10^0 C$

h (Watt / m² ⁰C)

Legend:
◆ H=25mm, θ = 0°
■ H=15mm, θ = 0°
▲ H=10mm, θ = 0°
✕ H=25mm, θ = 30°
✴ H=15mm, θ = 30°
● H=10mm, θ = 30°
+ H=25mm, θ = 45°
‒ H=15mm, θ = 45°
— H=10mm, θ = 45°
▲ H=25mm, θ = 75°
⊡ H=15mm, θ = 75°
△ H=10mm, θ = 75°

L / H
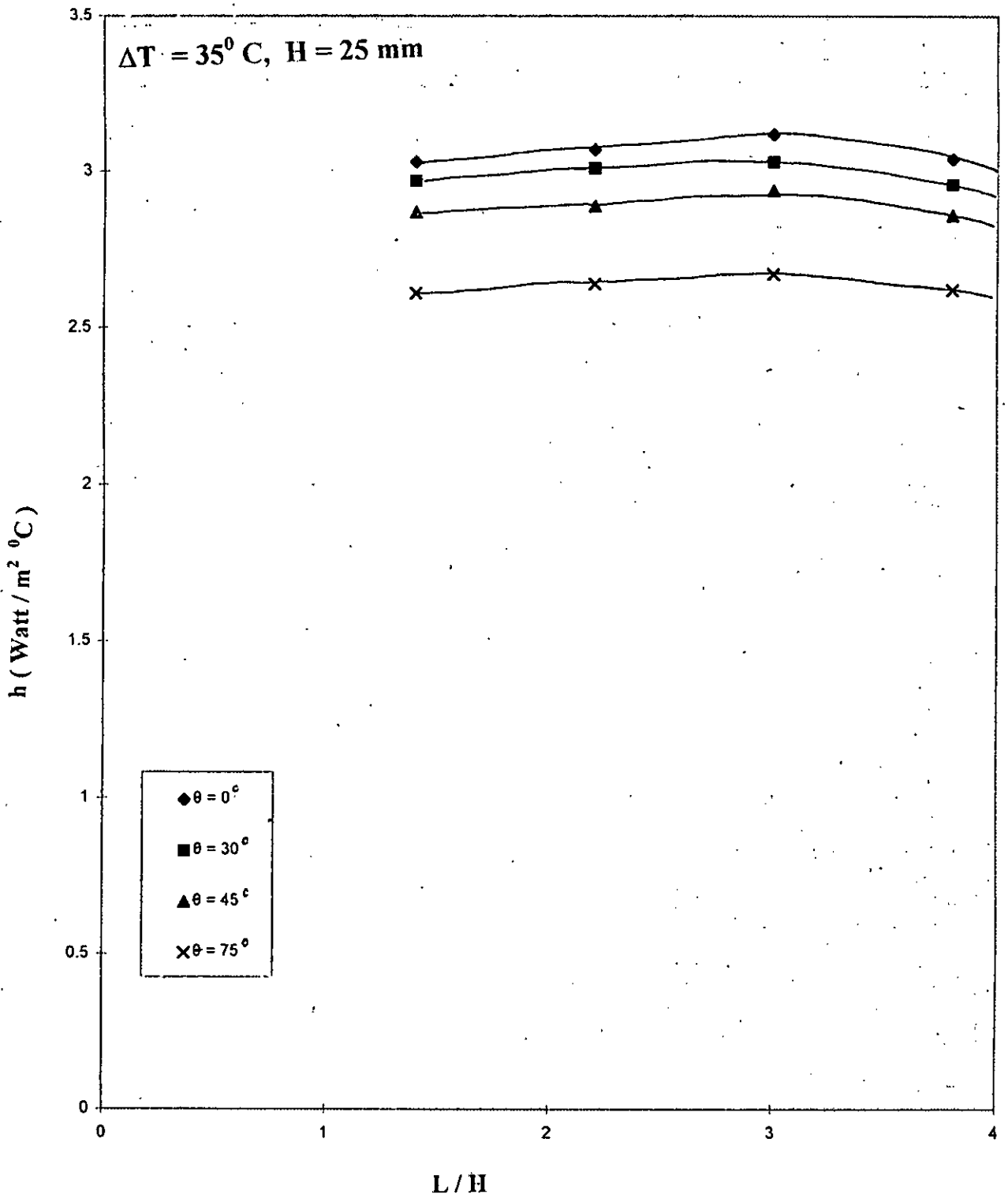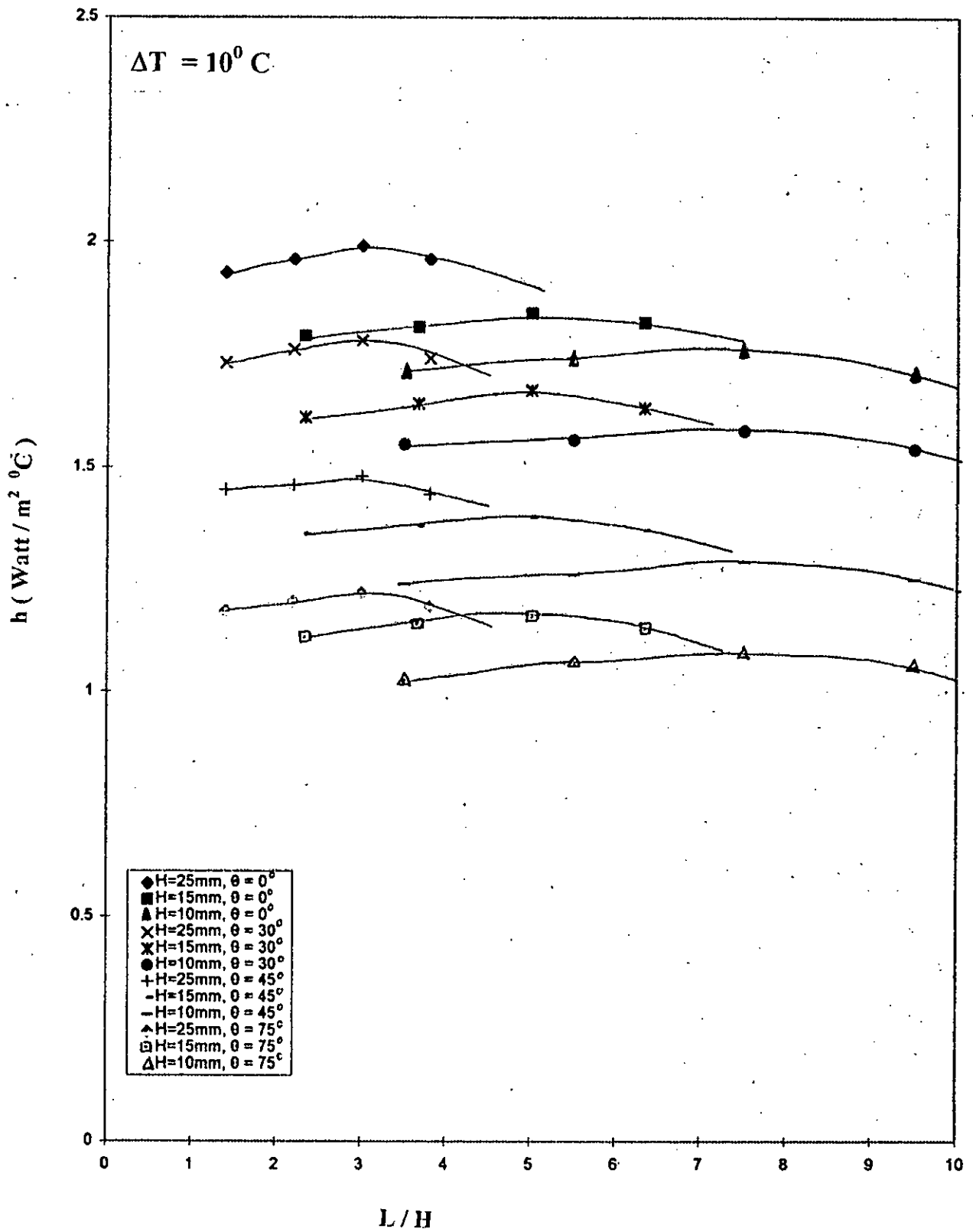
FIG 6.20 :   EFFECT OF ASPECT RATIO (A) ON AVERAGE HEAT TRANSFER COEFFICIENT FOR TEMPERATURE DIFFERENCE ΔT = 10⁰C.
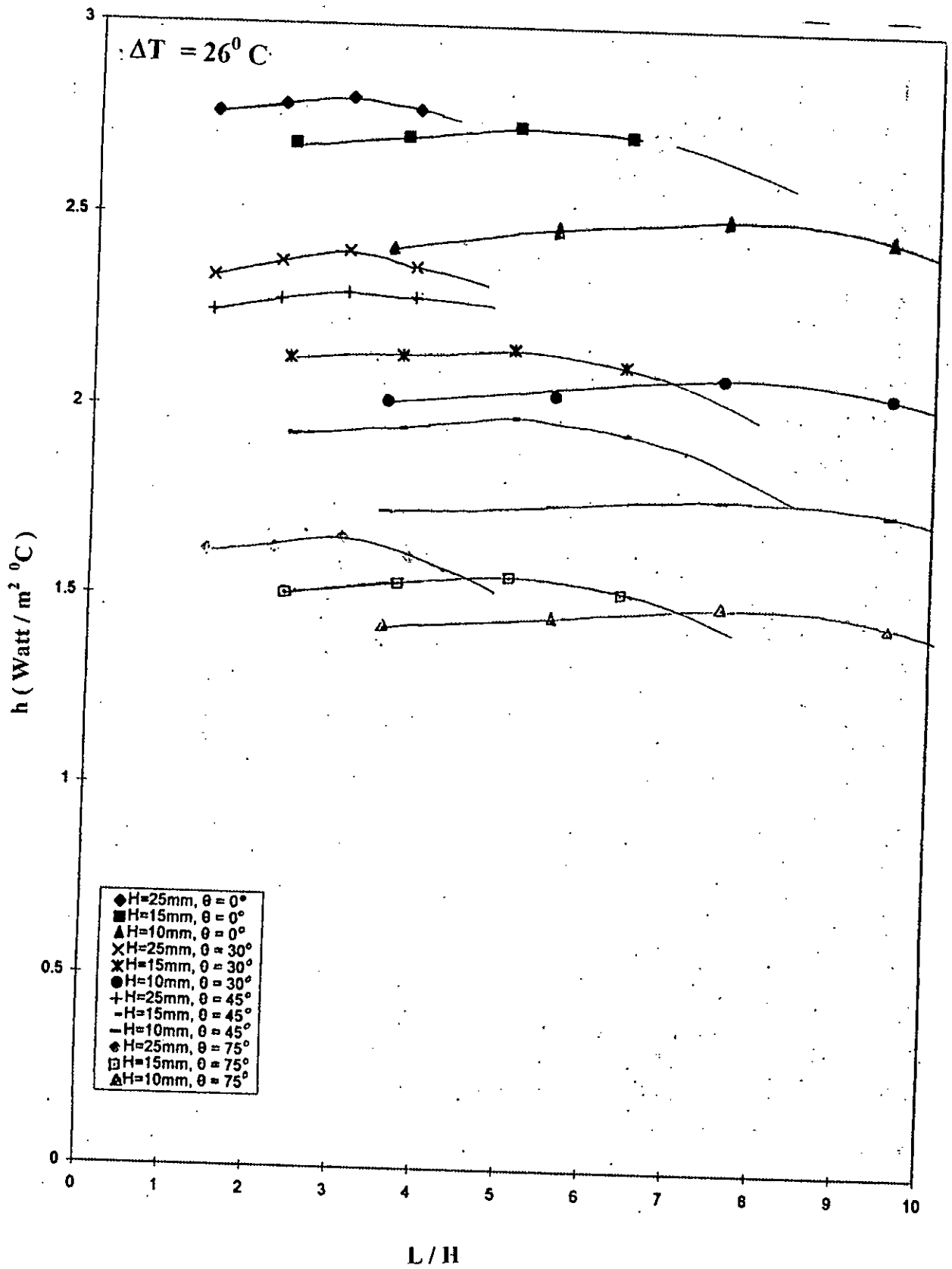
FIG 6.21 : EFFECT OF ASPECT RATIO (A) ON AVERAGE HEAT TRANSFER COEFFICIENT FOR TEMPERATURE DIFFERENCE AT = 26°C.
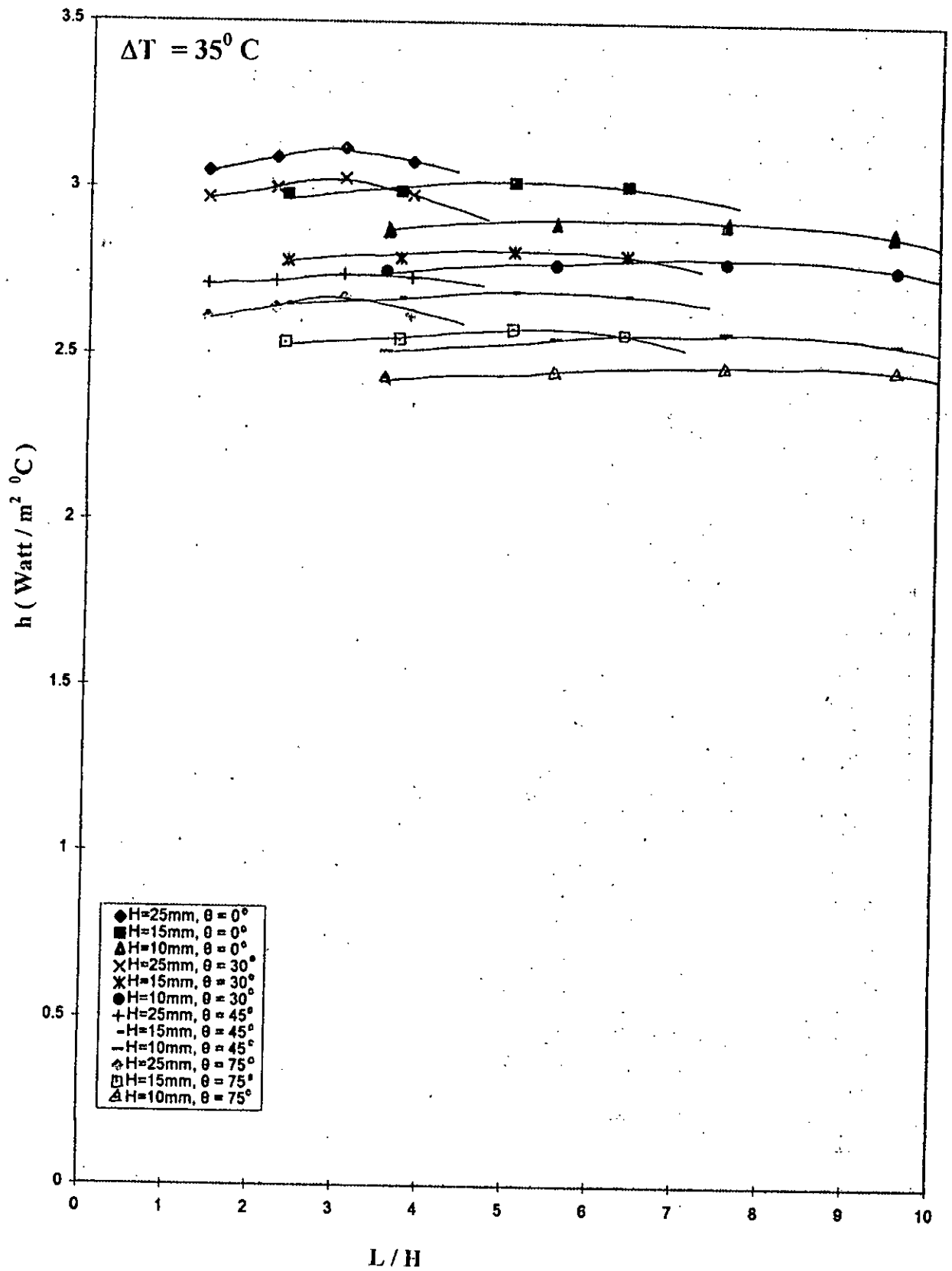
FIG 6.22 : EFFECT OF ASPECT RATIO (A) ON AVERAGE HEAT TRANSFER COEFFICIENT FOR
TEMPERATURE DIFFERENCE ΔT = 35°C.
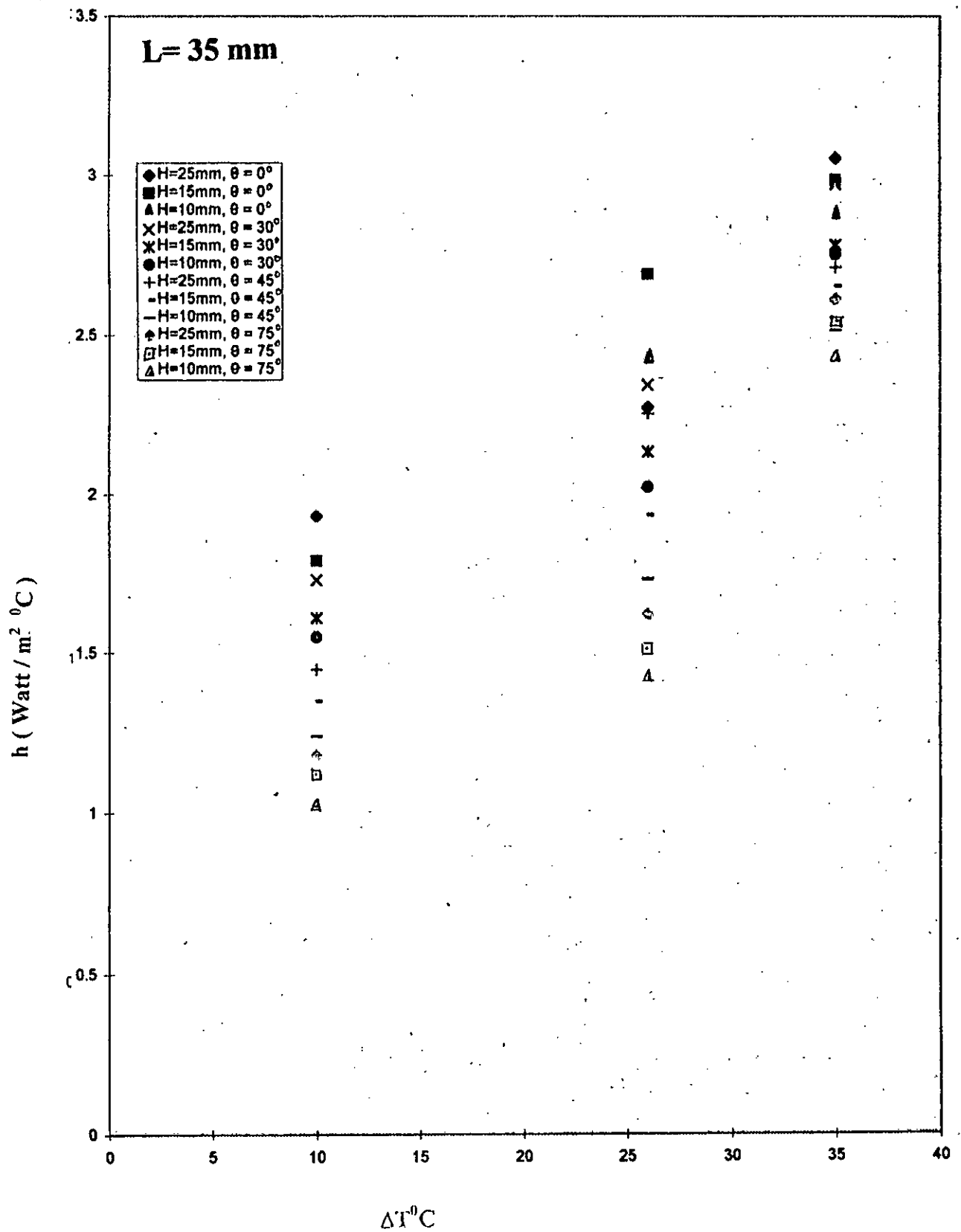
FIG 6.23 : EFFECT OF TEMPERATURE POTENTIAL (ΔT) ON AVERAGE HEAT TRANSFER COEFFICIENT FOR L = 35 mm.
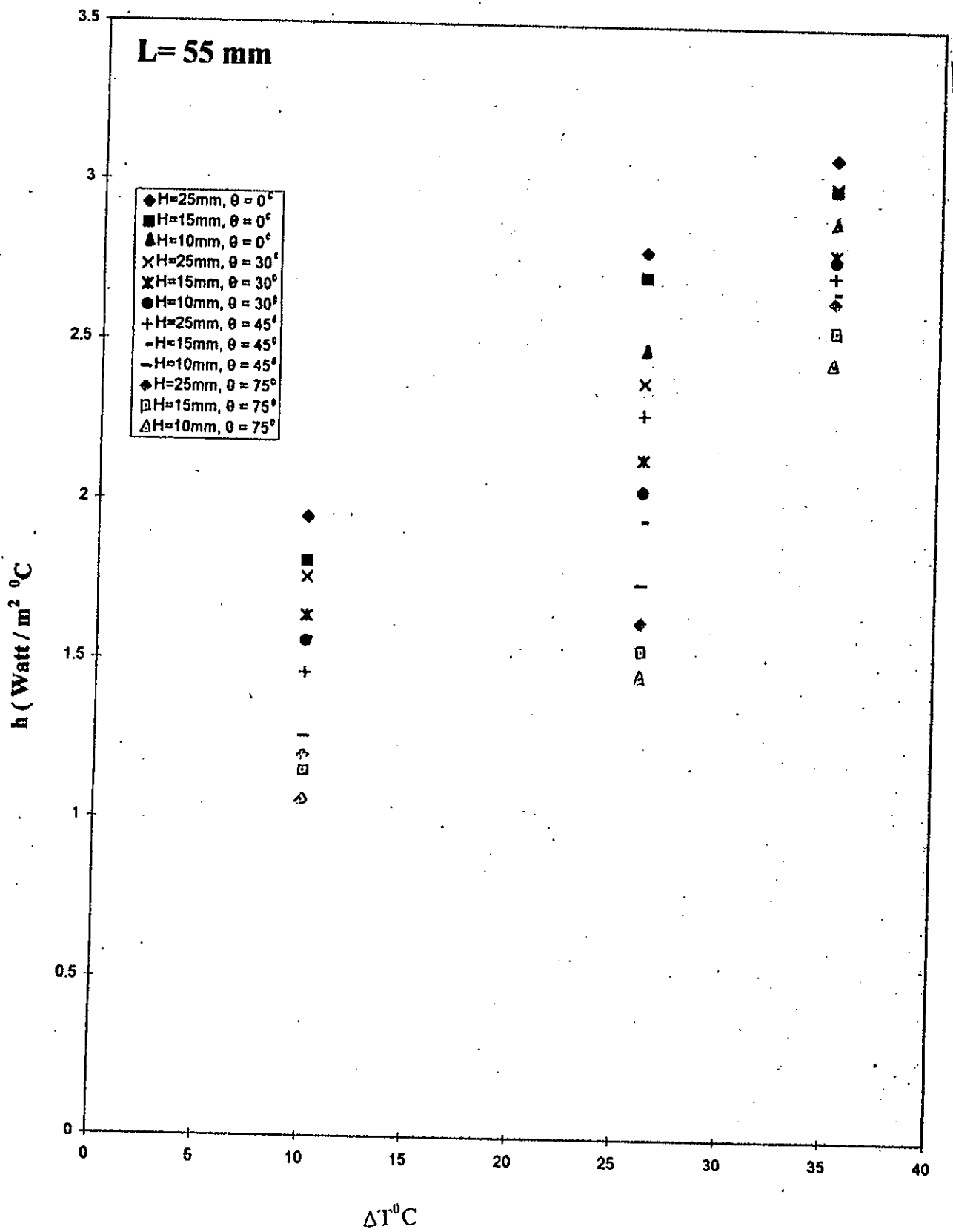
FIG 6.24 : EFFECT OF TEMPERATURE POTENTIAL (ΔT) ON AVERAGE HEAT TRANSFER COEFFICIENT FOR L = 55 mm.
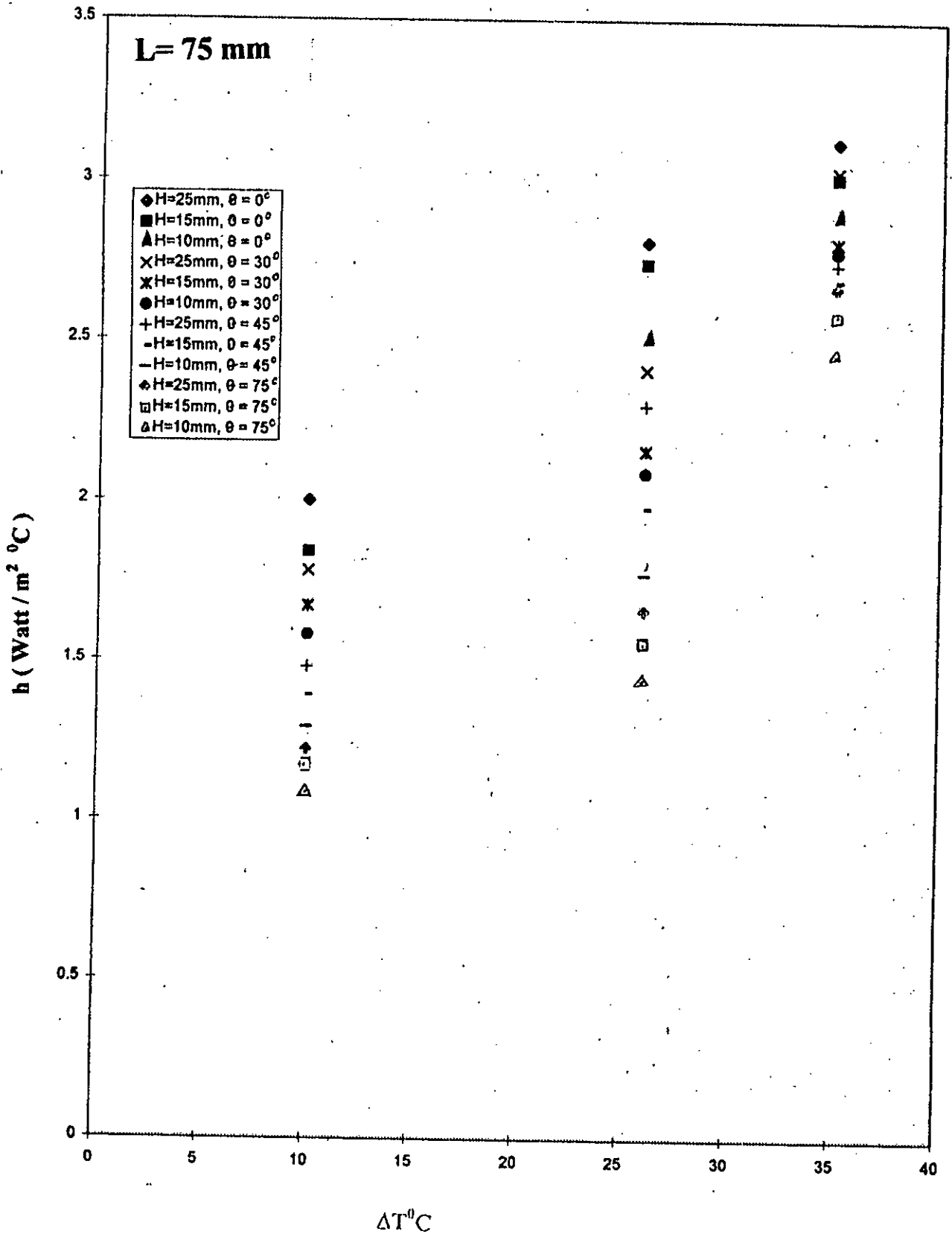
FIG 6.25 : EFFECT OF TEMPERATURE POTENTIAL (ΔT) ON AVERAGE HEAT TRANSFER
COEFFICIENT FOR L = 75 mm.
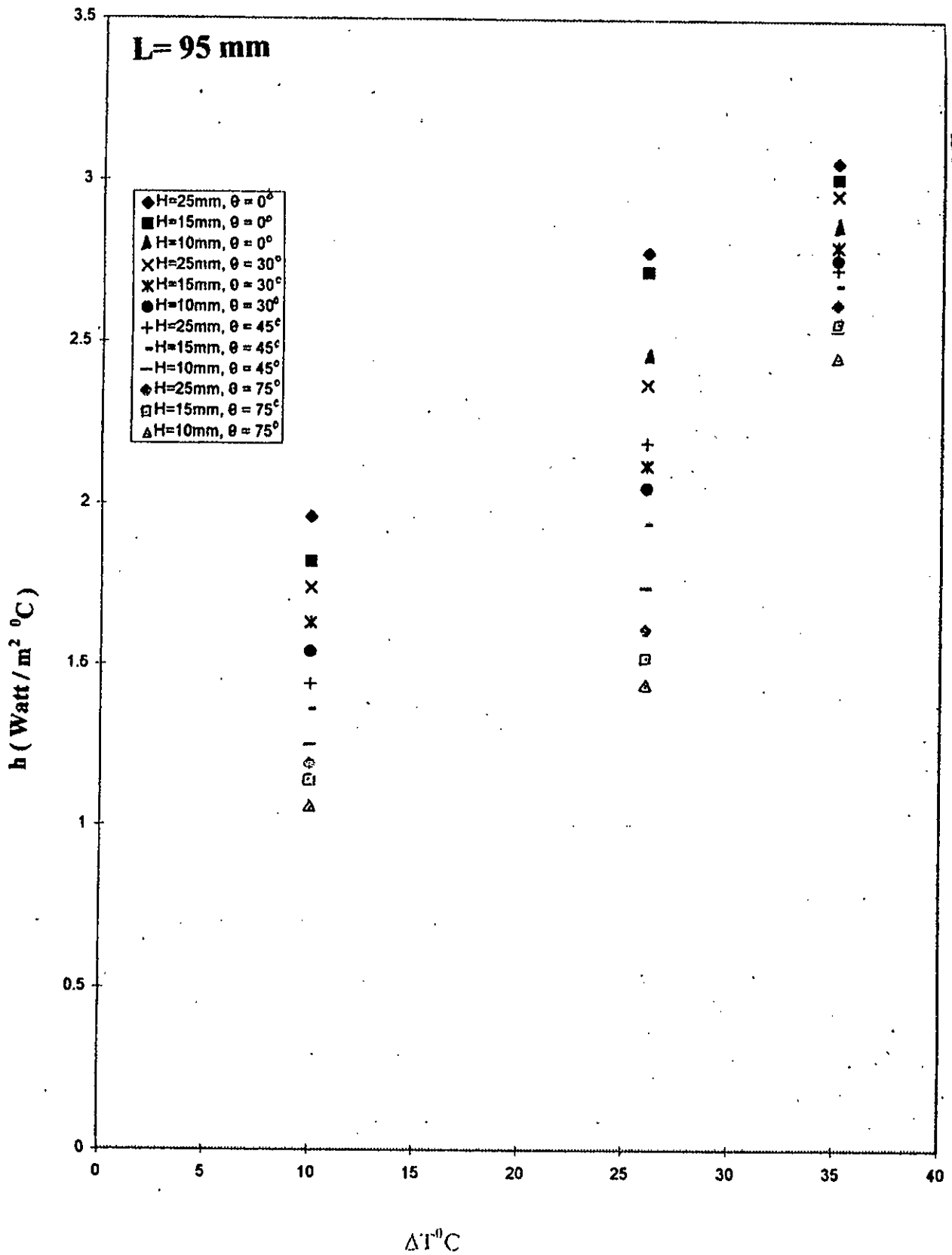
FIG 6.26 : EFFECT OF TEMPERATURE POTENTIAL (ΔT) ON AVERAGE HEAT TRANSFER
COEFFICIENT FOR L = 95 mm.
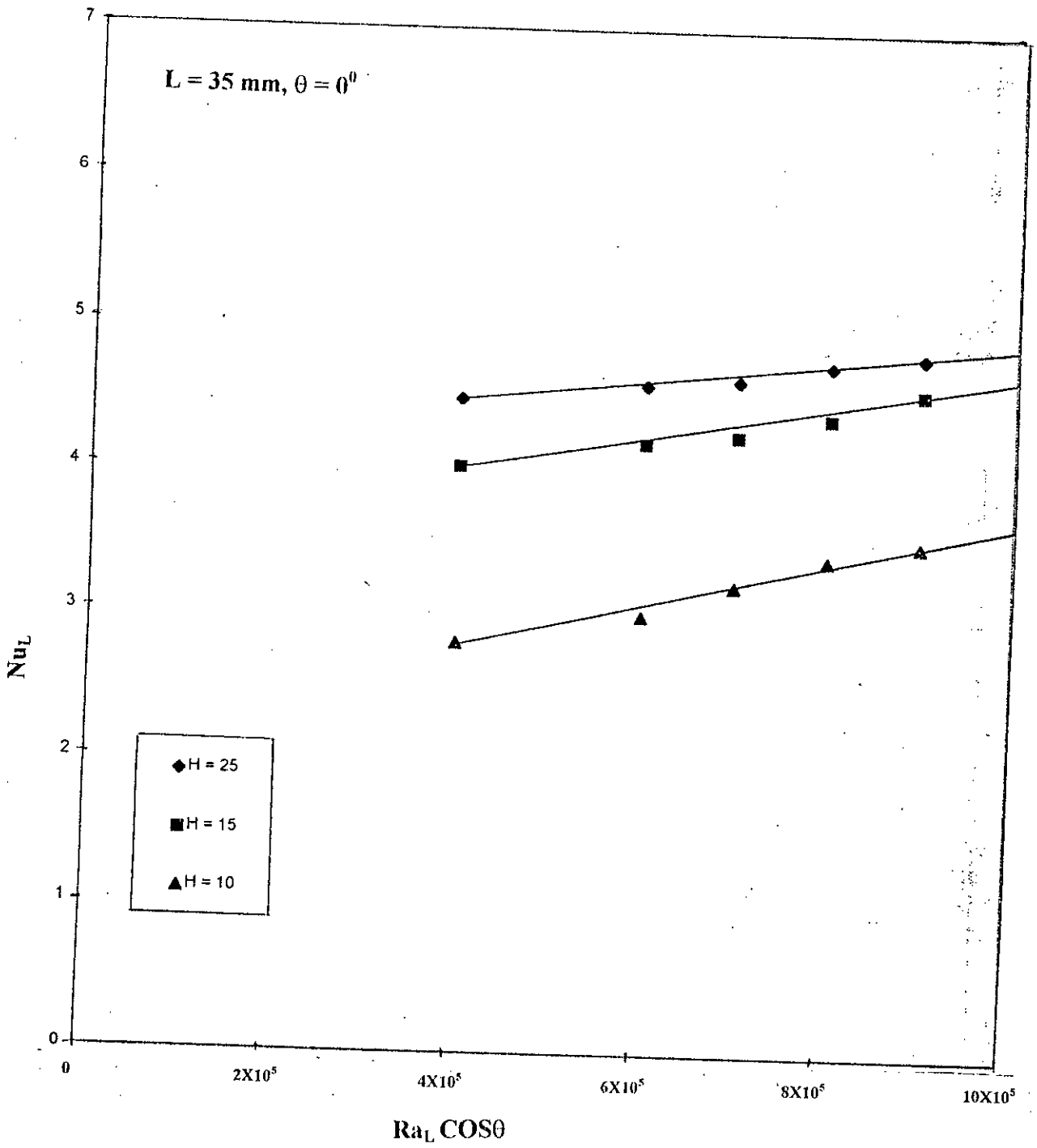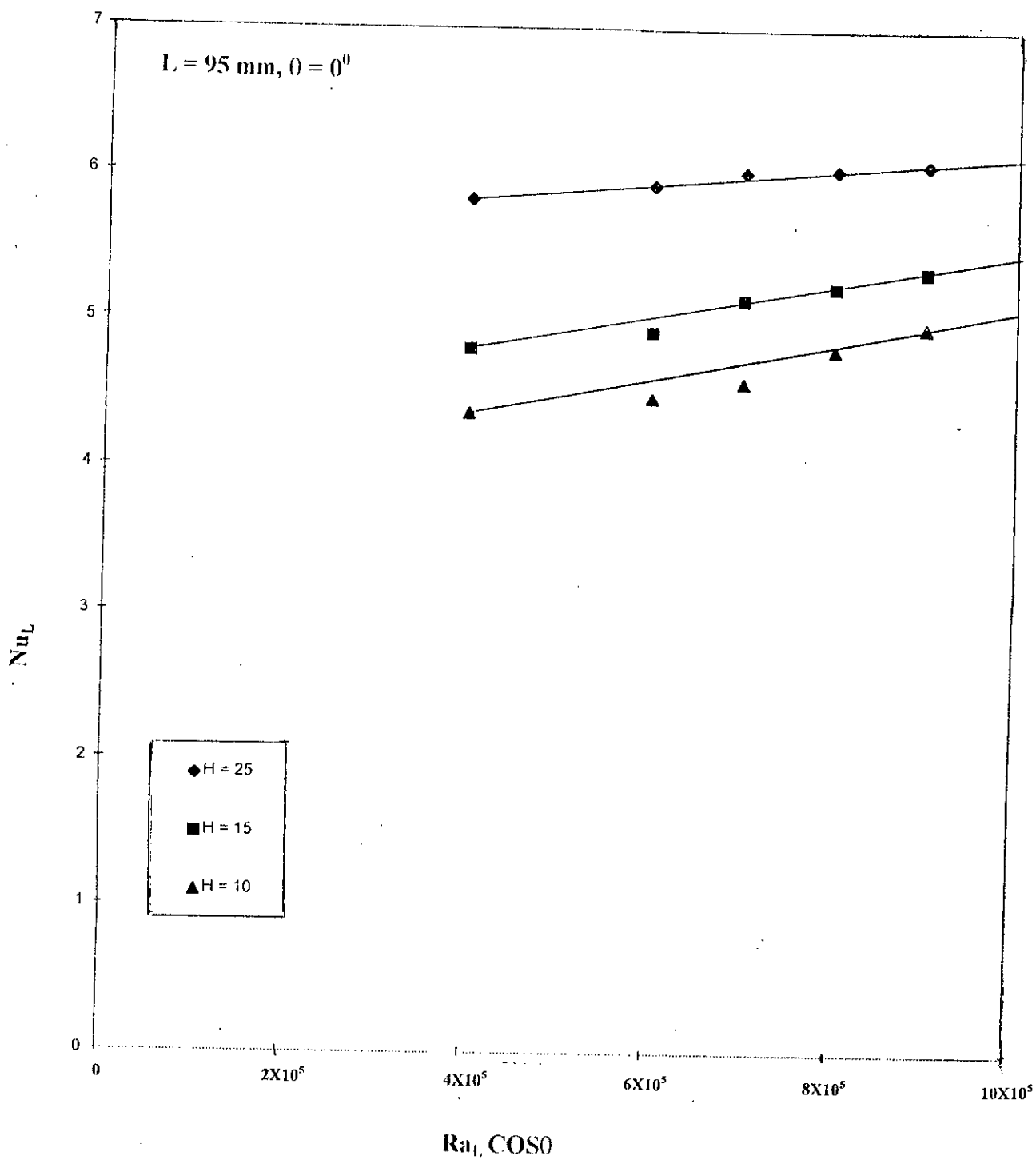
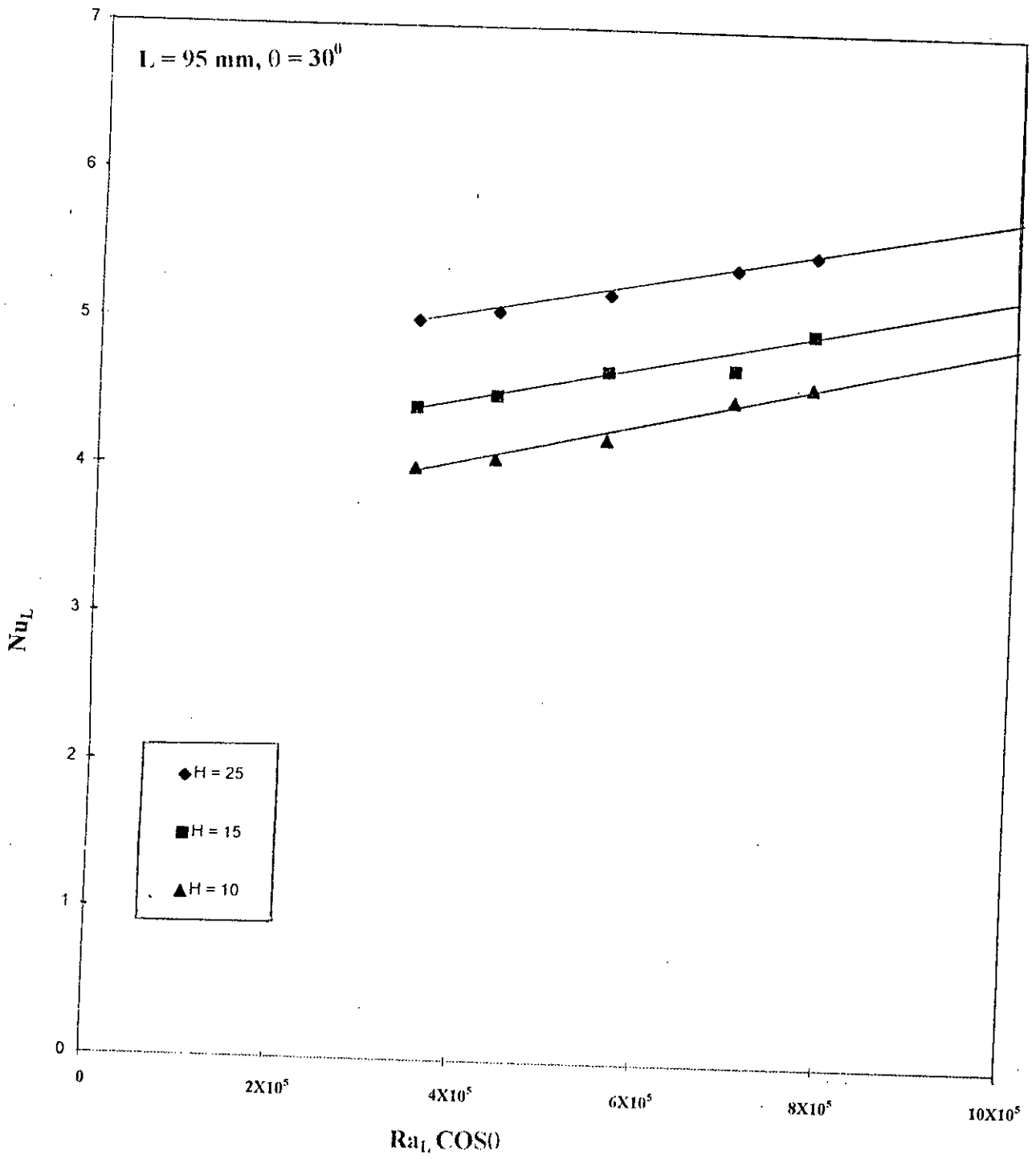FIG 6.27 :   EFFECT OF AVERAGE NUSSELT NUMBER VS $Ra_L COS\theta$ FOR L = 35 MM AT ANGLE OF INCLINATION $\theta = 0^0$.
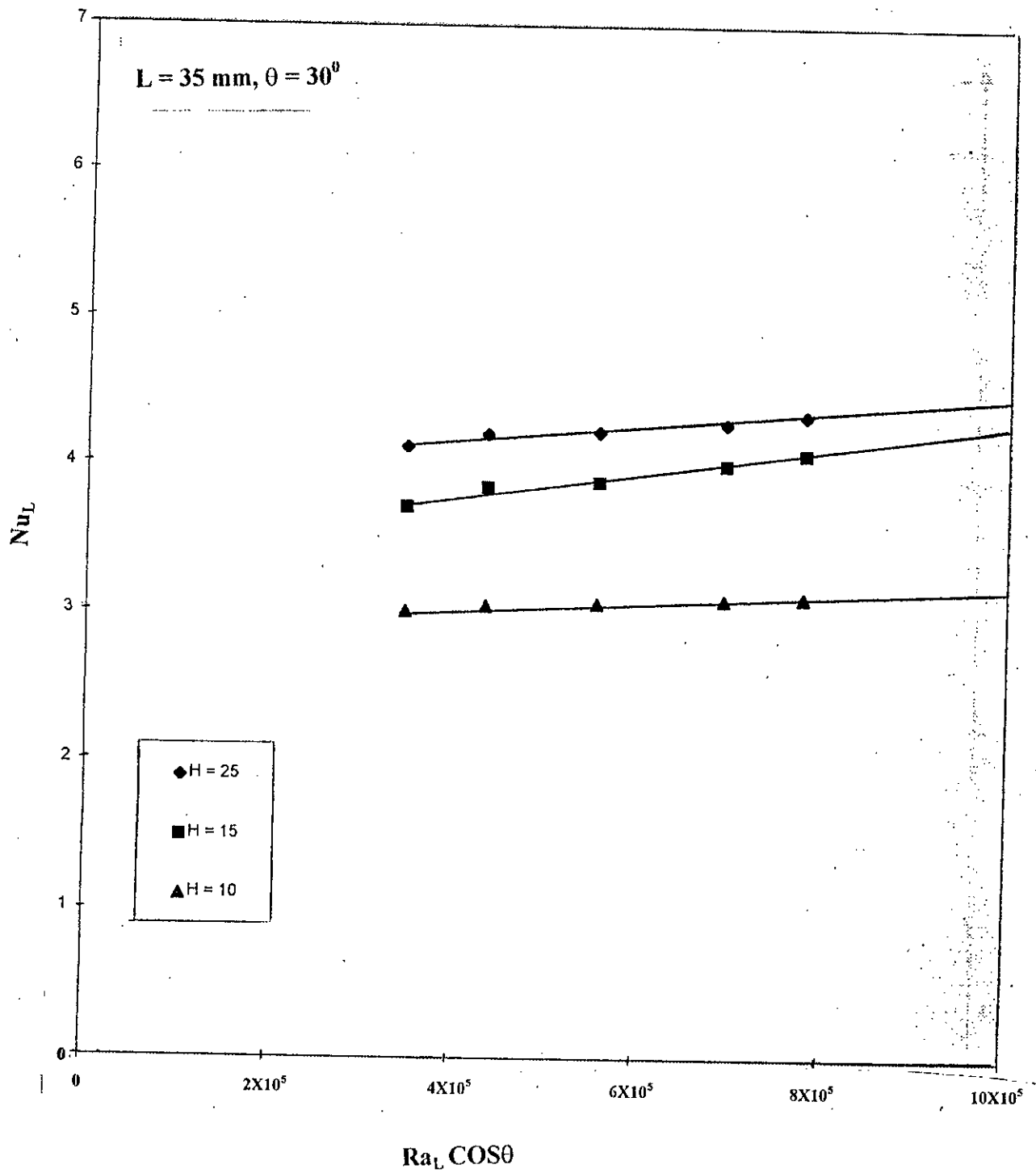
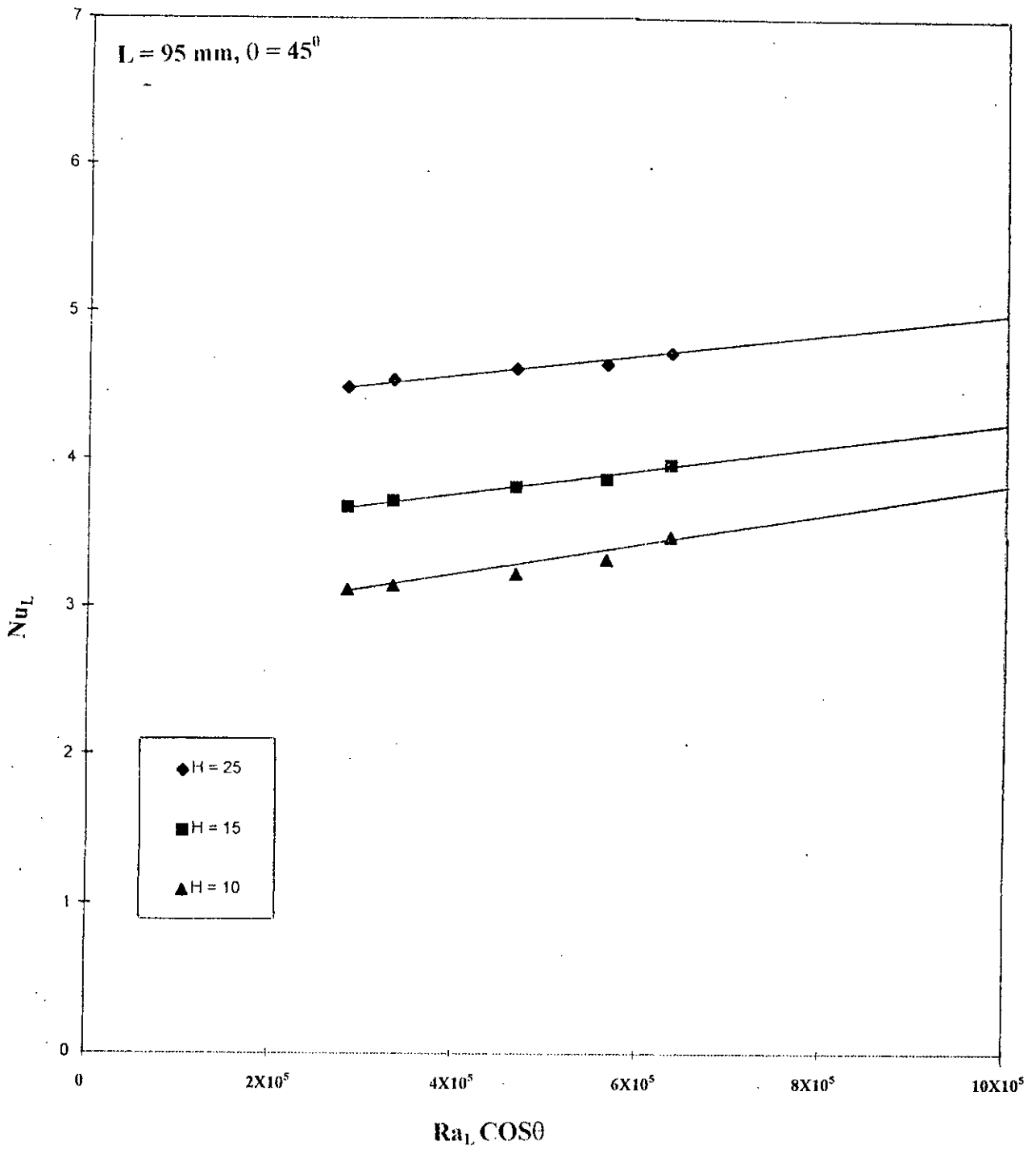FIG 6.28 : EFFECT OF AVERAGE NUSSELT NUMBER VS $Ra_L COS\theta$ FOR L = 35 MM AT ANGLE OF INCLINATION $\theta = 30^0$.
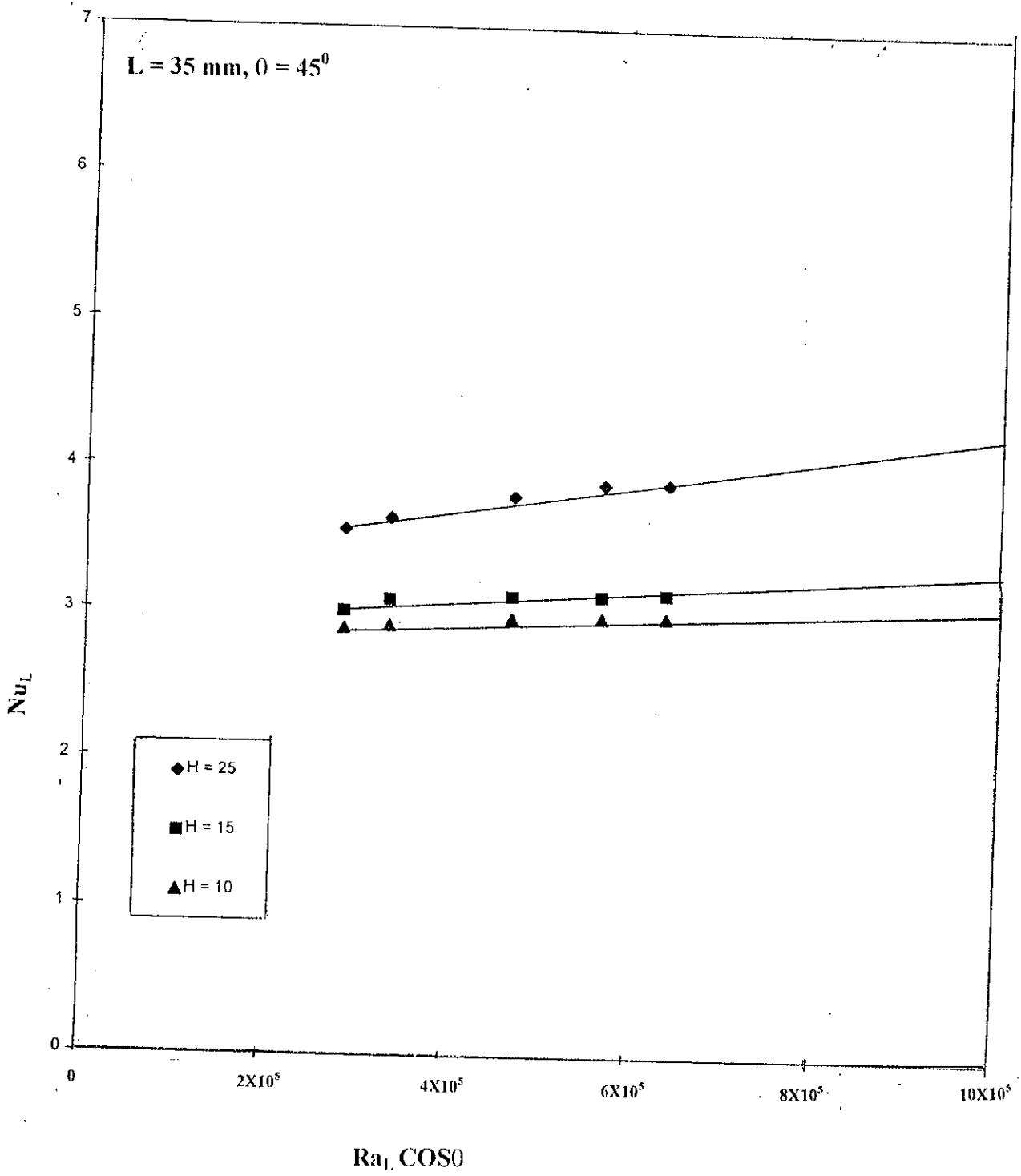
FIG 6.29 :   EFFECT OF AVERAGE NUSSELT NUMBER VS $Ra_L COS\theta$ FOR L = 35 MM AT ANGLE
OF INCLINATION $\theta = 45^0$.
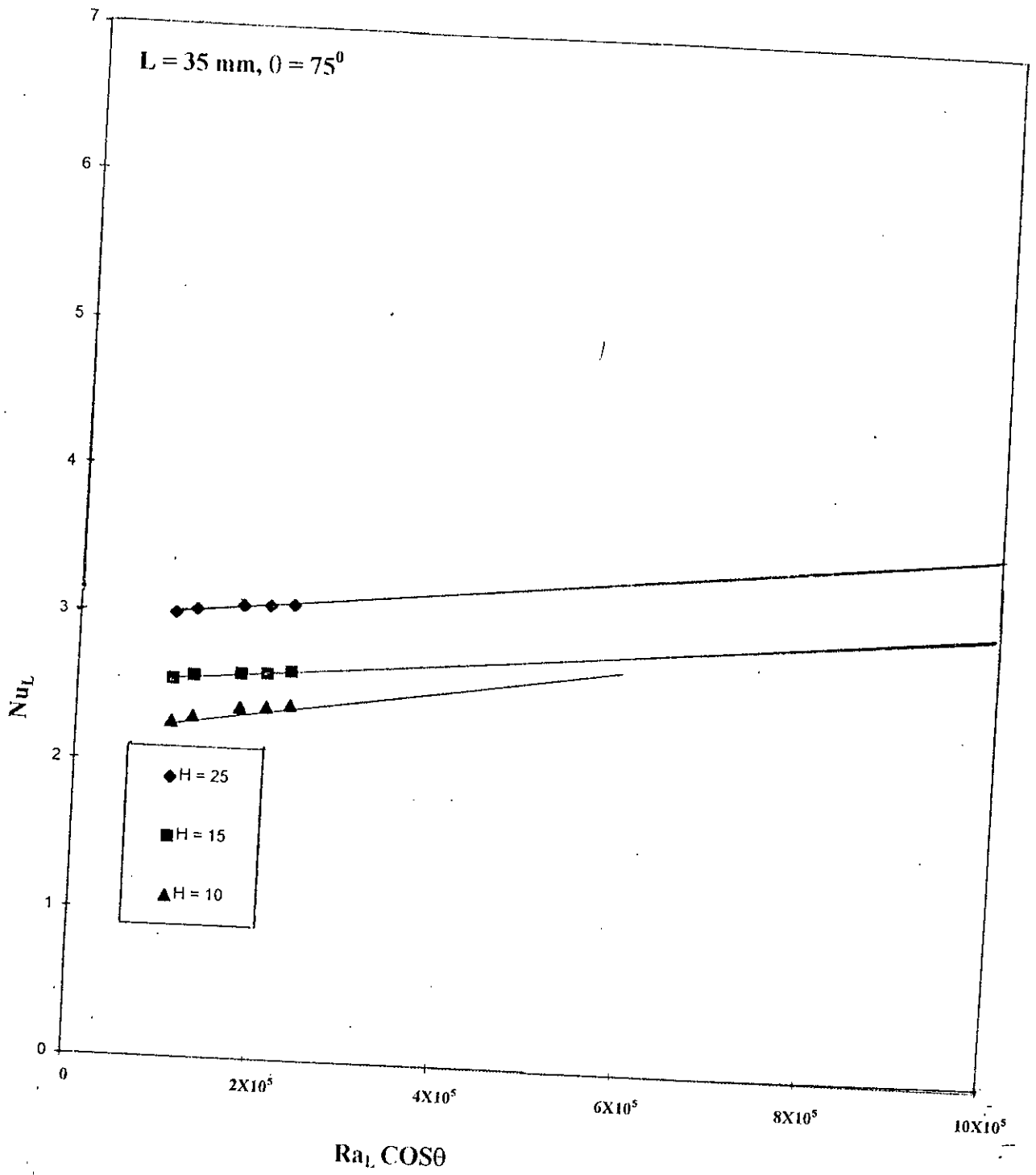
FIG 6.30 :   EFFECT OF AVERAGE NUSSELT NUMBER VS $Ra_L COS\theta$ FOR L = 35 MM AT ANGLE OF INCLINATION $\theta = 75^0$.
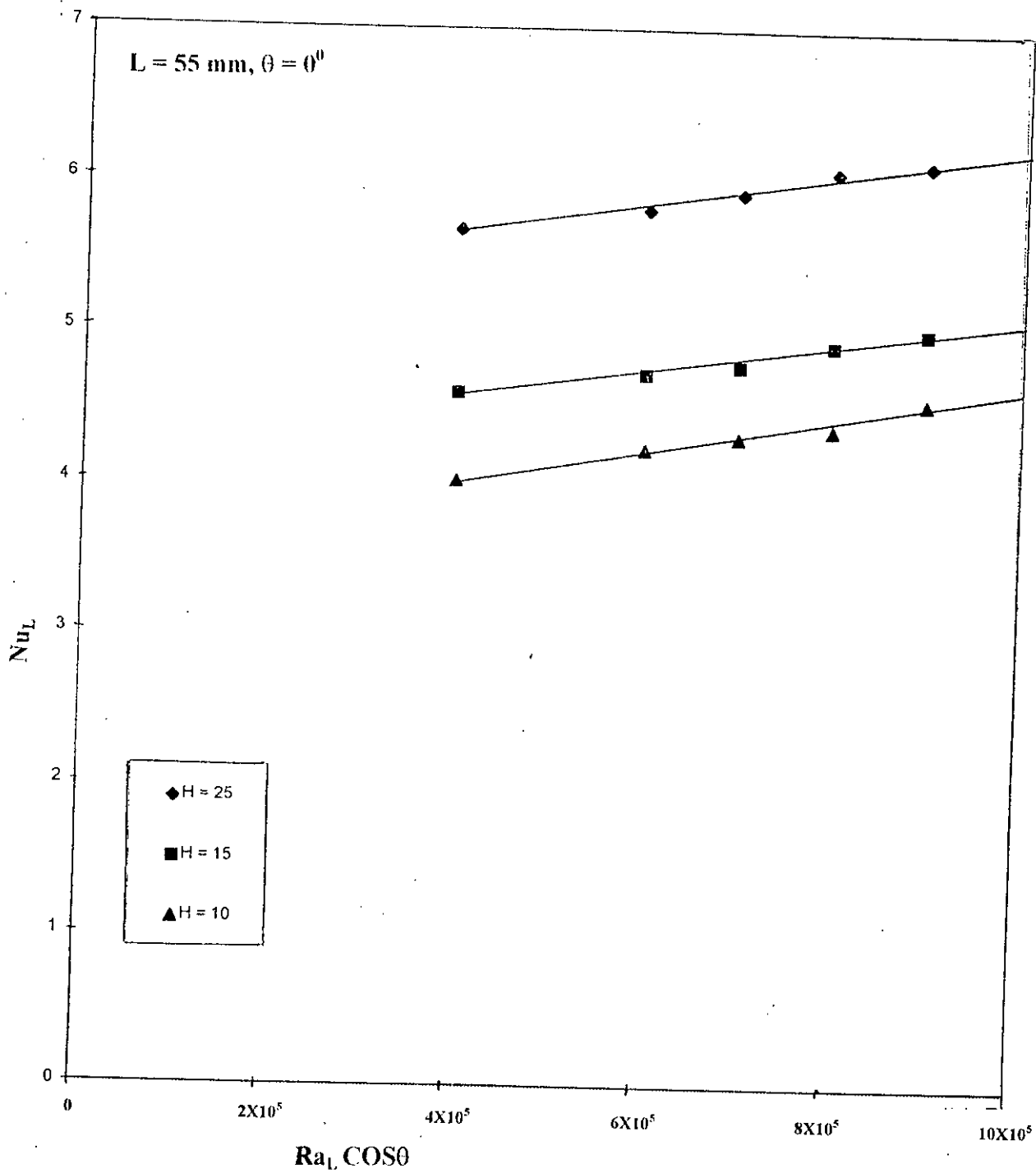
FIG 6.31 : EFFECT OF AVERAGE NUSSELT NUMBER VS Ra$_L$COS0 FOR L = 55 MM AT ANGLE OF INCLINATION 0 = 0^0.
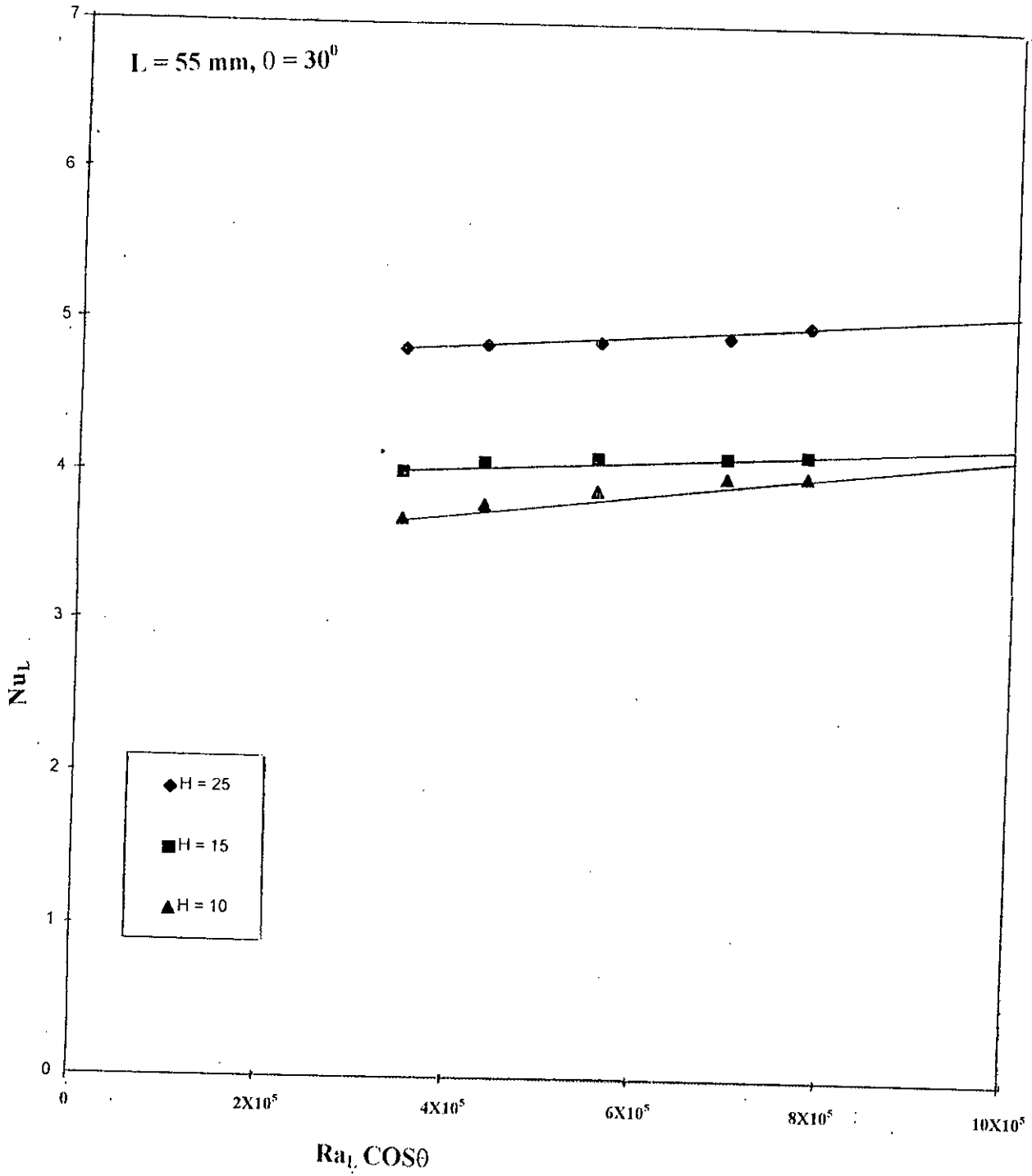
FIG 6.32 : EFFECT OF AVERAGE NUSSELT NUMBE VS Ra$_L$COSθ FOR L = 55 MM AT ANGLE OF INCLINATION θ = 30°.
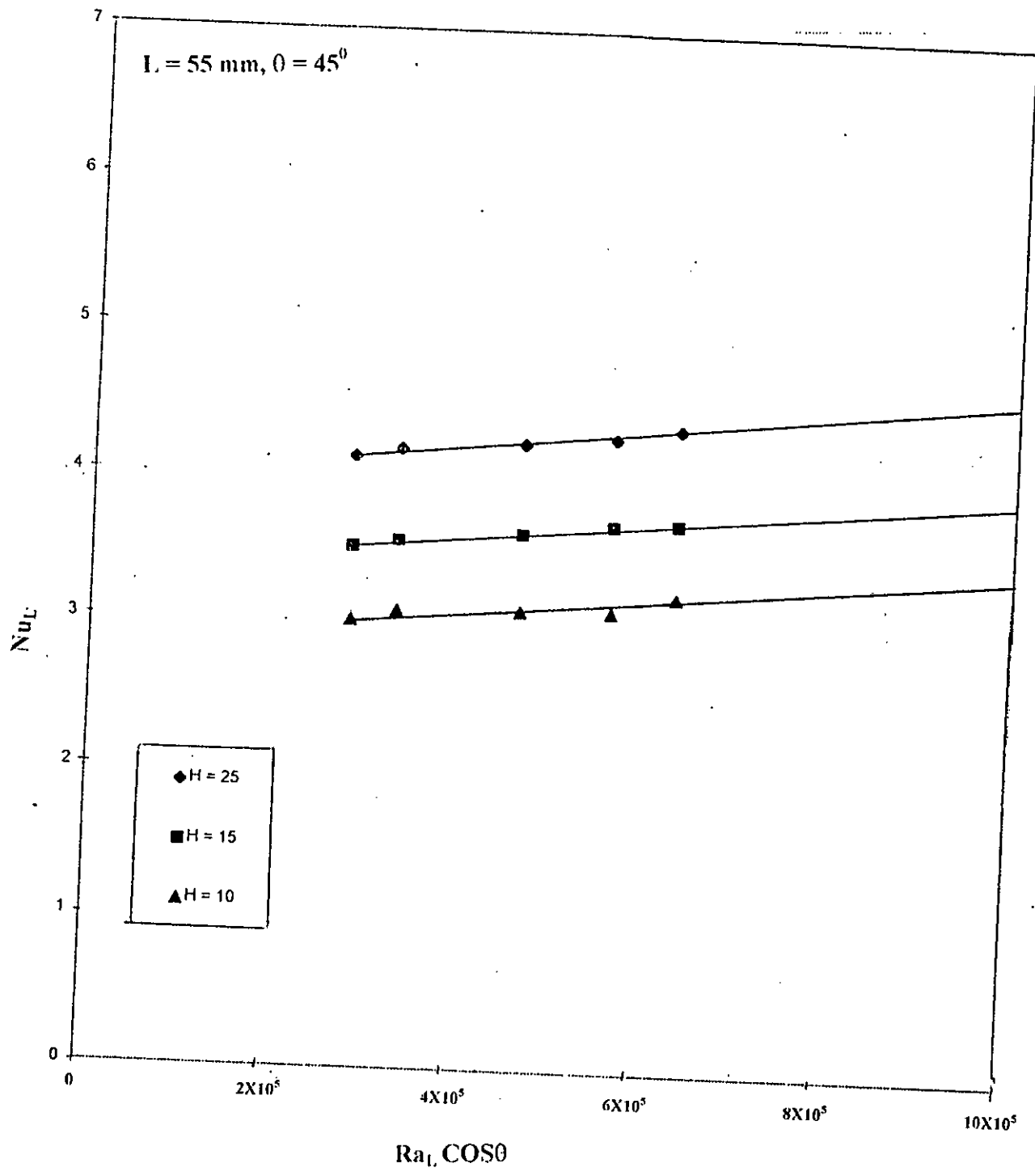
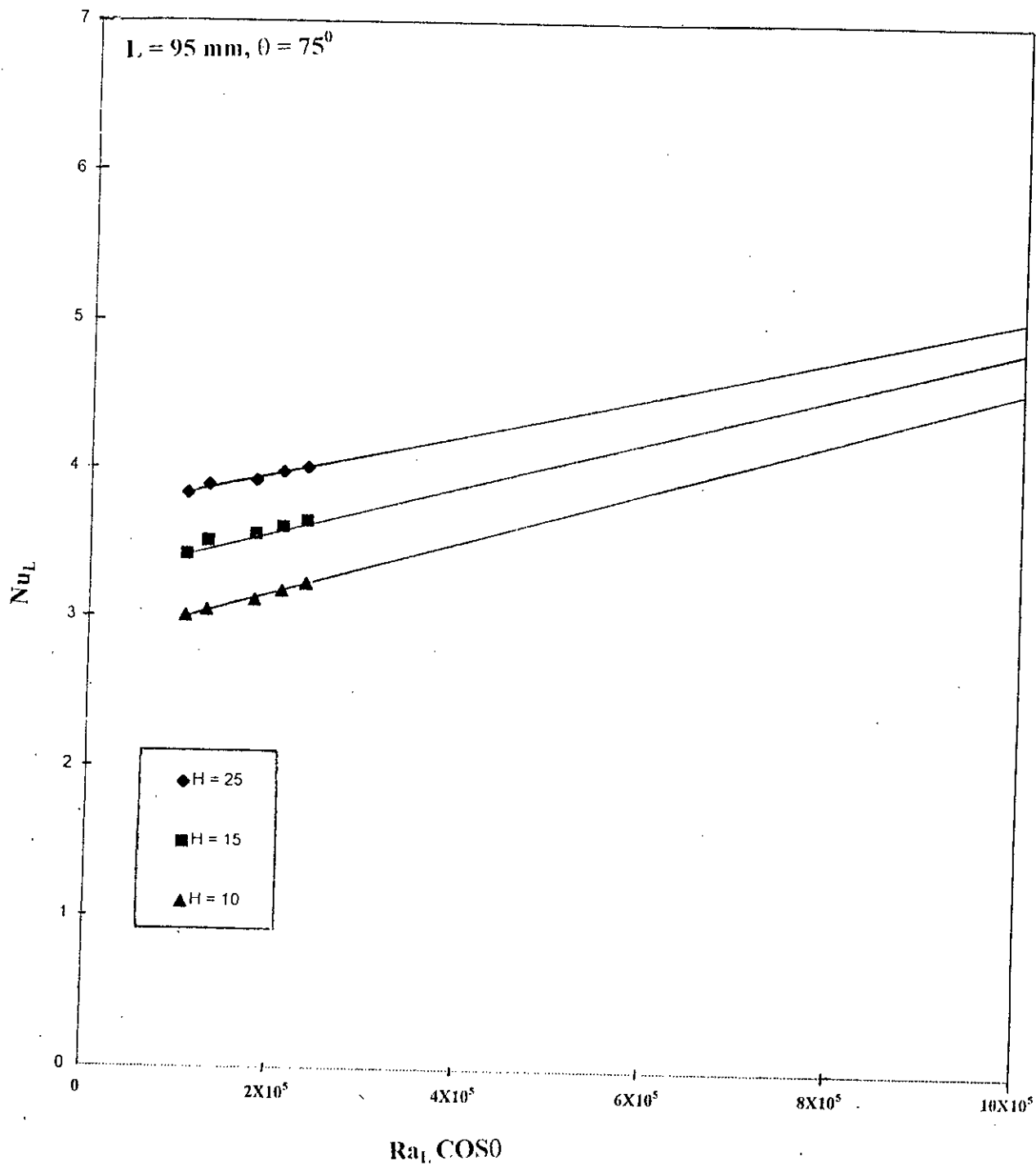FIG 6.33 : EFFECT OF AVERAGE NUSSELT NUMBER VS $Ra_L COS\theta$ FOR L = 55 MM AT ANGLE OF INCLINATION θ = 45°.
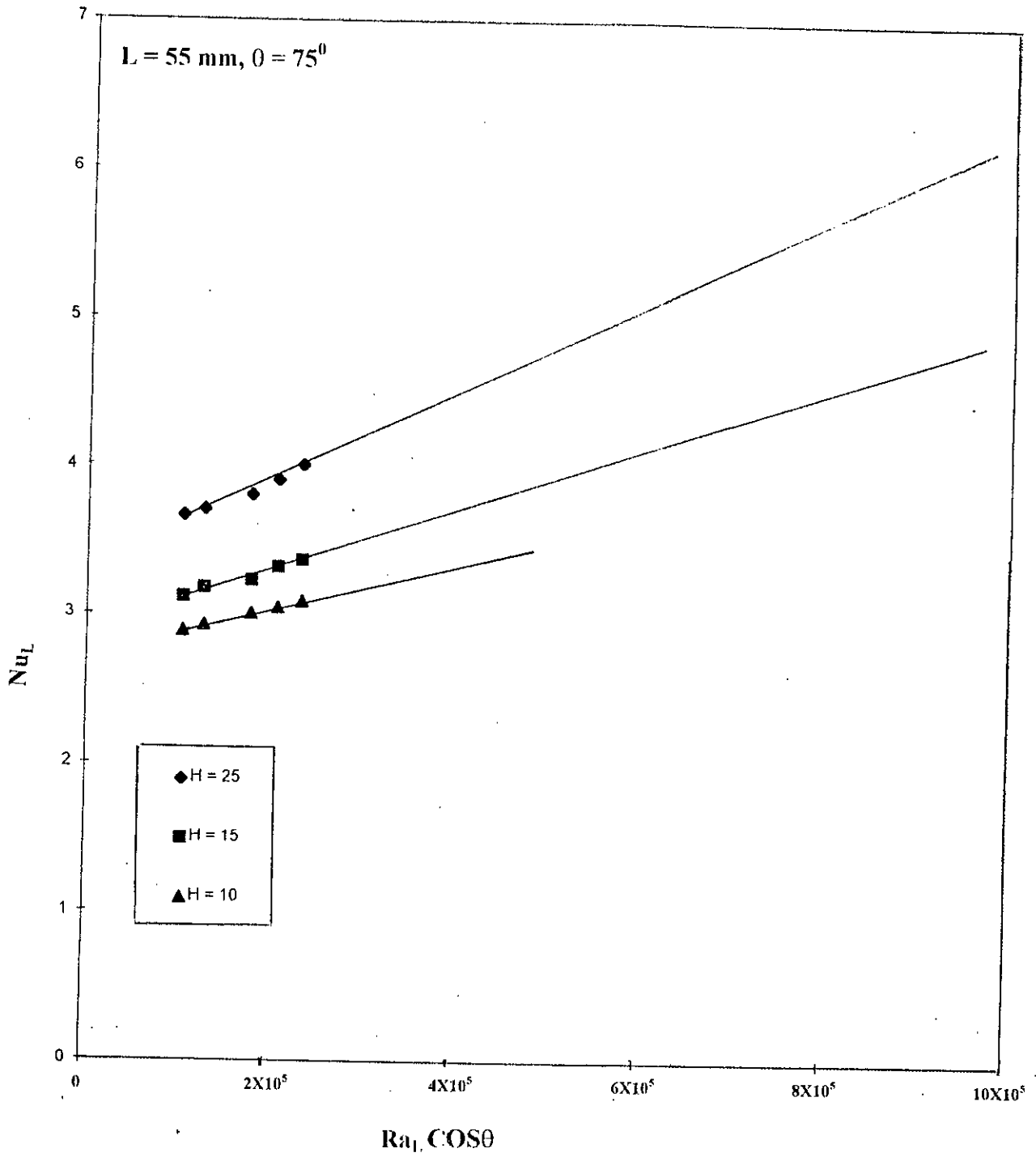
FIG 6.34 : EFFECT OF AVERAGE NUSSELT NUMBER VS $Ra_L COS\theta$ FOR L = 55 MM AT ANGLE OF INCLINATION $\theta = 75^0$.
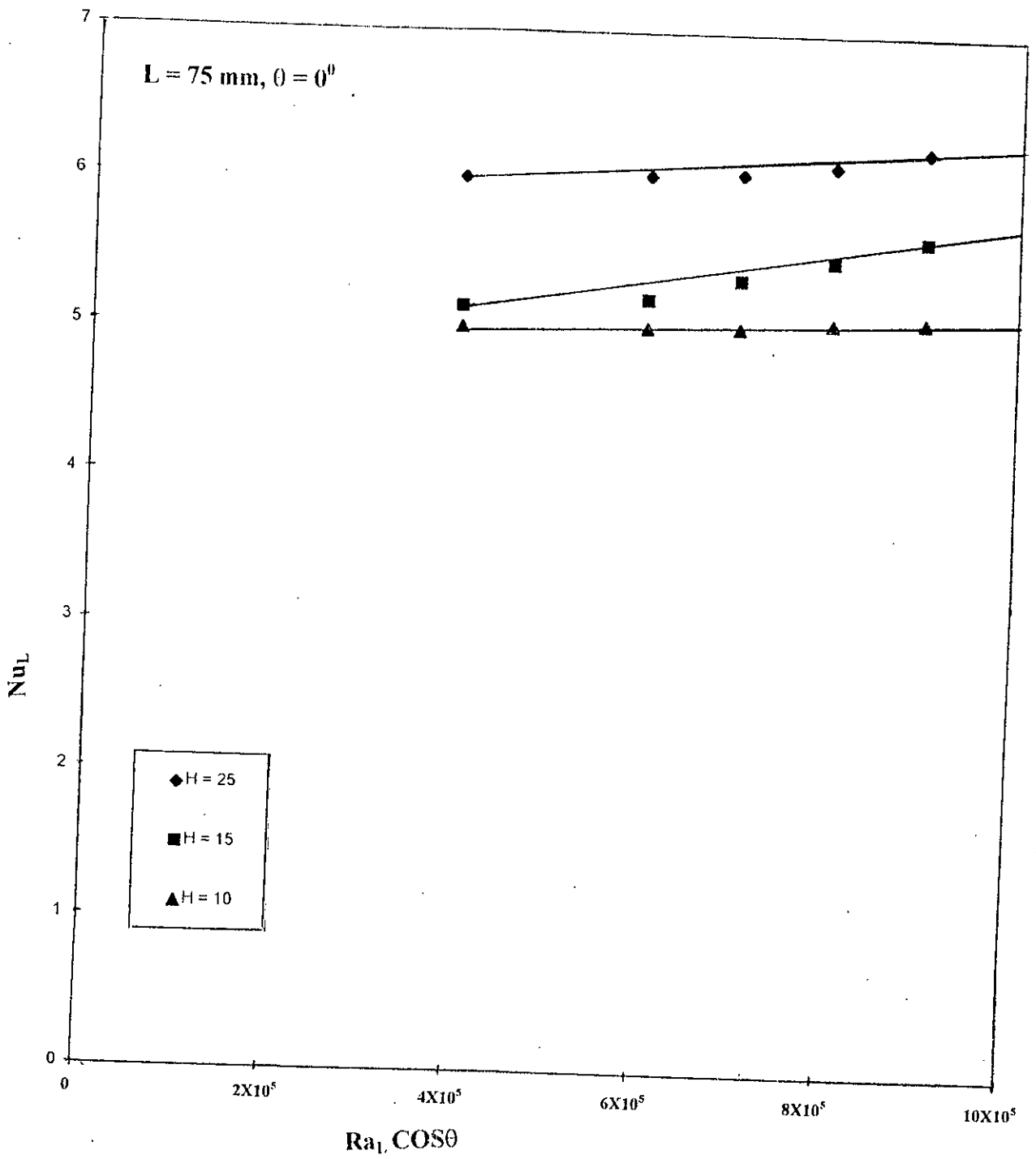
FIG 6.35 : EFFECT OF AVERAGE NUSSELT NUMBER VS $Ra_L COS\theta$ FOR L = 75 MM AT ANGLE OF INCLINATION $\theta = 0^0$
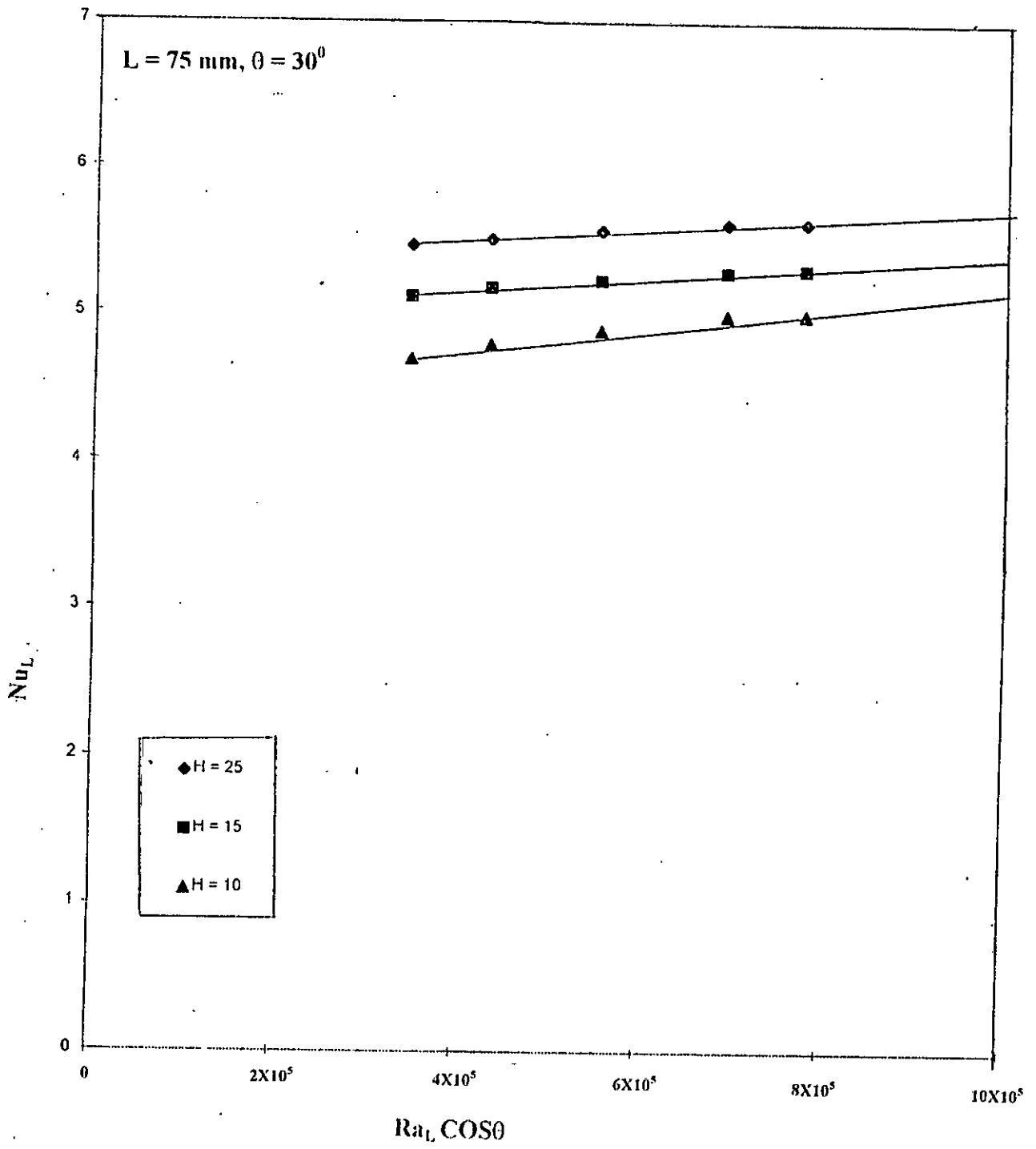
FIG 6.36 : EFFECT OF AVERAGE NUSSELT NUMBER VS $Ra_L COS\theta$ FOR L = 75 MM AT ANGLE OF INCLINATION θ = 30°
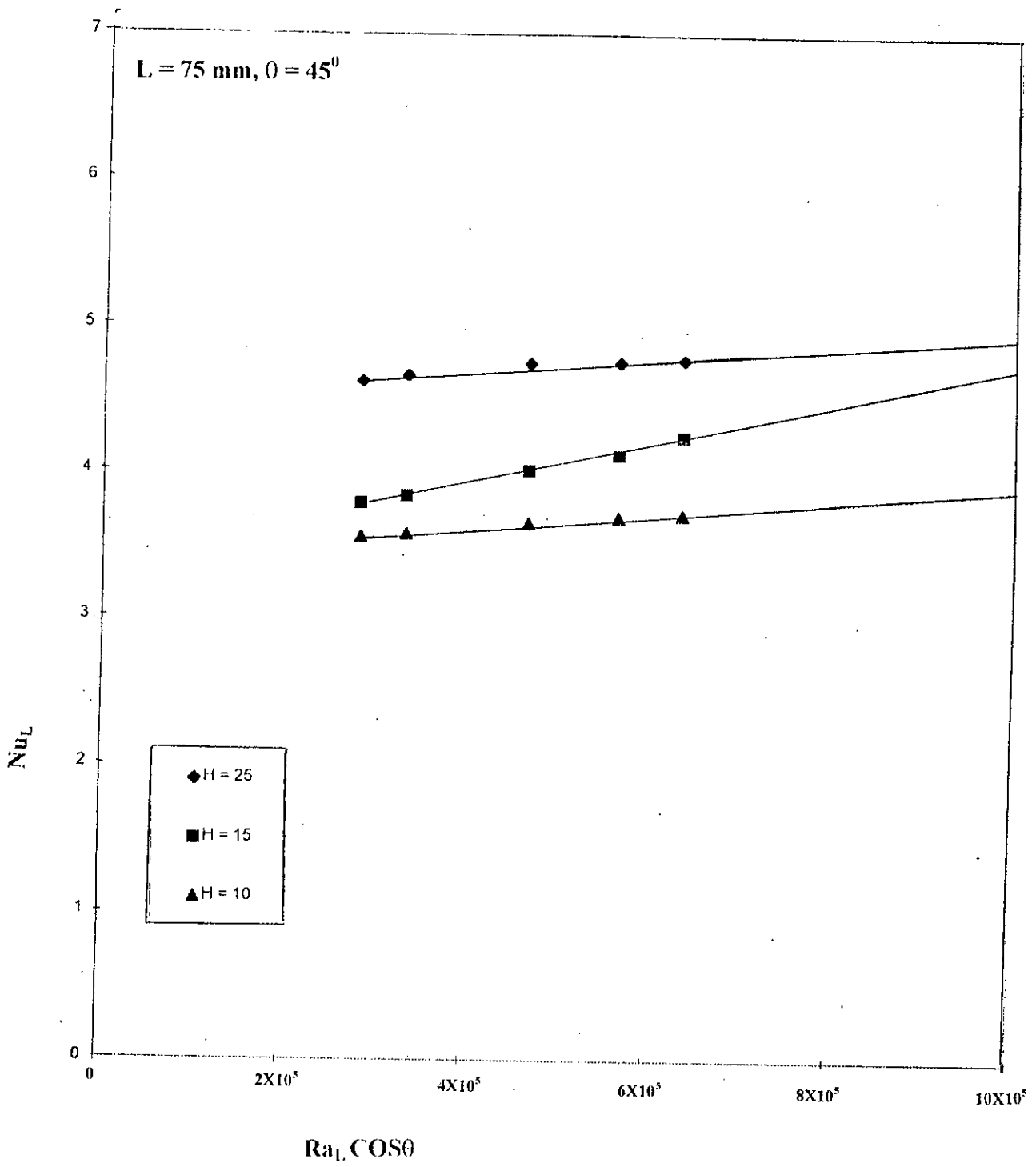
FIG 6.37 : EFFECT OF AVERAGE NUSSELT NUMBER VS $Ra_L COS\theta$ FOR L = 75 MM AT ANGLE OF INCLINATION $\theta = 45^0$
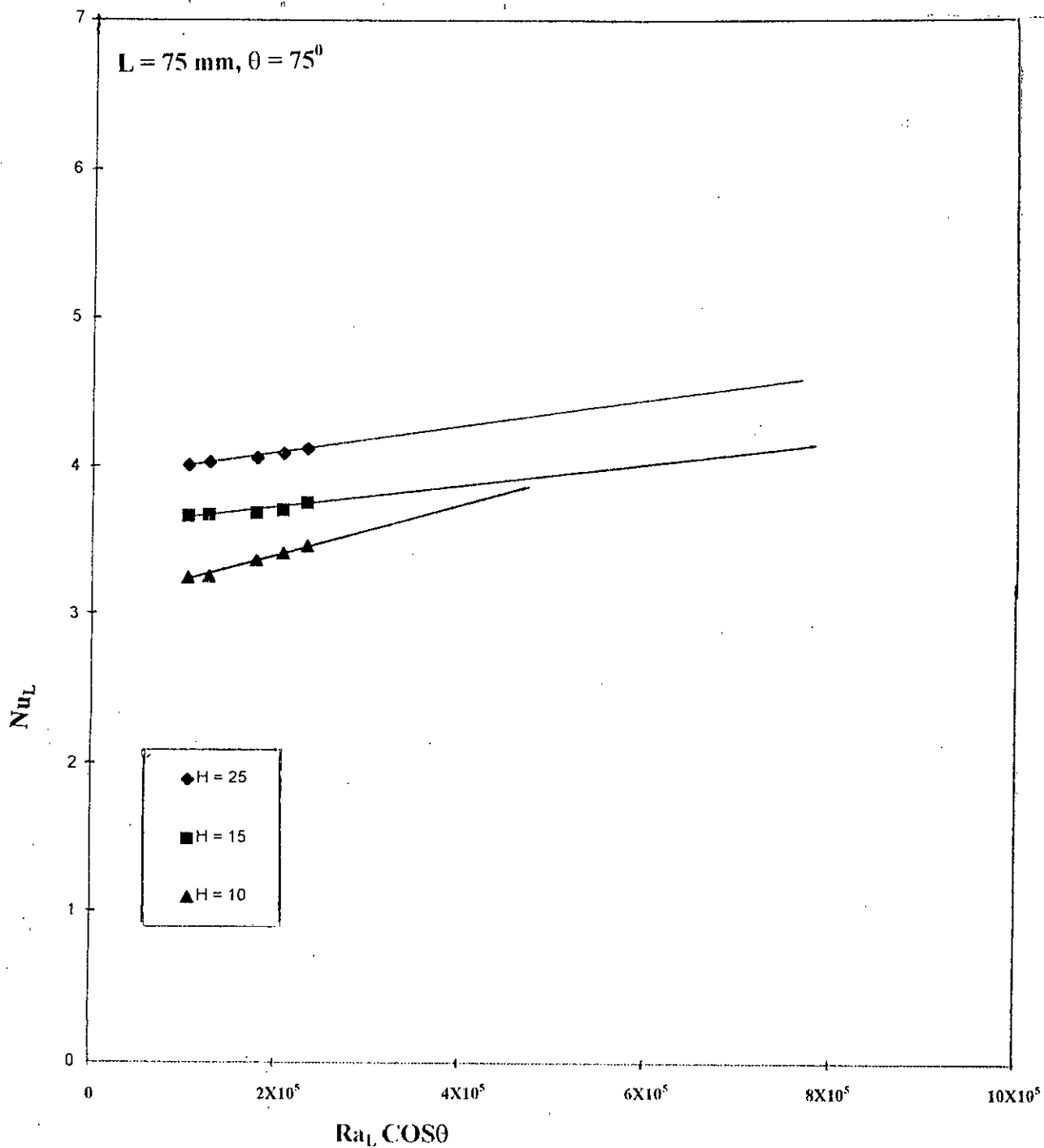
FIG 6.38 : EFFECT OF AVERAGE NUSSELT NUMBER VS $Ra_L COS\theta$ FOR L = 75 MM AT ANGLE OF INCLINATION θ = 75°.

FIG 6.39 : EFFECT OF AVERAGE NUSSELT NUMBER VS $Ra_L COS\theta$ FOR L = 95 MM AT ANGLE OF INCLINATION $\theta = 0^0$.

FIG 6.40 : EFFECT OF AVERAGE NUSSELT NUMBER VS $Ra_L COS\theta$ FOR L = 95 MM AT ANGLE OF INCLINATION $\theta = 30^0$.

FIG 6.41 · EFFECT OF AVERAGE NUSSELT NUMBER VS $Ra_L COS\theta$ FOR L = 95 MM AT ANGLE OF INCLINATION θ = 45°.

FIG 6.42 : EFFECT OF AVERAGE NUSSELT NUMBER VS $Ra_L COS\theta$ FOR L = 95 MM AT ANGLE OF INCLINATION θ = 75°.
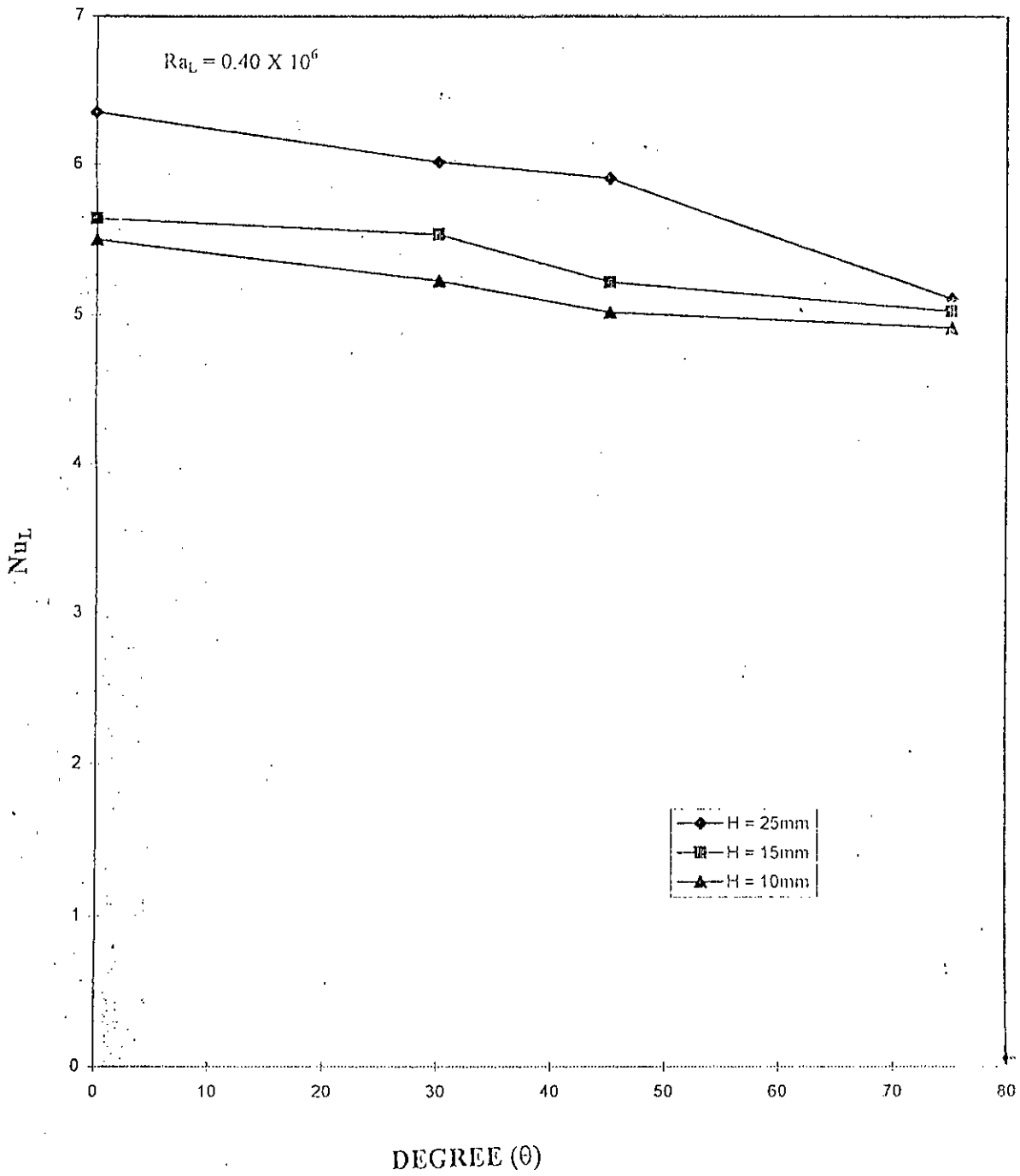
FIG. 6.43: EFFECT OF ANGLE OF INCLINATION ON NUSSENT NUMBER AT RAYLEIGH NUMBER (Ra$_L$) = 0.40 X 10^6 IN VARIOUS AMPLITUDES OF CORRUGATION(H=10mm,15mm,25mm)
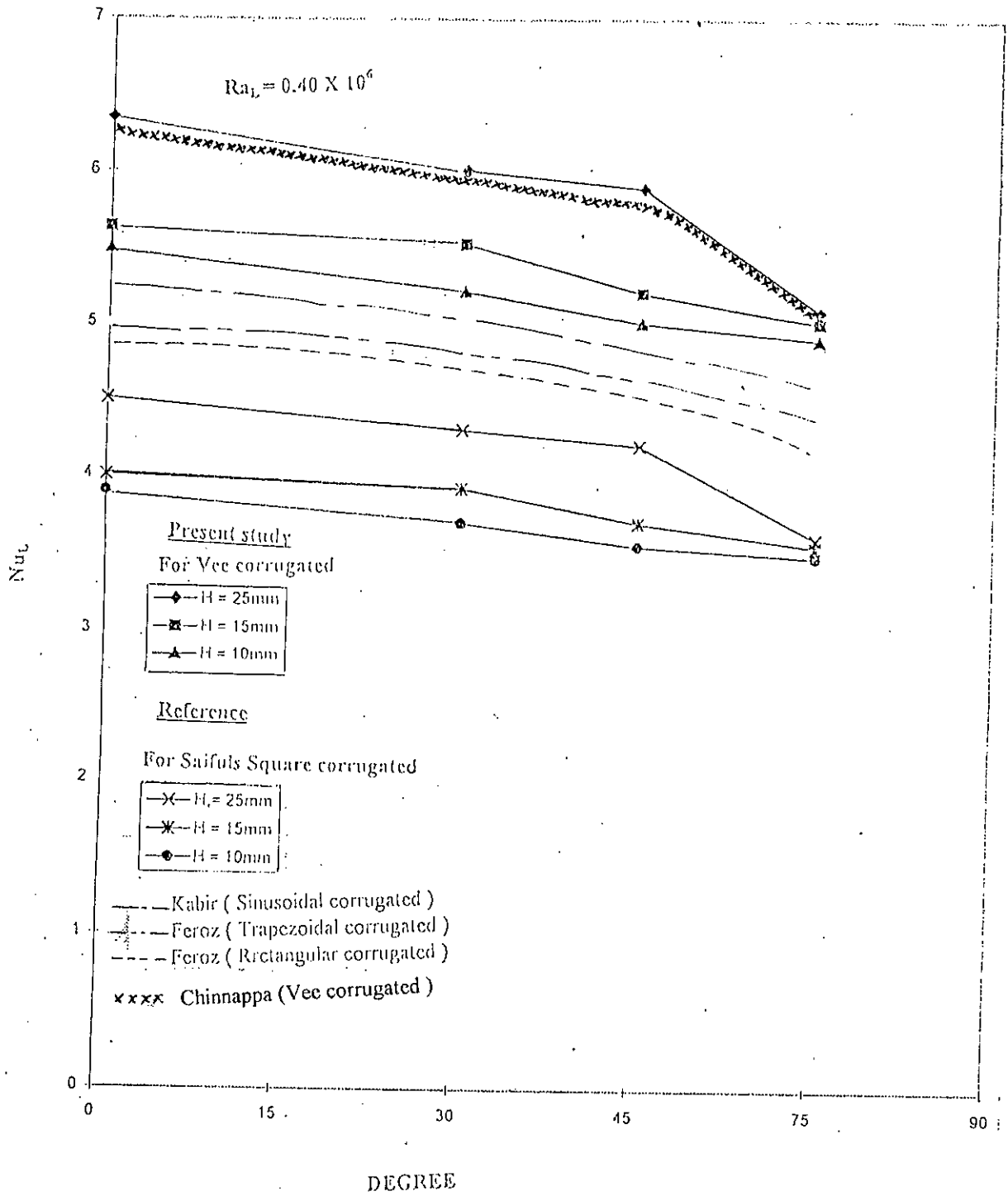
FIG. 6.44: COMPARISON OF THE EFFECT OF ANGLE OF INCLINATION (θ) ON NUSSELT NUMBER (Nu_L) OF THE PRESENT STUDY WITH NUSSELT NUMBER (Nu_L) OF OTHER RELATED WORKS AT RAYLEIGH NUMBER (Ra_L) = 0.40 X 10^6.
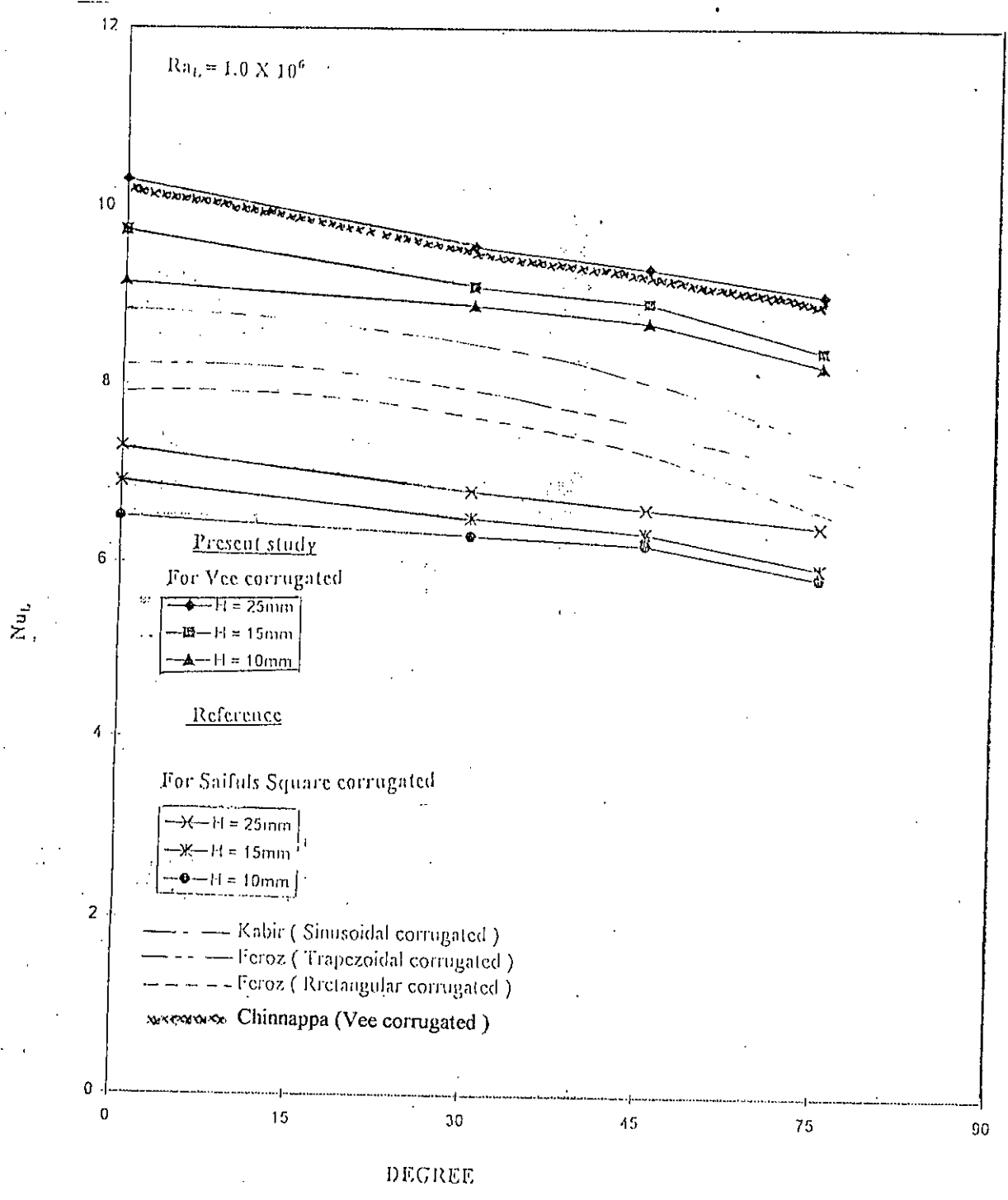
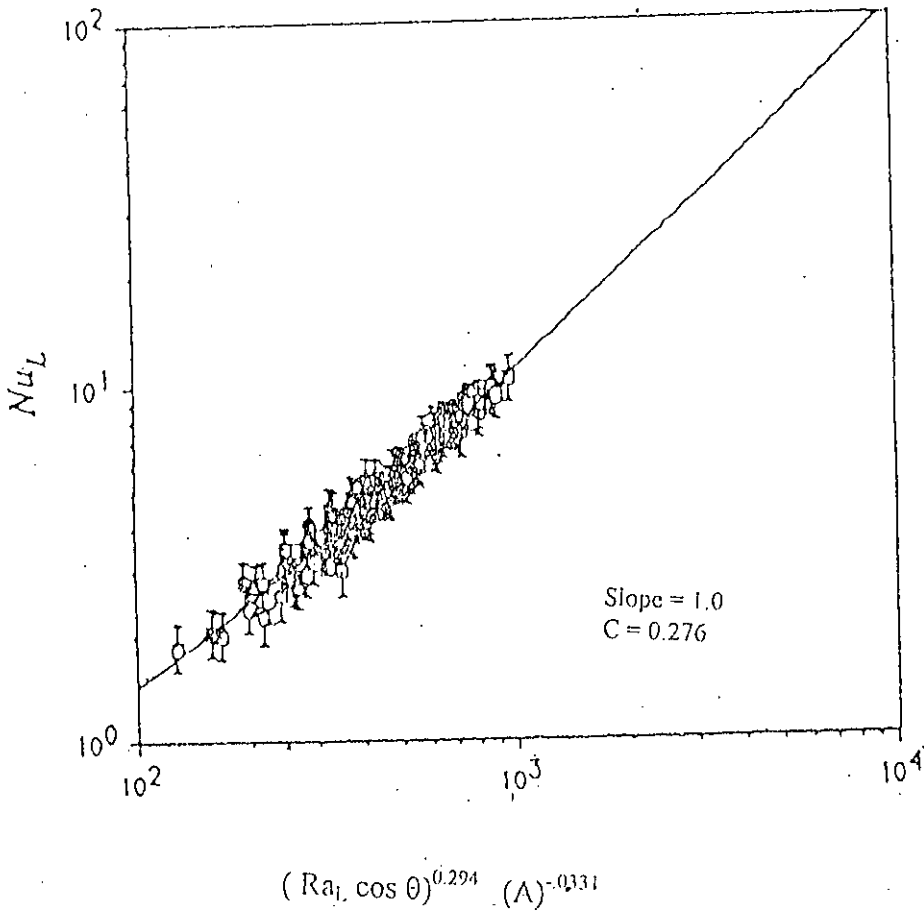FIG. 6.45: COMPARISON OF THE EFFECT OF ANGLE OF INCLINATION (θ) ON NUSSELT NUMBER (Nu$_L$) OF THE PRESENT STUDY WITH NUSSELT NUMBER (Nu$_L$) OF OTHER RELATED WORKS AT RAYLEIGH NUMBER (Ra$_L$) = 1.0 X 10^6.

Slope = 1.0
C = 0.276

$(Ra_L \cos \theta)^{0.294} \cdot (A)^{-0.131}$

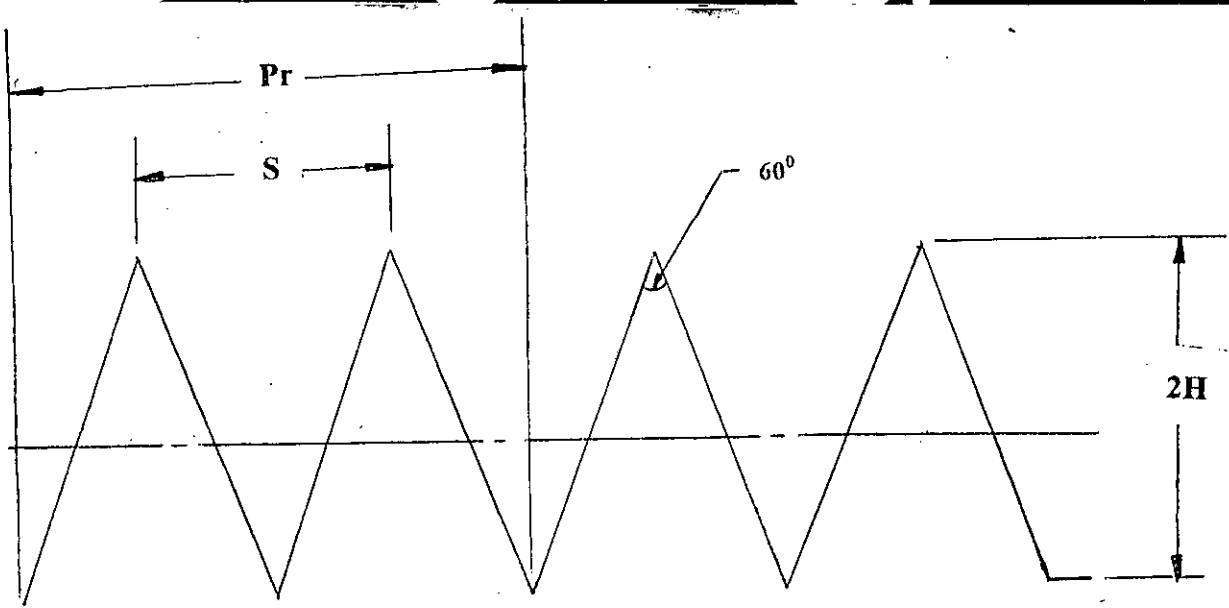FIG. 6.46 : GRAPHICAL REPRESENTATION OF CORRELATION FOR VEE CORRUGATION
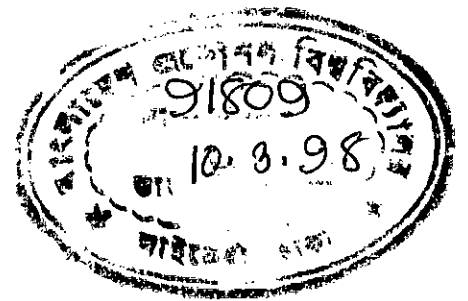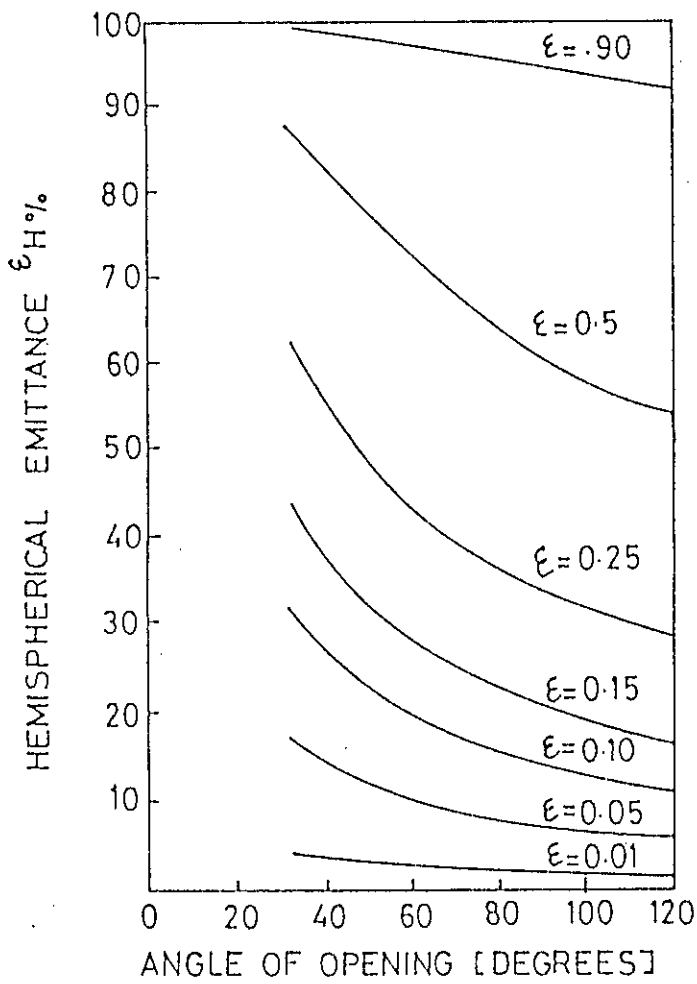
FIG. C. 1.   CORRUGATION GEOMETRY

FIG. C. 2. HEMISPHERICAL EMITTENCE Vs ANGLE
OF OPENING FOR SEVERAL PLANE
LONG WAVE EMISSIVITIES.